INL/EXT-16-39903
Revision 0

Light Water Reactor Sustainability Program

Framework for Structural Online Health Monitoring of Aging and Degradation of Secondary Systems due to some Aspects of Erosion

September 2016

U.S. Department of Energy

Office of Nuclear Energy

INL/EXT-16-39903
Revision 0

Framework for Structural Online Health Monitoring of Aging and Degradation of Secondary Systems due to some Aspects of Erosion

Andrei Gribok, Sobhan Patnaik, Christian Williams, Marut Pattanaik, and Raghunath Kanakala

September 2016

**Prepared for the
U.S. Department of Energy
Office of Nuclear Energy**

Light Water Reactor Sustainability Program

Framework for Structural Online Health Monitoring of Aging and Degradation of Secondary Systems due to some Aspects of Erosion

INL/EXT-16-39903
Revision 0

September 2016

ABSTRACT

This report describes the current state of research related to critical aspects of erosion and selected aspects of degradation of secondary components in nuclear power plants (NPPs). The report also proposes a framework for online health monitoring of aging and degradation of secondary components. The framework consists of an integrated multi-sensor modality system, which can be used to monitor different piping configurations under different degradation conditions. The report analyses the currently known degradation mechanisms and available predictive models. Based on this analysis, the structural health monitoring framework is proposed.

The Light Water Reactor Sustainability Program began to evaluate technologies that could be used to perform online monitoring of piping and other secondary system structural components in commercial NPPs. These online monitoring systems have the potential to identify when a more-detailed inspection is needed using real-time measurements, rather than at a pre-determined inspection interval.

This transition to condition-based, risk-informed automated maintenance will contribute to a significant reduction of operations and maintenance costs that account for the majority of nuclear power generation costs.

There is unanimous agreement between industry experts and academic researchers that identifying and prioritizing inspection locations in secondary piping systems (for example, in raw water piping or diesel piping) would eliminate many excessive in-service inspections. The proposed structural health monitoring framework takes aim at answering this challenge by combining long-range guided wave technologies with other monitoring techniques, which can significantly increase the inspection length and pinpoint the locations that degraded the most. More widely, the report suggests research efforts aimed at developing, validating, and deploying online corrosion monitoring techniques for complex geometries, which are pervasive in NPPs.

SUMMARY

This report describes the technical framework for online monitoring of secondary passive structures in nuclear power plants (NPPs) that is being conducted under the U.S. Department of Energy's Light Water Reactor Sustainability (LWRS) Program.

The LWRS Program, funded by the U.S. Department of Energy's Office of Nuclear Energy, aims to provide scientific, engineering, and technological foundations for extending the life of operating light water reactors (LWRs). This program involves several goals, one of which is ensuring safe operation of NPPs' passive components, such as concrete, piping, steam generators, heat exchangers, and cabling.

Within the LWRS Program, the Advanced Instrumentation, Information, and Control (II&C) Systems Technologies Pathway conducts targeted research and development to address aging and reliability concerns with the legacy analog instrumentation systems, structures, and components (SSC) and related information systems of the U.S. operating LWR fleet. This work involves two major goals: (1) ensuring legacy analog II&C systems are not life-limiting issues for the LWR fleet, and (2) to implementing digital II&C technology in a manner that enables broad innovation and business improvement in the NPP operating model. Resolving long-term operational concerns with II&C systems contributes to long-term sustainability of the LWR fleet, which is vital to the nation's energy and environmental security.

The goals of the LWRS Program are addressed through a number of pilot projects that target realistic opportunities for increasing sustainability, safety, and economic efficiency of the existing NPP fleet. It is generally recognized that the biggest challenge for existing NPPs is economic viability. Reducing operations and management cost is one of the most pressing problems facing the nuclear power generation industry. Operations and maintenance costs comprise approximately 60 to 70% of the overall generating cost in legacy NPPs. Only 15 to 30% of costs are attributed to fuel.

Furthermore, of the operations and maintenance costs in U.S. plants, approximately 80% are labor costs. To address the issue of rising operating costs and economic viability, in 2016, companies that operate the national nuclear energy fleet started the Delivering the Nuclear Promise Initiative, which is a 3-year program aimed at maintaining operational focus, increasing value, and improving efficiency.

The Delivering the Nuclear Promise Initiative is also expected to play a key role in achieving one of the major goals of the Paris agreement signed in December 2015, which sets a long-term goal of limiting global warming to well below 2°C or 1.5°C, if possible. The United States would not be able to meet its obligation under the Paris agreement, which goes into force in 2020, if they close their existing NPPs. The biggest threat to the current nuclear fleet in the United States is economic challenges and not technical challenges.

ACKNOWLEDGEMENTS

The author would like to thank Heather Feldman and Kurt Crytzer of EPRI for their help and leadership in organizing the joint workshop on structural health monitoring and for providing technical guidance and feedback during the development of the joint research plan. The author is also grateful to Kenneth Thomas of INL for his insights and encouragements during technical discussions.

CONTENTS

FIGURES

ACRONYMS

1-D	one-dimensional
2-D	two-dimensional
3-D	three-dimensional
AC	alternating current
AdvSMR	advanced small modular reactor
AE	acoustic emission
ANL	Argonne National Laboratory
ASME	American Society of Mechanical Engineers
BE	belt eye
BMG	bulk metallic glasses
BWR	boiling water reactor
CBM	condition-based maintenance
CCTV	closed-circuit television
CEM	Corrosion-Erosion Monitor
CFD	computational fluid dynamics
CPAD	Cable Polymer Aging Database
CRIEPI	Central Research Institute of Electric Power Industry
DC	direct current
DCPD	dicyclopentadiene resin
DNV	Det Norske Veritas
DOE	U.S. Department of Energy
DSS	duplex stainless steel
ECMS	Erosion-Corrosion Management System
E/CRC	Erosion/Corrosion Research Center
ECW	erosion-corrosion wear
EMAR	electromagnetic acoustic resonance
EMAT	electromagnetic acoustic transducers
EPRI	Electric Power Research Institute
ES-DCPD	Equipotential Switching Direct Current Potential Drop
ET	eddy-current testing
FAC	flow-accelerated corrosion
FBE	fusion-bonded epoxy
FFS	fitness-for-service

FPGA/RT	Field-Programmable-Gate-Array/Real-Time
GE	General Electric
GP	Gamma Process
GPM	General Path Model
GW	guided wave
GWT	guided wave testing
I&C	instrumentation and control
IAEA	International Atomic Energy Agency
II&C	advanced instrumentation, information, and control systems technologies pathway
INL	Idaho National Laboratory
IT	information technology
LDI	liquid droplet impingement
LIE	liquid impingement erosion
LTO	long term operations
LWR	light water reactor
LWRS	Light Water Reactor Sustainability Program
MDI	menu directed inspection
NACA	
NaRM	narrow range monitoring
NDE	non-destructive evaluation
NDT	non-destructive testing
NE	Nuclear Energy
NPP	nuclear power plant
NPS	nuclear power system
NRC	U.S. Nuclear Regulatory Commission
ODE	ordinary differential equations
OLM	online monitoring
OLP	online prognostics
PE	polyethylene
PHM	prognostics and health management
PNN/PZT	$Pb(Nb,Ni)O_3$-$Pb(Zr,Ti)O_3$
PSC	
PSZ	
PVDF	polyvinylidene fluoride
PWR	pressurized water reactor

PZT	lead zirconate titanate
R&D	research and development
RT	radiographic testing (or technique)
RUL	remaining useful life
RV	random variable
RVI	remote visual inspection
SCC	stress corrosion cracking
SDMS	self-diagnostic monitoring system
SEM	scanning electron microscopy
SFASL	Seoul National University FAC Accelerated Simulation Loop
SHM	structural health monitoring
SNC	superposition of the n^{th} compression
SPE	solid particle erosion
SSC	systems, structures, and components
SUNPP	South Ukrainian Nuclear Power Plant
TPP	thermal power plant
URANS	unsteady Reynolds-averaged Navier-Stokes
UT	ultrasonic testing (or technique)
VC	vena contracta
VT	visual testing (or technique)
WACOL	High-temperature On-line Monitoring of Water Chemistry and Corrosion
WACOLIN	Investigations on Water Chemistry Control and Coolant Interaction with Fuel and Primary Circuit Materials in Water Cooled Power Reactors
WATHEC	Wall Thinning due to Erosion Corrosion
WCB	
XRD	x-ray diffraction

Framework for Structural Online Health Monitoring of Aging and Degradation of Secondary Systems due to some Aspects of Erosion

1. CAVITATION EROSION

1.1 Introduction

Cavitation erosion can be defined as the process of surface degradation and loss of material from the surface due to the generation of vapor or gas pockets within the flow of liquid. These pockets are formed when the pressure is low and much less than the saturation vapor pressure of the liquid. Thus, erosion is caused when vapor bubbles are lashed against the surface.

Generally, cavitation erosion is a form of an attack on the surface by vapor or gas bubbles generating a rapid collapse due to a pressure difference close to the surface. A significant low pressure below the saturated vapor pressure is created hydro-dynamically due to different factors that affect the flow. Such factors consist of liquid viscosity, temperature, pressure, and type of flow. The main reason for the deterioration of the surface is the sudden, powerful upward or forward movement of the bubbles that bombard the surface, thus causing surface deformation eventually leading to pitting.

Cavitation affects the surfaces of both metals as well as non-metals. It gives rise to unnecessary noise levels and significantly declines the useful life of materials. For example, noise due to cavitation in submarines promotes vulnerability as it increases the possibility of detection by enemy craft. Another example is when small pipe diameters at the inlet side of pumps, combined with certain restrictions on the inlet pipe and high viscosity levels in the liquid, serve to increase the cavitation erosion risks in pumps. Furthermore, cavitation can damage various critical and expensive pieces of equipment used in industry, the military, and power stations. Certain important parts like pump impellers, propellers, and turbines can all be affected by cavitation. Not only can this damage lead to potential harm of workers and people associated with it, but also a loss of revenue, time, and energy. Hence, it incurs extra overhead costs on failure detection and analysis, repairs, and replacement work [1].

1.2 First Principles of Cavitation Erosion

According to Harold M. Crockett and Jeffrey S. Horowitz [2] a sudden pressure drop followed by a pressure recovery in a flowing fluid causes cavitation. Generally, if the flow is accelerated within a small area like valve internals, it gives rise to a difference between upstream and downstream pressure. According to Bernoulli's theorem, when the fluid moves through a smaller area, the velocity increases and the pressure drops. Bubbles are formed when the local pressure goes below the vapor pressure at the liquid temperature, and these bubbles (or cavities) collapse, when the downstream pressure goes beyond the vapor pressure. Thus, cavitation in a fluid is a mechanism in which vapor bubbles grow and collapse due to difference in local pressure. These pressure fluctuations lower the vapor pressure of the fluid. This process occurs at a constant temperature [3].

1.3 Cavitation Erosion in Nuclear Power Plants

According to Harold M. Crockett and Jeffrey S. Horowitz [2] a sudden pressure drop followed by pressure recovery in a flowing fluid causes cavitation. Generally, if the flow is accelerated within a small area, like valve internals, it gives rise to a difference between upstream and downstream pressure. When the fluid moves through a constricted area the velocity increases and the pressure drops, according to Bernoulli's theorem. Bubbles form when the local pressure goes below the vapor pressure at the liquid temperature, and these bubbles (or cavities) collapse when the downstream pressure goes beyond the vapor pressure.

Cavitation causes a variety of defects such as leakage, wall thinning in power plant piping, and severe damage to valve internals. It also damages hydroelectric turbine blades, shop propellers, and pump internals. In the case of power plants, cavitation mostly affects control valves and downstream of orifices in liquid filled systems. Generally, cavitation damages are sudden and localized. The damaged surface is usually very rough and irregular.

1.4 Wear Mechanism

A liquid contains gaseous or vaporous bubbles that act as the cavitation nuclei. When the pressure decreases to a particular level, bubbles become a kind of central storage or repository of vapor, or of dissolved gases. As a result, the bubbles rapidly increase in size. Furthermore, when the bubbles go into the low-pressure region, their size decreases due to the condensation of the vapors contained by them. This is a rapid condensation process that occurs which is accompanied by hydraulic shocks, sound emission, breaking material bonds, and other unfavorable processes. In most liquids it was observed that the reduction in volumetric stability is associated with the contents of various admixtures. These mixtures on a submicroscopic level might be unwetted solid particles and gas-vapor bubbles, which serve as cavitation nuclei.

One important aspect of cavitation is surface degradation and material displacement, which arise due to high relative motions between the material surface and the exposed fluid. These motions result in reduction of the local fluid pressure, which increases the fluid temperature up to its boiling point and causes the formation of small vapor cavities. When the pressure becomes higher than the vapor pressure of the fluid, implosions cause the vapor bubbles to collapse. As the bubbles collapse, shock waves are created that generate high-impact forces on adjacent metal surfaces and thus result in hardening, fatigue, and cavitation pits.

Thus, cavitation in a fluid is a mechanism in which vapor bubbles grow and collapse due to differences in local pressure. These pressure fluctuations lower the vapor pressure of the fluid. This vaporous cavitation process occurs at a constant temperature [3].

1.5 Types of Cavitation

Two major types of cavitation exist: vaporous and gaseous. When the liquid undergoes a sudden, rapid change into vapor, the bubbles grow explosively in an unbounded manner and hence vaporous cavitation takes place. During this occurrence of cavitation, the pressure level is quite less than the vapor pressure of the liquid. On the other hand, gaseous cavitation is a diffusion process. It occurs when the pressure decreases below the saturation pressure of the non-condensable gas dissolved in the liquid. Vaporous cavitation is extremely rapid, occurring at the rate of microseconds, whereas gaseous cavitation is much slower. The time taken depends on the degree of convection present.

Vaporous cavitation conditions cause cavitation wear where the shock waves and micro-jets damage the surface. Gaseous cavitation does not cause surface damage. It only creates noise, high temperatures, and degrades the chemical composition of the fluid by causing oxidation.

Cavitation erosion is a type of wear phenomena in which wear propagates from fluid to surface. This occurs when a part of the fluid is initially exposed to tensile stresses that cause the fluid to boil. It is then compressed under the action of compressive stresses, which leads to collapsing or imploding of the vapor bubbles. This implosion results in a mechanical shock wave and thus, micro-jets impinge against the surfaces. There is ample plausibility of cavitation wear to occur in a system that can repeat this tensile and compressive stress pattern. It can be said that cavitation wear is similar to surface fatigue wear; materials that have a high resistance against surface fatigue are also resistant to cavitation damage [3].

1.6 Cavitation Erosion in Various Materials and Their Behavior

According to a study by Laguna-Camacho et al. [4], cavitation erosion has an extensive impact on engineering materials. They studied a few of the specific material samples that have been described in this section. On conducting tests by only using only tap water as an impacting jet on the surface of pure aluminum, intense pitting was observed leading to surface damage. The extent of pitting was mild in the case of mild steel, even though it had an area of corrosion exhibiting thermal pits around it. Several aluminum samples used as ‘‘vibratory’’ specimens and Aluminum 6082 alloy used as the ‘‘stationary’’ specimen exhibited higher erosion damage as compared to the other two cases where pure aluminum was pitted against Stainless Steel 304 and Alloy 4340 of steel. When only tap water was used, it resulted in higher mass loss with abrasive particles such as silicon carbide (SiC) compared to others subjected to the test. When specimens were bombarded with silicon carbide (SiC), particles that roughened surfaces were less than compared to those that were damaged only by the direct implosion of small cavities. Along those lines, it was concluded that the damage on the surfaces were a result of a combination of small pits, irregular scratches, and grooves.

In a study by Moeny et al. [5], they conducted experiments on a modified NACA 66-series foil by impingement of an upstream vortex by means of a surface paint flow visualization and image acquisition. They induced intermittent surface cavitation in the secondary recirculation region, and the secondary flow advected cavitation bubbles away from the inception point prior to implosion. Then it was found that the mitigation greatly curbed the span wise flow, changed the nature of the induced cavitation, and was instrumental in minimizing the incidence of the advected cavitation bubbles from the point of inception.

Drozdz et al. [6], in their study of cavitation erosion on bulk metallic glasses (BMGs), made an important analysis. According to their results:

- The cavitation erosion resistance of BMGs, analysed by means of an ultrasonic vibration processor, was found to be greater than that of austenitic Stainless Steel S30431 by a factor 10. They can be arranged in the following manner in order of their resistance to cavitation erosion: Zr48Co > Zr48 > Zr58 > Zr65 > S30431 austenitic stainless steel.
- Cavitation erosion of BMGs originates in places with higher energy. It is followed by the formation of dimples and lines of deformation, which become large and create new gaps with the increase of cavitation time.
- BMGs normally tend to have a higher initial hardness, which becomes advantageous for cavitation erosion resistance. There exists an inverse proportionality between hardness and erosion rate. The higher the initial hardness, the lower the maximum rate of erosion. Therefore, the initial hardness becomes an important factor to predict cavitation behaviour of BMGs.
- Cavitation erosion is a cycling deformation process. Adding even a small amount of cobalt improves the erosion resistance of Zr-based BMG.
- Formation of high density of shear bands induces work-hardening, which results in the deformation of BMGs due to cavitation attacks.
- Good erosion resistance of Zr-based BMGs, along with their great mechanical properties, sheds light on new ideas in designing materials with high-cavitation resistance.

From their study on cavitation erosion mechanisms, Hattori and Nakao [7] observed that impact fracture is the predominant reason for the erosion during the starting and incubation stages. Afterward, during the acceleration and the maximum erosion rate stages, fatigue fracture occurs along with impact fracture. During the maximum erosion rate stage, the percentage of fatigue fracture is most dependent on the nature or type of material.

The growth rate of the crack on the eroding surface in the maximum rate stage can be given by:

$$da/dt = Ca^{1.2} \quad (1) \qquad (1)$$

where

t is the exposure time

C is a constant

a is defined as the crack length.

The value of the exponent 1.2, is obtained from regular fatigue tests. The volume loss rate was evaluated in terms of the material hardness and the fatigue crack growth rate.

In a study, Yu Kang et al. [8] gave some interesting ides concerning the cavitation erosion in diesel engine liners. It was found that the erosion of wet cylinder liners were quite different from the conventional corrosion mechanism. It differed on the basis of the macro appearance of the eroded surface and the micro-metallurgical investigations and analyses.

Only by corrosion is there even material removal from the exposed surface in the form of molecular combinations, but as for cavitation erosion, metal is removed as large particles from the surface. Mostly it has been inferred that the diesel engine liner erosion occurs mainly due to cavitation bubble implosion, and that cavitation arises from the vibration of the liner wall. As per the micrographs of the erosion tests performed by Yu-Kang et al., it was found that the primary reasons of the erosion were fatigue and fracture failure of the diesel engine liner walls.

While most research is focused on experimenting with the properties of different kinds of metals and their alloys, Hattori and Itoh [9] from Japan conducted a significant amount of research on the resistance of plastics to cavitation erosion. Quantitative evaluation of erosion and measuring the implosion of bubbles and fatigue strength led to certain interesting results. For example, on being compared to carbon steel SS400, it was found that in the case of plastics, the cavitation resistance varied from one half to 30 times for epoxy and polyamide 66, respectively. Due to the low thermal conductivity of plastics, there is a need for consideration of mechanical properties for quantitative evaluation of cavitation erosion. But essentially, the erosion propagation is similar to that of fatigue fracture. Due to the low noise impedance, loads impacting the surface of plastics are lower than metals. Cavitation erosion could be characterized from impact energy and fatigue strength.

Fairfield [10] conducted research on the damage due to cavitation on sewer and drain pipe materials. Based on his calculations of erosion rates and loss of material thickness, he proposed a list of five materials that displayed longer life span under the action of cavitation: concrete, clay, 30% (v/v) glass filled nylon, polysulphone, and polyetherimide. Also, the materials that showed excellent resistance even under very high pressure for 30 seconds were clay and some polymers like polyetheretherketone, polyetherimide, polyphenylenesulphide, and polysulphone. He also postulated that the smoother the material, less is the rate of induced cavitation.

In research based on vortex cavitation, Karimi and Avellan [11] suggested and inferred some interesting results. They found that the main reason behind the difference between flow and vibratory cavitation mechanisms is due to the spatial distributions of the cavities or bubbles, and the extent or intensities of implosion impingements. From work previously discussed [3], it can be described that flow cavitation is a kind of vaporous cavitation, where the propagation of shock waves and liquid micro-jets cause erosion on the material surface. While on the contrary, gaseous cavitation, like vibratory cavitation, creates noise due to vibration leading to a rise in temperature and ultimately destroys the chemical composition of the fluid by means of oxidation. Vibratory cavitation differs from flow cavitation based on the fact that there is no single factor responsible for causing the collapse impact. More or less, the damage is uniformly distributed over the area that is already exposed to cavitation and the area that gradually

develops over a period of exposure time. In case of flow cavitation, the thickness of the layers (subsurface) formed by hardening just below the exposed material surface is greater than that of the vibratory cavitation. Hence, the effective damage and surface degradation due to flow cavitation is more than vibratory cavitation.

Continuing with the study of cavitation effects on different materials, Howard and Ball [12] presented some good comparative results and analysis on Ti-Al alloys. Today in industry, Ti3Al-based super α2 alloy (Ti-25Al-lONb-3V-1Mo at.%) and TiAl-based (γ) alloys (Ti-52Al and Tid8Al- 2Mn-2Nb at.%) are being used for engineering applications. Their experimental analysis proved that the titanium aluminide alloys were effectively far more resistant to cavitation erosion even in comparison to erosion-resistant materials, such as WC-15Co (wt.%). Also, it was observed that the γ alloys of TiAl are more resistant to cavitation than theα alloy. The crystallographic line features obtained from x-ray diffraction (XRD) analysis confirm this fact. There is a reasonable assumption that both the γ alloys underwent a process during their short incubation period that eventually hardens the surface leading to same erosion rate, which is essentially less than that for the Ti-25Al-10Nb-3V-1Mo (α2 alloy).

Liu et al. [13] performed some tests to study the vibration cavitation behavior on Ni-Mn-Ga alloys. Generally, in materials science, this is an interesting combination of metals. Thus, the following conclusion could be incurred out of their study:

- The super plasticity and the twin variant arrangement of the Ni-Mn-Ga alloys essentially exhibited superior cavitation resistance when compared to austenitic stainless steel and to some NiTi alloys as well. Due to their material properties, the Ni-Mn-Ga alloys were able to dissipate the energy due to loading and thus, reduce the damage due to cavitation.
- The alloy with the cubic structure had the best resistant to cavitation followed by the one that had a T-martensitic structure. The 5M-structured alloy displayed the maximum material loss.
- Cavitation for the Ni-Mn-Ga alloys were characterized by the fact that the damage patterns on the Ni-Mn-Ga alloys were initiated and propagated locally, whereas the progress of cavitation occurred evenly in case of NiTi alloys.

The cavitation behavior of Hastelloy C-276, a nickel-based super alloy, has been studied and reported by Li et al. [14]. They made use of an ultrasonic vibratory system and the obtained cavitation behavior was compared to that of 316L austenitic stainless steel. It had been found that after 9 hours, the C-276 alloy's mean depth of erosion was one-sixth of the 316L austenitic steel. Also, the incubation time period for Hastelloy is three times that of the 316L alloy. Precipitates due to cavitation are formed in the damaged surface due to mechanical and thermal effects of bubble implosion. It was concluded that the dominating erosion mechanism for Hastelloy was selective cavitation erosion.

Different material combinations reflect different properties, and the interesting aspect of the study of cavitation is the resistances of materials towards it. Hong et al. [15] from Korea investigated the cavitation erosion behavior of Alloy SA 106B carbon steel after treatment with nano TiC particles. Ultrasonic cavitation tests conducted concluded the incubation time for the TiC-modified steel was 1.64 times more than the untreated steel. Along those lines, the TiC-treated steels exhibited 1.42 times more resistance to cavitation than the unmodified steel. The modified steel was found to be much more resilient due to better mechanical properties. The fine grain structure of the modified steels helped to enhance the surface density of the grain boundaries. This in turn impeded the cavitation and thus increased resistance to erosion due to a higher hardness value. Since the TiC particles used are nano particles, when they are homogenously distributed they stop the growth of cracks due to cavitation, which provides more resistance.

Cavitation erosion has taken the global materials science research world by storm. Chinese researchers Dong et al. [16] made their experimental analysis on the mechanism of cavitation of Ti-alloy radiation rods after treatment in molten aluminum. It was observed that the longer the cavitation effect, the rougher the surface became. On the contrary, due to plastic deformation, the effect by virtue of cavitation decreased the surface roughness quickly. High temperature coupled with cavitation helped in easier and faster dispersion of TiAl3 in the melt. The variation in intensity and direction of micro-jets is due to the increase in depth of the pits created from erosion. This led to the change of the pit shapes from V to U. When Dong et al. evaluated their findings, they found that the cavitation erosion mechanism of Ti alloy radiation rod in Al casting under ultrasonic testing confirmed that as the hardening layer tends to grow, cracks are generated, which leads to degradation along the axial direction.

1.7 Various Studies on Cavitation in NPPs

It has been observed that in boiling water reactor (BWR) and pressurized water reactor (PWR) steam systems, the moisture content varies up to approximately 15% and velocities vary up to 51 meters per second (167 feet per second). In restricted areas, such as orifices where the velocities are generally high or in drain lines that carry saturated and flashing mixtures, the erosion due to droplet impingement or cavitation would be more predominant [17]. Flow-accelerated corrosion (FAC), and several mechanical and electro-chemical mechanisms such as erosion, cavitation, and liquid droplet impingement, etc., play a significant role in the thinning of walls in secondary circuit piping in nuclear power plants (NPPs) due to loss of material in the pipes. The consequences of wall-thinning leads to leaking or breaking of pipes, which eventually is responsible for incidents or accidents [18]. Erosion/corrosion coupled with cavitation caused by severe flow conditions at the pump discharge elbows, are the primary mechanism that results in pipe wall thinning of the secondary piping in NPPs. The Surry incident was a first for a catastrophic failure occurring in an NPP, but it was no worse than previous failures in large steam turbine heat lines or in feed-water lines. The failure mechanism was different to some extent because the Surry incident was due to a pipe rupture that was induced by erosion/corrosion, whereas the wet steam pipe failures were caused by a cavitational-type erosion damage [19].

The resistive capacity to cavitation and jet impingement erosion of materials like Inconel 600 and the Inconel 625 has been systematically studied and the following conclusions have been drawn:

- Cumulative mass loss of the Inconel 625 is one-sixth times that of the Inconel 600 after being exposed to cavitation wear under tap water for 12 hours. Inconel 625 has a 4 times longer cavitation erosion incubation period in comparison to Inconel 600. The morphological evolution of cavitation erosion at a microscopic level shows that the twinning and hardness of the Inconel 625 has a significant role in cavitation erosion.
- The test results of jet-impingement erosion indicate that at an impacting angle of 90 degrees, the cumulative mass loss of the Inconel 625 is two-thirds that of the Inconel 600. While at an impacting angle of 30 degrees, it is as much as that of the Inconel 600.
- On the contrary, the higher hardness property of the Inconel 625 has a positive role as it lowers the jet-impingement erosion rate at a normal impact angle, which in turn, belittles its effect on the jet-impingement erosion resistance at the impacting angel of 30 degrees. Therefore, the resistance to the cavitation and the jet-impingement erosion of the Inconel 625 is greater in comparison to that of the Inconel 600 (except in the case of jet-impingement erosion at an impact angle of 30 degrees) [20].

On certain occasions, the failure of a parallel slide valve of an NPP before its designated life span has created concerns regarding the reason behind it. The failed part was on the belt eye (BE), which was manufactured from ASTM 216 WCB. The failure analysis on the parallel slide valve used in the secondary circuit in an NPP, gives us an outlook on the possible reasons and inferences. On visual investigation, it was observed that the reason of the failure was a combination of at least two mechanisms. Firstly, scallop morphology was found to be the dominant factor with very serious pitting at regions

where excessive wall thinning had occurred. This gave one plausible reason for the failure, which is FAC in single liquid phase. Further metallurgical analysis on micro structural levels confirmed the occurrence of FAC, which was largely responsible for the generalized wall thinning that happened on the belt eye. As a typical ASTM 216 WCB, on performing chemical composition analysis of the belt eye it was observed that the chromium content was below the threshold chromium content on the order of 0.04%. Hence, there was no protective oxide formed on the metal surface and thus there was no effect of the Cr concentration. The flow velocity and turbulence intensity inside the belt eye was enhanced due to the local constriction in the valve, consequently increasing the FAC rate on the wall.

In this study, the authors have discussed FAC occurring on the wall causing local wall thinning and cavitation on the downstream belt eye. Visual inspection shows FAC but it is evident from mathematical models that the misalignment between the reducer and the belt eye on the upstream side caused the formation cavities in the first place. Cavitation erosion occurred on the downstream belt eye, which led to the severe local wall thinning of the BE material. Furthermore, simulations have proved that when the misalignment is about 2 mm, the most sensitive section that suffered the cavitation erosion is determined to be in the middle section of the BE, which is in line with the practical observation. If the neighboring components had been perfectly fixed and the misalignment been avoided, there would not have been any occurrence of cavitation erosion phenomenon in the belt eye part of the valve [21].

1.8 Erosion-Corrosion Occurring in NPPs

1.8.1 Erosion

Erosion occurs when loose particles from solid or fluid bombard or lash against the surface of a material at a particular angle and velocity. In a case study by Chen et al. [22] on titanium tubes, when liquid droplets of high-pressure steam get lashed against the titanium tubes below the bypass pipes at a particular velocity, an exchange of energy takes place. These liquid droplets become energized from the steam medium, which carry them and eventually transfers this energy to the outer wall of the tubes. During higher energy and longer time periods which creates plastic deformation of the tube wall, indentation occurred. The material originally in the indentation now appeared to have a raised edge where thin peaks were observed. This can be seen in Figure 1(a) and 1(b) below.

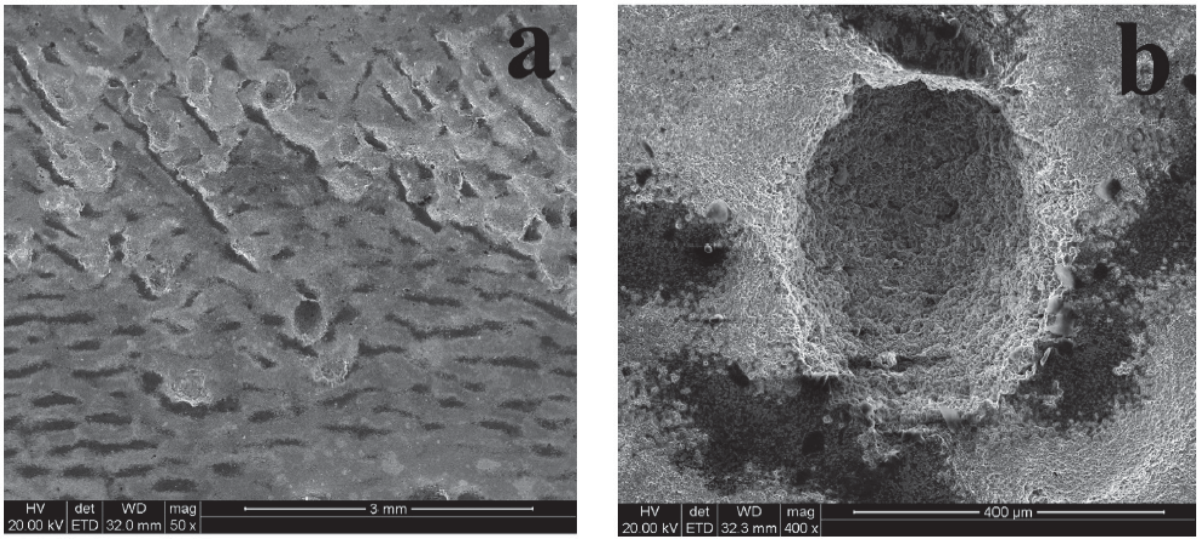

Figure 1. Microscopic morphology of defects on titanium tubes 052003-17, 18 (a) wavy erosion zone, (b) a large pit with thin, raised edge [22].

This resulted in the erosion zone, which was wavy in nature and the explanation for its morphology. Furthermore, the directional erosion traces occurred when high-pressure steam lashed against the tube wall at a certain angle.

1.8.2 Cavitation Corrosion

In a flowing fluid, when the pressure in a local region suddenly falls below the steam pressure at that local temperature for a certain reason, a part of the fluid also vaporizes. This results in the dissolving of the gas in the fluid and hence cavities are formed. This process is known as cavitation. On the one hand, as pressure decreases, the boiling point of water also decreases. Alternatively, the pressure of the fluid declines with the increase in the flowing velocity, which can be inferred from the Bernoulli equation:

$$P + (\rho v^2)/2 = C \tag{2}$$

where P, ρ, v, C stand for the pressure, density, flowing velocity of the fluid, and a constant respectively. At the point when the high-pressure steam is forced out of the bypass pipes, its pressure decreases significantly leading to a rise in its velocity and a decrease in the boiling point of water. In this way, cavitation occurred and the high-velocity steam ended up causing some serious cavitation corrosion to the tubes [22].

According to a study by Chen et al. [23], when titanium pipes were operational, the inner wall of borings was poorly designed with asperities and the non-uniform inner diameter led to wearing due to concentrated eccentric contact under the action of relative vibration. Secondly, sagging iron oxides were generated by the galvanic corrosion of the vertical carbon steel to support the plates into the internal borings. This, in turn, made the internal wall rough and eventually the position of the grindings and corrosion products changed due to vibration. Thus, three-body contact wear occurred. Last but not least, during overhaul some external new particles were brought into the condenser and deposited into the internal borings by airflow, thus resulting in the three-body abrasive wear.

Therefore, it was found that the reasons behind thinning failure was primarily the combination and interaction of contact wear, which was eccentric and three-body contact wear existing in the processing defect of internal borings, corrosion products deposit and sagging, and foreign particles.

1.8.3 Synergetic Effect of Erosion and Cavitation Corrosion

Erosion and corrosion due to cavitation occurring at the same time can both cause mechanical degradation of the material. The interaction between these two phenomena has also been deemed a cause of material degradation. On one side, cavitation corrosion creates pits on the tube wall where the passive oxide layer had already been eroded and the surface structure had been ruined. These pits serve as points where there exists the maximum likelihood of erosion to occur. This results in the mechanical degradation of the inner wall of the tube. On the other hand, erosion can hamper the structural surface of tube wall and create a wavy pattern making the tube wall structure loose and irregular. Therefore, the mechanical performance of the tube wall degrades and is more likely to deform and consequently more vulnerable to be affected by cavitation. By the interaction between these two processes, the pits and wavy zone become bigger and deeper; hence, a severe wall thinning can occur [22].

The literature review of cavitation erosion in the article by Tomarov et al. [24] provides ideas and certain important results, which should be always considered while making a choice of methods and techniques for predicting or monitoring cavitation erosion in NPPs. Some of the important conclusions are as follows:

- It is necessary to use the proposed and approved engineering methodologies for estimating the probable plausibility of manifestation and the intensity of cavitation attack by the water medium flowing through narrowing devices operating in the condensate feed path of NPP and thermal power plant (TPP) power units.

- As much as 30% of throttling devices of the condensate feed channel of NPP power units are subjected to cavitation erosion; around 60% of them falls on technological lines of the main condensate channel.
- It is quite possible to observe both cavitation erosion and local erosion–corrosion mechanisms predominant in the process of wall thinning of throttling device components.
- Some of the existing and developed methods of cavitation erosion estimation along with the erosion–corrosion computational code RAMEK, one can solve practical problems on determination of the dominating mechanism of wall thinning and the causes of damage for components of pipelines and equipment of power plants operating with one phase water flows.

The U.S. Nuclear Regulatory Commission (NRC) has been keenly interested in both corrosion and flow-accelerated corrosion of piping systems. However, in recent times, the NRC has not exhibited an optimum level of interest in cavitation erosion. In their paper, Dr. David Alley and James Gavula from the U.S. Nuclear Regulatory Commission at The Corrosion 2014 convention held in San Antonio, Texas [25] threw some light on the following aspects of cavitation and the role of NRC to control and mitigate erosion:

- Practical application experience indicates that erosion occurs at nuclear power plants when they are close to the expiration of their original licenses in components that are in line for license renewal (long lived, passive components). The NRC has determined that the management of aging for this aging effect is very much essential.
- The NRC has decided to create a single management aging system for flow-accelerated corrosion as well as erosion. This is an outcome of successful use of the FAC aging management program adopted and fruitfully used by several plants.
- The differences between erosion and FAC essentially demands for significant changes to the traditional flow-accelerated corrosion aging management system. These amendments are necessary to acknowledge that there are ample chances of erosion occurring in pipes on a much larger scale than flow-accelerated corrosion. Along these lines, it can be noted that the response to components affected by erosion are more complicated in comparison to a similar response for FAC.
- The current guidance about cavitation suggests that cavitation will be discovered and resolved during the initial license period, and for up to 100 hours in a year it can be tolerated without evaluation. This appears to be inconsistent with the current operating experience.

Ozol et al. [26] have laid out the following list of the various problems with valves resulting from cavitation in NPPs:

- Physical damage to the valve and downstream piping. This is usually characterized by surface pitting and can lead to failure, similar to the case at the Surry Power Station Unit 2.
- Flow limiting. Choking the valve due to flashing. Besides the potential damage, flow limiting can change the valve and control system characteristics.
- Noise and vibration. Cavitation can cause noise and vibration. Excessive vibration can result in damaging the valve.
- Vibration damage to the associated equipment. Damage to the attached equipment and piping supports.

On certain occasions in NPPs, surveillance alone might not be helpful enough to detect the problems in the valves; hence, there is a need to watch for the following problem indicators:

- Valve maintenance. A history of frequent repairs is often an indicator of a cavitation problem. Field reports of valve problems are also an indicator.

- Abnormal noises. While all valves are noisy, cavitation problems are indicated by popping or buzzing noises or a sound as if gravel were flowing in the piping system.
- Vibration of the valve or attached piping. While some flow vibration is normal, excessive vibration usually results from cavitation.
- Signs of piping support damage near the valve. Even if no other indicators are present, this may indicate cavitation problems but only at certain operating conditions.

Once the problem valves are identified, a systematic inspection methodology can be planned out. An effective technique at Commonwealth Edison has been the spectral analysis of vibration measurements made on valves suspected of having issues. Control valve cavitation is one of the most difficult problems faced by operational nuclear plants and is a source of major operational and maintenance cost. In most cases, the conditions that produce cavitation can be predicted with current analysis methods, but providing a working solution is often difficult and expensive. To avoid the costly plant shutdown associated with cavitation-induced failure and to ensure continued plant operation, efforts to monitor and inspect as well as repair damages in severe duty valves and piping are vitally important. Such efforts are a part of the nuclear utility industry's practice.

In their study on cavitation, Isaka et al. [27] performed cavitation tests for the same types of cylindrical orifices that are currently being used in the NPPs. The cavitation parameters at inception downstream of orifices and inside the orifice were clarified. It was also confirmed that neither the length nor the diameter of an orifice affects the inception, and the design criteria for prevention of cavitation erosion has been determined in their article. Cavitation erosion found in a cylindrical orifice with the hard material used at plants was actually obtained in the erosion tests that have been performed and the validity of the criteria has been justified.

Chinese researchers Ma et al. [28] researched the wall-thinning mechanism of three different carbon steel pipes and reported the following in their paper:

It was observed that the cause of wall thinning in the elbow of the first pipe was due to erosion corrosion. This erosion corrosion was attributed to a high flow rate inside the pipe and low chromium content of the steel material. The solution, which was explained, talked about increasing the diameter of the pipe or by lowering the flow rate. Improving or increasing the chromium content is also a solution, but it might not be the ultimate solution for the said problem.

For the second elbow in another pipe, the wall thinning was attributed to FAC due to the low chromium content in the steel. A couple of ways this problem can be addressed is by controlling and monitoring the properties of the fluid like pH, temperature, oxide content, etc.; however, a more practical approach would be to increase the chromium content for the material or to try to use other materials with optimum chromium content so that they do not get affected by FAC.

The orifice of the third steel pipe observed crevassing due to cavitation. The approach to solve this issue can be redesigning the orifice with attention to diameter and length of the bore to adjust and be effectively functional to the fluid conditions.

1.9 Conclusion

Cavitation corrosion causes serious design and service problems for practicing engineers. This wear mechanism, if left un-checked, can rapidly reduce the life of a part. However, consideration and regular examination and maintenance of these kinds of effects during the design stage can reduce and possibly eliminate the effects of these forms of corrosion. Cavitation erosion causing wear and tear in machine parts and industrial appliances can in turn affect the productivity, the capital of a project/industry, and its impact on the people who depend on the machines. Hence, a routinely timed quality check and design assurance analysis must be performed on the cavitation erosion parts to keep up with its maintenance and prevention of the wear. It is not appreciated by industry to lose money on parts and machinery due to

cavitation erosion. Thus, it should be controlled and minimized. A dedicated team of engineers with an understanding of the situation and a sincere approach to check and control cavitation can really yield good results, which in turn is beneficial for everybody as a whole.

2. LIQUID IMPINGEMENT EROSION

2.1 Introduction

Liquid impingement erosion (LIE), often termed as liquid droplet impingement (LDI), can be defined as a gradual or progressive degradation of the parent material from a solid surface as it is continuously exposed to impacts of liquid droplets or micro jets. Impingement by liquid droplets or jets causing repetitive collisions between the discrete liquid drops and the surface that degrades due to the impact. However, this broad definition does not take into account the various other erosion mechanisms arising from these impacts. Examples, such as continuous jet impacts, single-phase liquid flow over the surface, cavitating flow, or progressive material loss due to a jet flow containing solid particles, are all methodologies that are responsible for causing erosion under certain situations.

Impulsive contact pressures are created on the target solid surface by the discrete liquid droplets from the micro jets, the impacts of which are more extensive than those generated by steady flows. Hence, the yield strength and the limit of endurance can be exceeded, resulting in damage because of mechanical interactions. Conjoint chemical interactions also cause material loss and degradation in under certain circumstances. At very high velocities, a single liquid droplet can induce material loss from the surface. In advanced stages, erosion due to liquid impingement shows surface features that appear jagged, and are composed of sharp peaks and pits [29].

The major source of most erosion is the water entrapped in the flow of steam and the non-discharged condensate moving at very high speeds. The recurring impacts of impinged flowing water jets induce progressive wall thinning at the bends and fittings of pipes. These water jets, due to their mass and higher impact velocity, create the damage, which is analogous to that of water jet cutting [30].

2.2 First Principles of Liquid Impingement Erosion

LIE can be defined as a gradual or progressive degradation of the parent material from a solid surface as it is continuously exposed to impacts of liquid droplets or micro jets. Impingement by liquid droplets or jets causing repetitive collisions between the discrete liquid drops and the surface that degrades due to the impact. Impulsive contact pressures are created on the target solid surface by the discrete liquid droplets from the micro jets, the impacts of which are more extensive than those generated by steady flows. Hence, the yield strength and the limit of endurance can be exceeded, resulting in damage because of mechanical interactions. Conjoint chemical interactions also cause material loss and degradation under certain circumstances. At very high velocities, a single liquid droplet can induce material loss from the surface. In advanced stages, erosion due to liquid impingement shows surface features that appear jagged, and are composed of sharp peaks and pits [29].

Also, Crockett and Horowitz [2] suggested that high-speed liquid droplets impacting upon a solid surface lead to loss of material from the surface, thus inducing liquid impingement erosion. When there is a high drop in pressure in the two-phase stream of a flow, for instance over an orifice on a pipeline to the condenser, LIE is observed. Consequently, such high-liquid velocity causes rapid acceleration leading to a situation where the impact of the liquid on a metal surface shall lead to surface degradation.

2.3 The Phenomenon of Liquid Impingement

It has been found that carbon steel substances suffer damage when liquid droplets travelling at speeds more than 100 m/s strike against the surface. In the case of flashing erosion mechanisms, the fluid is considered to be of low quality as the majority of its composition is liquid with some amount of steam. Alternatively, for LIE the fluid is considered to be of superior quality as it mostly composed of steam

with very little liquid. Also unlike flashing erosion, LIE damages make the affected surfaces irregular and rough.

In a turbine, when work and steam are separated, the pressure falls down to such a point where the droplets start nucleating and begin to travel downstream. A portion of the liquid droplets cause impacts and become hooked up to the low-pressure stationary blades of the turbine. Some of the water also becomes re-entrained and goes downstream. Some serious investigation has confirmed that the larger re-entrained droplets are responsible for the majority of the damage caused, but there is no such mechanism in the downstream flow of an orifice or valve.

During the 1940s, it was found that heavy raindrops damaged the metallic front-facing parts of military aircrafts that travelled at speeds greater than 350 mph. The significant areas of concern included windshields, canopies, and radomes. Due to the requirement of transparency to light and radio waves of these materials, non-metals have mostly been used for this purpose [2].

2.4 Liquid Impingement Erosion in NPPs and Other Areas

Four primary methods exist in which LIE causes damage and degradation of materials based on the means of material removal: direct deformation, stress wave propagation, lateral outflow jetting, and hydraulic penetration [31].

Undoubtedly, one of the world's most phenomenal forms of energy is nuclear energy. The fluid flowing in the main pipeline of a nuclear power plant is of high-temperature, pressure, and velocity. It is very essential to ensure the safety of the main piping system in an NPP. Due to the presence of these fluids at higher temperatures, pressures, and speeds, material loss occurs in the form of erosion corrosion and jet impingement erosion due to the impact of highly subcooled coolant on the reactor assembly and fuel rods. The main pipe through which the coolant flows carries with it particles that cause physical wear and tear, chemical corrosion, FAC, erosion corrosion, and many more surface degradation mechanisms. All of these can eventually lead to a rupture the main pipeline. Yao et al. [32] studied and found that both austenitic Stainless Steel 304 and 306 exhibit very high resistance to corrosion. These materials also have good resistance to higher temperature. Such superior resistances make the suitably of these materials usable in a variety of industries like aeronautical, aerospace, marine, and nuclear applications. The primary and secondary pipelines of NPPs are mostly built out of 304 and 316 austenitic stainless steels.

Upon further experimental analysis of the 304 and 316 stainless steels, Yao et al. studied the various operational conditions of high-velocity jet impact. They came up with the following observations:

- Both the 304 and 316 stainless steels exhibit linear variation of mass loss per unit area, irrespective of the sand effect, if any. This confirms that the erosion under the jet impingement erosion is steady in nature.
- 304 stainless steel has a greater erosion rate than 316 stainless steel.
- As particle size increases, greater is the effect of erosion on mass loss for both 304 and 316 stainless steels.
- Material loss due to erosion is greater in the case of quartz sand than sea sand for both 304 and 316 stainless steels.
- Higher particle concentration contributes more to the loss of mass due to erosion than particle size. This is true for both 304 and 316 stainless steels.
- Formation of ploughing or microcutting along the flow direction marks the erosion features for both of the materials.

In other research, in work based on several erosion tests comparing cavitation erosion and LIE, Hattori and Takinami [33] inferred that erosion by both cavitation and liquid impingement has certain

identical features such as incubation, acceleration, and maximum rate stages. For both LIE and cavitation, the maximum depth of erosion rate is tentatively determined when a straight line passes through the origin. Thus, the correlation between these erosion rates tends to be quite high. Fatigue helps in propagating the erosion mechanisms for cavitation and LIE. This indicates that asperities, which are found at the crystal grain boundaries, are formed due to plastic deformation. Hence, those areas generate greater stress concentrations, thus resulting in material degradation and the formation of cracks due to fatigue.

Some Japanese researchers (Ikohagi et al. [34]) suggested and analyzed various methods and models as to predict and study the wall thinning phenomena due to LIE. Measurement of parameters such as velocity, diameter, and number density of liquid droplets were performed by techniques involving light (optical) inside a spray-jet type of apparatus. This assisted in the understanding of the relationship between droplet parameters and the rate of erosion. Thus, it was found that the rate of erosion could be characterized by the velocity of the droplet as well as its parameters.

Numerical analysis confirmed the following aspects of LIE:

- The liquid film on the surface of the solid causes a depreciating effect. As a result, the pressure at impact is affected, which confirms the fact that the effect of LIE erosion is reduced due to the wetness of the solid surface.
- Due to multiple and repeated liquid droplet impacts, as the surface of the solid becomes rough, the erosion rate due to LIE increases. This indicated that dented or disturbed surface morphology enhances the effects of particle pressure at the point of impact.

Along those lines, using multiple laser pulses by means of laser shock method processes like exfoliation, the mechanical fatigue of an oxide layer formed on carbon steel was studied. The yield strength appeared to be more or less equivalent to the strength of exfoliation. Such minimal variation in strength indicated a higher mechanical fatigue cycle.

The authors suggested an oxidative thinning model according to which the oxidative rate of thinning is directly proportional to the square root of impingement frequency. On the other hand, the mechanical model of thinning shows that the mechanical rate of thinning varies linearly with the impact frequency. Hence, it became evidently conclusive that the mechanical model can be used for LIE tests in laboratories as the mechanical damage is seen to occur mostly at higher frequencies of impact. However, for a real-life system as well as fretting testing in laboratories, the oxidative thinning model could be used as it is effective at lower frequency levels of impingement.

Visual investigation revealed that piping without an orifice has a lower LIE risk than that of a piping system with an orifice. This is because of the existing liquid film in the upstream of the orifice, which results in the formation of larger sized droplets and misty flow of the jet.

Li et al. [35] conducted experimental investigation by performing computational fluid dynamics (CFD) analysis of a single-impacting, high-speed liquid droplet impingement onto a rigid wall and made the following observations:

- The evolution of liquid droplet impingement greatly depends on the compressibility of the liquid medium. Solutions to the fluid dynamics continuity and momentum equations determine the formation and propagation of the shock waves.
- It was confirmed from numerical calculations that the maximum critical pressure was highest at the point before jet eruption and after the angle of contact, and not at the center of the droplet contact on the surface. They also proposed a droplet impact angle, which could be essentially helpful for global liquid droplet impingement study and monitoring.

There are certain limitations that came out of their study. As LIE is a three-dimensional (3-D) process, the calculations associated with it should also be done in 3-D space. The damage to the wall

needs to be taken into account based on the solid elasticity concept. Moreover, during impingement it is essential also to consider the droplet film effect during impact.

In an analysis of causes responsible for wall thinning and leakage, Hwang et al. [36] studied and exemplified the leakage of a 1-inch small bore piping, which branched from the main line. The leakage was due to wall thinning in a 1000-MWe PWR NPP in Korea. Hence, a control valve, which had a vertical flow path, was placed in front of the orifice. Several commonly used analytical methodologies were performed on the small-bore piping. These methods included ultrasonic testing (UT) thickness measurement, visual investigation, scanning electron microscopy (SEM) imaging, and numerical analyses. Multiple and repeated liquid drop impingements to the pipe wall was found to be the reason behind the leakage. However, the leakage did not occur at the point where there was maximum frequent impingement (i.e., behind the orifice). Instead, the leak occurred most probably to downstream from the orifice, near the vortex flow reattachment point. This clarifies and throws light on the fact that even though the main piping system contains dry steam, it can still be affected by wall thinning from liquid impingement erosion.

Fujisawa et al. [37], in their study on the wall thinning rate of deep erosion by LIE, found that as the depth of erosion increases, the rate of wall thinning decreases. This mainly attributed to two reasons: the damping effect of the liquid film on the rate of wall thinning, and the impact of the side jet of the LIE. The model proposed to study wall thinning of deep erosion brought in an attenuation factor, which also has a function of the depth of erosion. The attenuation factor helps to provide a more accurate correlation of the uniform erosion rate.

In an experimental analysis, Hattori and Lin [38] calculated the volume loss per liquid droplet by using several experimental methods, namely rotating disk method and high-pressure test method. On further detailed analysis of the obtained data points, it was found that the loss of volume per liquid droplet increases at approximately 4.67th power of the droplet diameter. In another study, Hattori and Kakuichi [39] studied the effect of impact angle on LIE induced erosion. They conducted tests, namely jet nozzle tests and spray nozzle tests that provided different results. The jet nozzle tests concluded that the maximum depth of erosion by LIE for many types of steels can be given by $sin\theta^n$. The spray nozzle tests provided information on the rate of mass loss by the following equation:

$$V = V_0 \sin\theta \tag{3}$$

where V_0 is the flow velocity and θ is the angle of impact. At acute impact angles, the liquid film is extremely thin and is destroyed easily, causing erosion. However, when the liquid strikes the surface at 90 degrees, a thick water film is observed, reducing erosion.

Furthermore, Fujisawa et al. [40] conducted research on LIE experimentally by using high-speed spray for liquid droplets having a diameter in the range of some tens of micrometers. This size corresponds to the prototype pipeline condition of NPPs. Various properties of the droplets, such as velocity, diameter, and number of impacting droplets, were measured using different methods like particle image velocimetry, shadowgraph, and sampling probe, respectively. High-speed spray tests showed that the maximum rate of erosion happens to exist at a particular distance from the exit of the nozzle. The tests revealed that the rate of erosion is a function of the droplet velocity to the power of 7.0 for maximum rate. This was a deviation from the previous study of 4.8 where the droplet size was 1 mm. Thus, it was confirmed that the erosion rate is dependent on the diameter of the impinging liquid droplet.

Choi et al. [41] designed an experimental system where they studied LIE effects on materials under an extensive period of time and under severe conditions. For carbon steels, the erosion rates are directly proportional to erosion time. However, it was found that for aluminum, the erosion rate becomes saturated with time. Aluminum exhibits the formation of localized pores, whereas carbon steels show initiation of line cracks. There was hardly an effect on the mechanical hardness of aluminum, but carbon steels saw a phenomenal change in their hardness. The formulation and calculation of erosion rates as per air-to-water

ratios, both for aluminum and carbon steel, shall help manage, mitigate, and monitor LIE-induced damages in plant industries.

Fujisawa et al. [42] used a high-speed conical spray to study LIE under the condition that the specimen size is less than the diameter of the spray. It was concluded that as the specimen diameter decreases, the rate of erosion increases. Along the same lines, the erosion rate also increases with increasing standoff distance. Hence, by combining their experimental data along with theoretical information regarding liquid film, it was inferred that as the liquid film thickness decreases, the erosion rate increases. Here, the LIE erosion has been predicted in terms of the thickness of the liquid film.

Continuing the remarkable work in LIE, Fujisawa et al. [43] conducted some experimental analyses to observe the variation of erosion rate in the terminal stage of erosion with the thickness of the liquid film. Hence, it was found that rate of erosion decreases with increase in the thickness of the liquid film as well as Vickers hardness number. The fundamentals of LIE like velocity of droplet, local volume flux, Vickers hardness, and the liquid film thickness, were perfectly correlated to the experimental rates of erosion that were obtained from the study. Experimental erosion rates varied within a factor of 1.5 with the predicted erosion rate, which determines the accuracy of the experimental investigation and hence the authenticity of the results. Furthermore, research has been done by Fujisawa et al. [44] by incorporating certain critical considerations on the rate of wall thinning of metals due to LIE. Several researchers over the world have come up with different power indices as far as the velocity of the droplets is concerned. However, when factors like the erosion mechanism, the thickness of liquid film, and the accuracy of the measured velocity are concerned, the values of the indices come to be consistent varying in the range of 6-to-8-in. water jet and spray jet tests. However, in a rotating disk test, the value was found to be a little lower (around 5.8), which is quite close to the theoretical value of five. Such differences in the velocity indices are observed because of the impact of the thickness of the liquid film, which is instrumental in determining these higher power indices in the tests conducted for wall thinning prediction in real life plants.

Ohira et al. [45] conducted a study for predicting liquid impingement erosion trends in actual NPPs. They made use of an evaluation system in CRIEPI, for monitoring liquid droplet impingement in the fourth heater vent line in Tokai-2 NPP in Japan. It was determined that the ratio of maximum thinning rate to that of average thinning rate was related to the average thinning rate. The evaluation system excludes the average thinning rate, and thus the relationship maximum/average was used and the maximum thinning rate could be calculated. Thus, it showed that experimental maximum thinning rates matched the measured value. This LIE evaluation system could be used in actual NPPs to predict and monitor liquid droplet impingement.

A study performed by Nicolici et al. [46], presented the idea of modeling and simulating fluid-structure interaction occurring in liquid droplet impingement erosion. Their study was based on determining the fluid-solid interface pressures and the transferring of the plastic energy from liquid droplet to solid. Thus, they proposed a new technique of computational analysis as a new perspective, which would assist to figure out the resistance to erosion of materials undergoing LIE damage. It was concluded from CFD simulations that the maximum pressure at 90 degrees impacting the interface was almost three times greater than the water hammer pressure. This maximum pressure induces material degradation by causing loss of surface material. It also proves that tangential velocity has almost no effect on the LIE damage as the liquid droplet is easily deformed by the solid surface. Tangential velocity could only be significant if the surface is very rough and if the height of the roughness is more than the thickness of the liquid film formed on the surface. This method can be used for evaluating the damage due to erosion in cases of ductile materials where the damage is caused due to continuously increasing plastic deformations. However, for brittle fracture, when the surface cracking occurs with accumulation of cracks in the subsurface level, it results in material removal from the surface.

P. Veerabhadra Rao and Donald H. Buckley [47] proposed some empirical relationships for cavitation and liquid impingement erosion processes. The rotating disk test gave certain data points, which were represented by power-law relationships. The acceleration zone equation is expressed as:

$$V/t = AV^n \tag{4}$$

where V is the cumulative volume loss (in mm^3), t is the exposure time corresponding to V (in minutes or hour), A is a constant depending on the material, and n is an exponent determined empirically. According to their study, this empirical power-law relationship between the rate of erosion and volume of erosion described the acceleration and deceleration zones of erosion.

2.5 Conclusion

In concluding lines, liquid particles or droplets under high velocity and pressure cause tremendous impact on the surface of solid materials like metals, plastics, etc. Generally, LIE tests are conducted to test the resistance of materials. This is useful in working process applications where solid surfaces are exposed to continuous repeated strikes from water jets [48]. Normally, choosing the right kind of material with higher resistance can sometimes help to solve the problem in fluid machineries. Moreover, the techniques and methods discussed above by various researchers can be used to monitor, manage, and mitigate erosion mechanisms. Overall, even if there are proposed methods to tackle erosion due to liquid droplet impingement, none of them can be considered as a silver bullet technique to solve the surface damaging issues. Hence, further studies and experiments need to be performed to keep discovering new and better ways to handle the damage caused by LIE impacts.

3. SOLID PARTICLE EROSION

3.1 Introduction

Similar to cavitation and liquid droplet impingement, there is another erosion phenomenon that consists of a very typical process of wear caused by virtue of material loss resulting out of repetitive impingement or impact of small solid particles, which is known as Solid Particle Erosion (SPE). When a liquid or gas medium entraps hard particles, which then get impacted onto a solid surface at a high velocity, this causes solid particle erosion. When SPE occurs, the solid particles undergo acceleration or deceleration, and the fluid impacting has the plausibility of changing their directions of motion. SPE acts as a useful phenomenon in the case of sand blasting and water jet cutting under high-speed abrasive water. However, SPE can cause serious problems in several process applications in industries like steam and jet turbines, piping systems, valves carrying particles, and fluidized bed combustion systems. SPE involves various processes. Mechanical impact, being the primary process, is caused by the impact of solid particles on the target material. There are also certain secondary processes, such as thermal, chemical, and physical interactions, within the counterparts during the wear mechanism. The failures of mechanical components undergoing erosion and the decreased life span have led to research and studies for a better understanding of the SPE wear phenomenon [49].

3.2 First Principles of Solid Particle Erosion

A particle of solid, flowing along or carried by a fluid, which impacts the target material causes solid particle erosion. The kinetic energy of the high-velocity particles is distributed through ductility, fracture, heating, transformation of phases, etc. The medium of energy dissipation is determined by the target surface, nature of particle, and the operating factors. The behavior of any material undergoing solid particle erosion is most likely to be of two types: brittle and ductile. When the maximum kinetic energy of the particle is transferred to the target surface on impact, and eventually is distributed by formation, propagation, and intersection of crack, it is known as the brittle form of SPE. Generally, this causes the loss of material when the angle of impact is 90 degrees, or normal to the surface. On the other hand,

ploughing or cutting mechanisms arising out of plastic flow cause ductile SPE. In this case, the maximum material degradation occurs at a low incident angle, between 20 to 40 degrees [50].

According to Patnaik, A. et al. [49], similar to cavitation and liquid droplet impingement, another erosion phenomenon consists of a very typical process of wear caused by virtue of material loss resulting from repetitive impingement or impact of small solid particles, which is known as solid particle erosion. When a liquid or gas medium entraps hard particles, which then get impacted onto a solid surface at a high velocity, this causes solid particle erosion. When SPE occurs, the solid particles undergo acceleration or deceleration, and the fluid impacting has the plausibility of changing their directions of motion.

3.3 An Introduction to Solid Particle Erosion in NPPs

Crockett and Horowitz [2] investigated various erosive mechanisms in NPPs and found that for solid particle erosion, the damage is caused by solid particles that are transported by the fluid stream rather than by collapsing cavities and liquid water droplets. The primary reason behind the SPE mechanism is the bombardment of hard, large solid particles against the surface of the material with significant high velocities. Solid particle erosion mechanism has the following manifestations:

- Thinning of components
- Gas or particle flow field generates a scooping like appearance
- Variable surface morphology from polishing to severe surface roughness, but this is dependent on particle diameter and velocity of the particle
- Direction-less, grooving nature of abrasion
- In few occasions, ripple pattern generation on metals.

Solid particle erosion has affected several industrial engineering applications over the years. Some of the major, more severe areas are:

- Steam turbines
- Rotors of helicopters
- Gas turbines
- Valves and piping systems that carry particulate material
- Boilers of the fluidized bed type
- Rocket motor nozzles.

As far as NPPs are concerned, SPE is predominantly observed in the blow down system of the steam generator in PWRs, and also in the case of raw water systems. Moreover, solid particle erosion has been shown to cause damage to valve internals and leakage in piping systems.

3.4 Mechanism of Solid Particle Erosion

Solid particles cause solid particle erosion, flowing along or carried by a fluid, which impact on the target material. The kinetic energy of the high-velocity particles is distributed through ductility, fracture, heating, transformation of phases, etc. The medium of energy dissipation is determined by the target surface, nature of particle, and the operating factors. The behavior of any material undergoing solid particle erosion is most likely to be of two types: brittle and ductile. When the maximum kinetic energy of the particle is transferred to the target surface on impact, and eventually is distributed by formation, propagation, and intersection of crack, it is known as the brittle form of SPE. Generally, this causes the loss of material when the angle of impact is 90 degrees, or normal to the surface. On the other hand,

ploughing or cutting mechanisms arising out of plastic flow cause ductile SPE. In this case, the maximum material degradation occurs at a low-incident angle, between 20 and 40 degrees [50].

3.5 Solid Particle Erosion in NPPs and Various Materials

Branco et al. [51], in their study regarding the solid particle erosion of ceramic coatings, gave certain interesting ideas about the ways porosity affects the erosion process. First, as the material near the edge of a void does not have a mechanical support, porosity reduces the strength of materials against plastic deformation. It can then be noted that the particle impacts the concave surface inside the void, at an angle that is greater than the usual impact angle, which is made on the target surface of the material. This is good for ductile materials, but damaging for brittle materials. Finally, porosity decreases the strength of a material as it induces stress concentrations and eventually impairs the impact load surface.

Upon studying resistance to solid impingement, Satapathy et al. [52] found that an industrial waste known as redmud could be used effectively as a resistant material to sustain SPE. A solid particle entrapped by flowing fluid, upon impact of the target surface causes severe damaging effect to the material and induces erosion. They studied the erosive behavior of plasma sprayed redmud coatings after exposing them to jet air solid particle impingement. Redmud has shown substantial resistance to SPE; hence, it has been used as the coating material in several tribological applications. The erosion wear rate was investigated and they concluded that the rate of wear was smallest at an acute impact angle of 30 degrees, and it was largest at 90 degrees of impact angle. Thus, it was observed that the net loss of mass due to solid particle impingement with due course of time of impact could be evaluated by varying the angle of impingement.

Researchers Levin et al. [53] suggested a model for ductile alloys undergoing SPE. Their proposed model not only takes into account the mechanical properties under the conditions of deformation when SPE occurs, but also the development of such properties when deformations are induced by virtue of solid impingement erosion. In their study, they analyzed the deformation behavior and the resistance towards erosion of certain ductile alloys such as nickel, cobalt, and iron. Energy loss analyses helped to generate a factor based on erosion and it revealed better dependence on rates of erosion obtained from experiments. Materials exhibited better resistance to erosion, which at high-strain rates have higher tensile toughness and hardness. Hardness significantly decreases the transfer of energy form the impinging particle to the target material and toughness characterizes the tendency of the material to absorb the energy without undergoing fracture.

Laguna-Camacho et al. [54], in their investigative study on different metallic materials, tested Aluminum 6061 and Stainless Steels 304 and 316. At room temperature, Aluminum 6061 exhibited superior erosion resistance than that of 304 and 316 stainless steels. It was found that at greater impact angles such as 60, 75, and 90 degrees, the rate of erosion was significantly reduced as compared to the maximum rates of erosion at lower angles of incidence like 30 and 45 degrees. However, stainless steels 304 and 316 showed considerably greater material degradation at 60 degrees. Specifically, in this study, the researchers observed the following kinds of erosion induced wear features affecting the surface morphology. They are ploughing, pitting, scratches, irregular indentations and peaks, craters, fragments due to abrasion, and smudged debris from wear. Cracks that formed at random locations led to brittle fracture. At low-incidence angles like 30 degrees° and 45 degrees, the damage from wear reflected an elliptical shape. On the contrary, an almost circular shape was seen in cases of the impact angles 60 and 90 degrees.

Research work by Arabnejad et al. [55] developed a semi-mechanical erosion correlation to figure out the erosion of different metallic materials. The relation had two aspects. One was to determine the cutting erosion that was characterized by the impacting solid particles as they cut through the surface of the target material at various impinging angles. The second relation was deformation erosion that occurred by virtue of repetitive collision of particles at 90 degrees to the surface, thereby resulting in platelet generation and eventual surface failure. Micrographs from scanning electron microscopy showed the differences between

such erosion methods. Indented rough surfaces denoted the case of a 90-degree impingement of particles, whereas lengthy craters were seen when the particles were incident at grazing angles. It was also reported that this relationship could be used for varieties of geometries and materials to evaluate the damage due to erosion by using it in CFD analysis and particle tracking codes.

Islam et al. [56] studied the effect of microstructure on erosion in the case of carbon steels like AISI 1018 and AISI 1080. The conclusions that resulted have been mentioned below:

- For AISI 1018 and 1080 steels, the erosion rate goes down as the impact angle increases, but the rate of erosion tends to be higher as the particle velocity increases.
- At impact angles 45, 60, and 90 degrees, the erosion resistance increases significantly for AISI 1080. On the other hand, AISI 1018 steel shows higher resistance to erosion at low acute impact angles like 30 degrees.
- High-angle particle striking creates certain erosive features like flat ridges and fractures that cause loss of material, whereas small angle impingement creates erosion mechanisms of ploughing and low-angle metal cutting, which are predominant.
- Owing to its lamellar structure, the pearlite phase has a higher resistance to erosion than the ferrite phase. At the same time however, when the impact angle is small, the embedded Al_2O_3 has greater erosion resistance than the pearlite.
- Even AISI 1018, at a low-impingement angle, exhibits better erosion resistance as it is low on hardness and has more embedded particles. Pearlite displays the maximum resistance to material loss and surface damage if the plate is at a 90-degree orientation to the incoming impacting solid particles.

While conducting extensive research on stainless steel, Shimizu et al. [57] studied the impact and mechanical behavior of SPE on alloys of stainless steel at higher temperatures. Two types of stainless steels were considered: SUS403 and SUS630. These two steels were subjected to high-temperature erosion tests, tensile tests, and also high-temperature hardness tests. It was found that material loses its hardness and tends to soften at higher temperatures in case of high-temperature erosion. At a normal angle of incidence, it was observed that the percentage decrease in hardness varies directly with the rate of erosion. One significant inference drawn from this study was that at a lower angle of impact, the material that exhibits a greater elongation shows protrusion easily and is eventually removed by continuous erodent impingement.

A modified, better way of understanding erosion wear was suggested by Siddhartha and Bisht [58]. They suggested a mathematical model, which considered both the vertical and horizontal components of the impinging velocity of the particle corresponding to the plane of the target material. Incorporating the physical dimensions of the erodent particles showed that the rate of erosion remains constant. The idea of using the mathematical model to evaluate the erosion rate produced a contradicting outcome. It was generally observed that dimensions of the erodent particle also influence the angle of impact. However, in a real occurrence for a given dimension, the erodent particle can cause an impact at any angle. Hence, the opposite approach is not applicable. Under this model as proposed, the erosion rate varied from the 0-15% on the error scale. Furthermore, the superiority and accuracy of this model was more cemented when it was found that for a 90-degree impact angle, the error percentage ranges from 1 to 15% unlike the previously studied models where it was as high as 33%.

An analysis and study of solid particle erosion from an impact zone perspective by D. R. Andrews [59] inferred certain new aspects regarding the wear phenomenon. Measuring flux at the point of impact was studied to determine the average rate of arrival of particles on to the impact zone. Flux can be measured in terms of mass per unit area per second, average particle size, and the average mass of a single particle. One more conclusion was the knowledge regarding incubation times, which means that erosion is a cooperative process. Incubation times could be evaluated by cooperative melting, which is

also instrumental in determining a threshold value for flux to initiate erosion. Along those lines, deformation and delamination wear also helps to predict incubation times.

Some the most important and significant contributions to the study of erosion mechanisms has been done by I. Finnie. Finnie [60], in his study on solid particle erosion suggested that the surface wear due to SPE is based on two parameters:

- Motion of the solid particles entrained in the fluid.
- Behavior of the surface of the target material under impact.

Considering these two factors, it became clear that the surface roughness induced due to erosion makes the fluid more turbulent and thus speeds up the material loss process.

H. M. Clark [61], from his experimental study on impact rate and impact energy of solid particles, brought out the role of viscosity in SPE—as the viscosity of the liquid carrying the solid particles increases, the velocity of impact decreases significantly. This happens because smaller particles have lower inertia than the bigger particles. Furthermore, an increase in viscosity reduces particle size and lower velocity reflected a decrease in the collision efficiency. Therefore, there is a decreased rate of erosion because:

- Higher viscosity of liquid carrying solid particles
- Smaller particle size
- Lower speed.

These factors above mark the variations in eroded surface, flow interaction of liquid, and particles. Hence, there is a need for studying the particle trajectories for a better knowledge of erosion by liquid suspensions.

In further studies about slurry erosion regarding the particle size effect, Lynn et al. [62] made certain interesting conclusions. Their findings were:

- A smaller particle size ensured lower impact velocity and much less collision frequency.
- Rate of mass loss is directly proportional to the rate at which the kinetic energy is scattered for impacting particles of 100 μm and more.
- At a certain limiting erosion rate, the collision frequency approaches to one and the rate at which the particle tends to retard is low.
- From the tests conducted by Lynn et al., they found that for uniform particle size in a cylindrical erosion specimen, the circumferential erosion angle can help predict the collision efficiency.

Desale et al. [63], by virtue of their experimental investigations, concluded that at a certain minimum value of kinetic energy, the material removal methodology transforms from erosion to three-body abrasion. This process induces wear mechanisms through small-sized particles, and thus the wear rate is higher than that caused by larger particles. From the power law relationship (discussed above), it was observed that particles travelling at a kinetic energy less than the minimum value, the exponent particle size value is 1, whereas for greater values of kinetic energy for different angles of impact, the exponent value is greater than one.

Solid particle erosion effects on brittle materials, with focus on the interaction of SPE with the properties of material and the effect of the impact particle on wear mechanism, was studied by Wada and Watanabe [64]. The following inferences were reported:

- They studied gas pressure sintered Si_3N_4, PSZ, sintered SiC, and soda-lime silica glass. In these four materials, it was observed that there was significant dependence of the erosion rate on the particle-to-target harness ratio.

- One interesting finding was that the erosion rates varied from 0 to 10^{-4} cm^3/cm^3 for Si_3N_4 and PSZ and SiC, respectively. The variation in the rates of erosion was because of differences in the fracture toughness of the material.

Liebhard and Levy [65] conducted research on the effect characteristics of erodent particles on the erosion of metals, and thus the outcome is as follows:

- Particle size was instrumental in determining the erosion rate for spherical and angular particles.
- As particle size increases, the erosive nature of spherical particles also increased. This held true until a peak value after which it began to decrease, even though the particle size was still larger.
- Similarly, as the angular particle size became larger, the erosion rate also increased. At a certain point, the erosivity became consistent with size for lower velocities, but eventually, as the velocity increased, it increased progressively.
- Erosivity also depended on the shape of the particles.
- The erosivity of a stream of particles was characterized by: (a) size of the particle, (b) particle concentration on the target material at the point of contact (number of particles impacting the surface per unit time), (c) mass and velocity (kinetic energy) of the particle and lastly, (d) intervention between particles hitting the surface and those coming back after striking.

Considering the subsurface damage in SPE mechanisms, S. Jahanmir [66] reported certain inferences. They are:

- Ductile metals having second-phase particles can be characterized by structural changes like formation of micro-voids in subsurfaces and micro-crack nucleation.
- Voids are created due to contributing factors like velocity of the eroding particle and the angle of impact.
- Impact angle in the range of 15 to 20 degrees is the peak angle of impingement for ductile metals, which corresponds to the formation of voids.
- The number of voids formed depends directly on the impact velocities.
- Inter-particle spacing of the second phase particles and their number causes a substantial effect on the rate of erosion.

3.6 Conclusion

Solid particle erosion is a type of erosion that removes the material from a surface when a flow stream carrying solid particles impinge against the target material at a significant velocity and at some angle of incidence. Erosion in any form is not suitable or affordable for industries and practical applications. It is an expensive repair mechanism, but it cannot be avoided as well. In NPPs, there are flowing streams of fluid carrying various kinds of materials; sometimes liquid droplets causing liquid impingement erosion, and sometimes solid particles causing solid particle erosion. An NPP is one of the most critical power-generating sources in a country. Piping systems and valves for different purposes, and the materials with which these are made, define the structural outline of any power plant. Over years of relentless service and power generation, like every mechanical and functional component, piping systems and the valves also reach a fatigue point. At that point, they cannot be used further or it leads to rupture, breakdown, fracture, and cracks. It creates a serious matter of concern as the entire plant comes to a situation where it might have to be shut down, which in turn can ruin the life of millions of people. At the same time, the leakage of harmful chemicals to the atmosphere also poses a direct threat to human lives.

Hence, such an adverse situation can be tackled by periodic monitoring, diligent managing, and of course, designing thoughtful and practical mitigating plans. Therefore, the proper choice of material for

making the pipelines, studying and analyzing the erosion resistant behavior of various materials, knowing the mechanical behavior and properties of those materials are a few options that can help minimize the disastrous or sometimes catastrophic failure of pipelines in NPPs. Erosion, like friction in the physical world, is a necessary evil. Therefore, apart from studying metallurgy behind the materials for manufacturing, there is also a need to monitor the flow of the fluids. The concentration of particles travelling in a stream of flow also matters when it comes to minimizing erosion. Thus, it can be inferred that the damaging effect can be reduced by varying the velocity of the flow causing impact and the angle of impact. All in all, the overall consideration and proper channeling of resources can definitely help in reducing the material loss and surface degradation due to erosion in NPPs. Various organizing bodies, such as the Electric Power Research Institute (EPRI) and the NRC along with the U.S. Department of Energy (DOE), have provided several commendable efforts and have been instrumental in deploying new and efficient techniques so as to keep a continuous vigil on the longevity and life span of components undergoing erosion on a daily basis in NPPs.

4. FLASHING EROSION

4.1 Introduction

Flashing erosion originates when the pressure of a fluid decrease below its vapor pressure, while changing from a liquid to a vapor. This process involves small vapor cavities or bubbles, which are created that eat away or degrade away at the outlet of the control valve and its trimmed components. This sort of damage is earmarked by shiny, smooth gouges in material surface body [67]. In this stage, the fluid is converted from a liquid to a vapor, both of which have similar chemical composition and characteristics. The vapor pressure depends on the fluid temperature; therefore, flashing erosion is characterized by both the pressure and temperature of the flowing fluid. For the fluid to undergo flashing, heat transfer has to occur from the liquid while vaporizing and this phenomenon needs time [68].

4.2 First Principles of Flashing Erosion

Control valves that are predominantly used in applications involving fluids are prone to flashing or cavitation erosion. Flashing generally is initiated in the liquid flow when the internal pressure of the liquid not only is less than the vapor pressure, but also it continues to stay below it. This phase marks the formation of vapor cavities and liquid downstream flow velocity increases, thus resulting in erosion in valves and piping. It is known that pressure at the outlet valve and the fluid vapor pressure are not under the direct control of the valve; hence, the best way for the flashing medium is to decide on using control valves that minimize such effects [69].

4.3 How Flashing Occurs? – A Case Study

The end of cavitation marks the initiation of flashing when the pressure difference, $p_2 - p_v$, becomes less than or equal to 0 where, p_2 is the valve outlet pressure and p_v is the vapor pressure. Vapor cavities exiting the valve in the two-phase flow do not collapse, but remain intact (Figures 2, 3[a] and 3[b]) [69].

Figure 2. Visualization of flashing with flow coming from below [69].

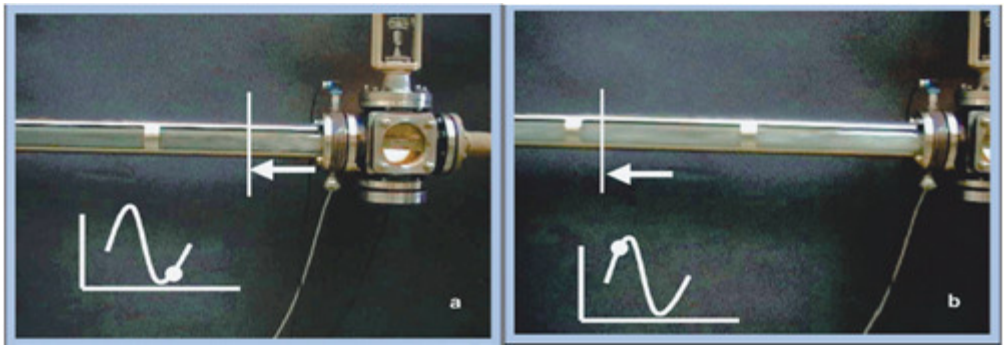

Figure 3. Propagating shock waves during flashing result in pipeline excitation (a) beginning shock wave, (b) ending shock wave [69].

As a result, there is a significant reduction in the density of the liquid-vapor mixture on the downstream side of the valve in comparison to the only liquid phase on the inlet side. This increases the average velocity of the flow. With flashing, the average velocity is a factor of the inlet velocity of the valve. For example from Figure 4, outlet velocity is close to 40 m/s, which is higher than the inlet velocity of 2 m/s. The higher the average flow velocity at the outlet of the valve, the greater is the imbalance between the liquid and vapor phases. From Figure 3(a) and 3(b) it can be clearly seen that the moving shock waves arising from the imploding bubbles. As a result, the entire pipeline responds and becomes excited to mechanical vibrations less than 10 Hz (i.e., low-frequency vibrations).

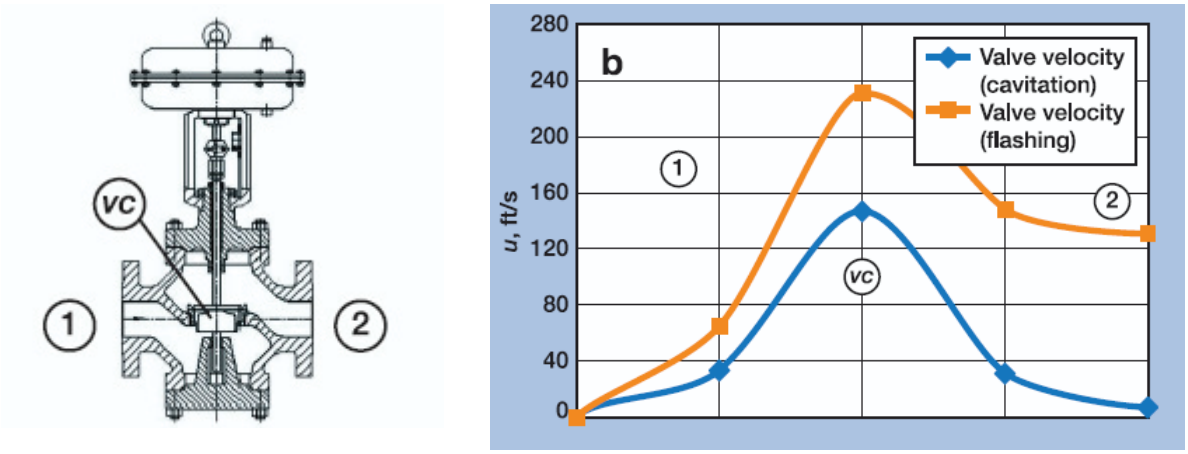

Figure 4. Pressure and velocity during cavitation and flashing (1) valve inlet, vena contracta (VC) and (2) valve outlet [70].

In the presence of a two-phase liquid and vapor mixture, during process applications when there is a higher pressure at the inlet side of the valve than the vapor pressure, the described effects are much intensified. Subsequently, flashing, which is a true two-phase flow, might create some serious problems like:

- Noise excitation. Figure 5 shows that the excitation by noise during flashing was at significant low levels.
- Intensive damage is caused by corrosive constituents to the valve components and pipelines by erosion by virtue of impact from the liquid droplets.
- The disturbance and imbalance between the liquid and vapor phase creates shock waves whose propagation from the outlet of the valve cases the excitation of the pipeline due to vibration (Figure 3[a] and 3[b]).
- The inlet side of the valve has a significantly low and choked flow rate in case of two-phase fluid flow.

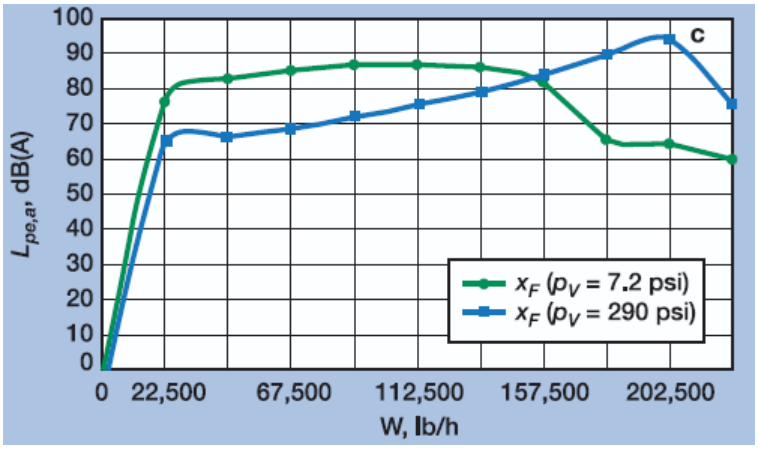

Figure 5. Typical refinery conditions for sound level [69].

4.4 Flashing vs. Cavitation

Flashing can be termed as a change of state when a liquid exiting an outlet valve has a pressure lesser than the vapor pressure of the liquid in its upstream, which leads to vaporization of the liquid. The liquid actually begins to flash at that point when there is the maximum drop in pressure and that occurs as the liquid medium tends to move through the vena contracta (VC) of the valve.

In case of flashing, unlike cavitation the downstream flow vapor stays there intact because the pressure at the outlet tends to stay below the vapor pressure of the liquid. As a result, serious degradation concerning a cavitating flow is often observed in a flashing pipe. Normally cavitation-induced damages are more severe and are more bothersome than the damage caused by flashing. On contact with the materials involved in processes, the high-speed flow and the moisture-entrained vapors result in maximum material degradation in case of valves and piping.

Mostly these damages are found in valve subassembly, in the trim, and wall of the valve. The degradation of the trim and the body of the valve is characterized based on the flow path and the saturation levels of the liquid near the inlet of the valve. Flashing caused damage, which has been observed to be smooth and polished in appearance. When left unattended over a period of time, such damages lead to loss of material to such an extent that it results in the low-performance ability of the material. The moisture contained inside the vapor also induces damage in the piping on the downstream side. If the affected valve is followed directly by elbows or fittings, the elbows also become quite severely damaged due to erosion.

There are few options, such as hardened materials, expanding outlet piping, and unobstructed outlet flow paths, that are available to counteract flashing erosion. The user will manage and monitor the flashing medium. Even though these methods are not very cost effective when compared to a standard trim design, they are essentially helpful in handling the flow [70].

4.5 Effect of Flashing Erosion on Flow

Flashing results in a choked flow. This is the maximum allowable or possible flow that can pass through the restriction under a particular pressure in the upstream. Such a phenomenon is termed as super cavitation. Increasing the upstream pressure, also increase the flow. At this condition, the velocity of sound is attained in the two-phase mixture. An analogy can be drawn as a gas passes through a convergent nozzle at sonic velocity. However, note that sonic velocity in two-phase mixtures contributes to a very minute fraction of the speed of sound as in a pure liquid or pure vapor phases. Flashing not only causes erosion but also creates unstable disturbing conditions in the downstream pipe. Under such conditions, harmful vibrations are created.

Normally cavitation occurs when the local vapor pressure is lower than the downstream pressure, resulting in implosion of bubbles or cavities. In the case of flashing, it is the opposite as the local vapor pressure is above the downstream pressure not to allow the bubbles to collapse; therefore, the bubble will move downstream. Even if cavitation can be prevented by changing the design of the control valve, it would result in the downstream pressure to be lesser than the vapor pressure of the incoming stream, which will eventually cause flashing. In most occasions, flashing generally occurs on the downstream of valves or orifices in liquid pipelines that connect the condenser. Flashing is also seen in the downstream of valves in the case of cascading drains. There are few other probable locations, such as the downstream of valves. Valve manufacturers install erosion-resistant materials to address flashing in valves, which are expected to face severe erosion, including flashing in the downstream part of valves. However, flashing erosion in piping is not even addressed unless there is a leak or a rupture in the pipe [2].

4.6 More about Flashing

When the vapor pressure in liquid applications is equal or greater than the local downstream pressure, the vapors in the VC remain intact and do not implode. Such a regime is observed because the recovery of

the pressure difference is quite high. Figure 6 shows such a phenomenon called flashing. During flashing the vapor liquid mixture has a higher moving velocity, which causes damage in the valve in the downstream piping (Figure 7) [71].

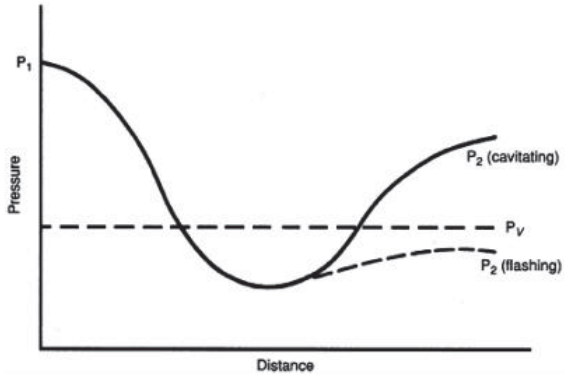

Figure 6. Pressure curve showing outlet pressure below the vapor pressure, resulting in flashing [72].

Figure 7. Plug damaged by flashing [72].

4.6.1 Controlling Flashing

If flashing could at all be completely eradicated, then that would require modification to the system as a whole, most likely the local pressure or the vapor pressure of the fluid. However, this option is not entirely feasible and reliable in the majority of the systems. Another option is to consider the location of the valve if the valve exits downstream in a bigger vessel, condenser, or a tank. In this case, the placement of the valve is significant. On that note, if the valve is placed closer to the larger vessel, then the flow will impinge a greater volume of the vessel that is separate from any critical surfaces. Practical analyses and utility have proven that any particular solution cannot be designated in the design of the valve. For instance, in cavitation control trim, the only plausible solution is to use hardened trim materials [71].

In a discharge stream, if the flashing steam is not well handled, then it is a matter of concern in the condensate recovery piping as it becomes more prone to erosion. Condensate piping is responsible for transporting the condensate. However, during this transportation, if flash revaporization occurs, then it results in an atmosphere that is identical to t wet steam flows at a high velocity inside the steam distribution pipeline. This type of liquid droplet impingement erosion is also known as “flashing erosion.”

Flashing erosion is aggravated by two factors:

- High velocity of the flash steam (also known as water-cutting effect, which is a result of undersized condensate return lines)
- Low-temperature condensate can be related to corrosive substances like carbonic acid [30].

Flashing is a single-stage process that is similar to cavitation, but differentiated because the downstream local pressure does not make an optimum recovery to be more than the vapor pressure of the fluid. Hence, vapor bubbles in the liquid remain as vapors and there is no implosion or collapsing. As only a certain part of the fluid undergoes vaporization, the remaining downstream flow in the valve exists in two phase (i.e., vapor and liquid). Flashing is not as severe as cavitation. Cavitation can be controlled or prevented, unlike flashing. Irrespective of the valve's trim, if all of the outlet valve's pressure is lower than the vapor pressure, flashing is bound to occur.

4.7 The Flashing Phenomena

When flashing occurs, the liquid flow after vaporization of part of the liquid now exists in two phases comprising of flashed vapor and the remaining liquid. The liquid will tend to continue flashing as long as it achieves thermodynamic equilibrium and complete saturation of vapors. Most of the time it has been observed that most of the volume will be vapor and the remainder of the liquid will form droplets suspended in the vapor. When the velocity of the vapors is at par with the sonic velocity at such high velocities, these liquid droplets cause extensive damage to the valve body and downstream pipeline. The flashing process has high turbulence as the liquid impinges at a high velocity, which causes a strong impact at the valve trim. If the impinging liquid strikes the control surfaces of the plug then it could easily result in trim instability. Consequently, plug control trim is not ideal for flashing. Certain special designs of cavitation-reducing trims disperse, which creates a distribution of the flashing dividing it into several microjets that bring down the net turbulence effect and minimize the vibrations on the plug. This also greatly reduces the erosion effects on the valve body. In most cases, an angled body direction along with downstream flow characterizes a flashing service. The main aim is to avoid any body contact as much as possible while getting the flashing in a valve. As Warren [73] did not have an anti-cavitation trim, avoiding body contact was a good idea. If the pressure difference that needs to be recovered is lower than 50 PSI, then such kind of flashing ensures low turbulence; hence, the standardized-hardened trims with specific patterns of flow could be of ideal utility.

4.8 Measures against Flashing

Selecting an optimum large nominal size for valve helps to reduce the average downstream flow velocity during flashing. It minimizes a majority of the problems due to cavitation and flashing in piping systems. It has been observed that the limiting value is 200 fps [69]. Some basic, yet important measures for flashing applications are discussed below:

Body Material. Flashing results in erosion on the body surface and degrades the body's wall thickness severely. Due to high turbulence in the two-phase fluid in the downstream flow of the valve can cause extensive erosion damage to body materials, which do not have enough resistance to erosion, such as carbon steel.

Trim Selection. Use of Balanced Plug Control must be avoided as flashing makes the valve trims unstable. Special cage control trim with several small orifices reduces the vibration due to turbulence on the trim; therefore, it best addresses the concern of high-pressure differences during flashing. Along those lines, Unbalanced Plug Control Trims with tungsten carbide or ceramic might also be considered for the needful [73].

4.9 Conclusion

Process conditions and process applications fluid properties characterize flashing and cavitation as thermodynamic regimes. During the selection of valves and their applications, it is very essential to understand both fluid properties like vapor pressure and also system properties, such as process pressure and temperature, so as to determine if flashing or cavitation are probable issues.

Even clean fluids without any solid content might also create very severe flashing and cavitation erosion damages to valves. Few known and used valve designs to counteract flashing and cavitation can

be classified as the use of resistance, isolation, and elimination [74]. Understanding these three general principles can help in selecting the ideal valve design for tough applications and industrial utility. This is a brief summary of flashing erosion mechanisms that have been found in NPPs. The U.S. NRC, along with EPRI, is conducting research in this area to improve the safety and reliability of NPPs.

5. PITTING CORROSION

5.1 Introduction

Pitting corrosion can be defined as the phenomena of localized areas of corrosion characterized by the formation of holes, or pits, on the material surface. The formation of these pits can be either uncovered or covered by a semi-permeable membrane of products due to corrosion. Due to the formation of these covered pits makes pitting corrosion difficult to detect and mitigate the effects thereof compared to that of uniform corrosion. Other than the localized reduction in material thickness, the pits also serve as stress points that increase the probability of fatigue and stress corrosion cracking (SCC).

Pitting corrosion typically occurs under the following scenarios:

- Localized damage to the oxide film due to mechanical or chemical interactions. Water chemistry parameters can induce a disruption in the oxide film (e.g., acidity, low dissolved oxygen concentrations, and high-chloride concentrations).
- Localized damage of protective coatings, including damage due to poor application.
- Existence of discontinuities in the structure of the material (e.g., inclusions) [75].

5.2 Mechanism of Pitting Corrosion

Pitting corrosion occurs when the material surface is exposed to anionic species, such as chloride ions. Exposure of the anionic species to the surface, and therefore initiation of the process of pitting, is typically characterized by a breakdown of the oxide, or passive, film. Once the material surface is exposed, an autocatalytic reaction occurs when oxidation of the metal surface produces metal cations resulting in the electromigration of the anionic solution (e.g., chloride ion) to the area to maintain neutrality. Once this process is initiated and the environment becomes more enriched in metal cations, pit growth is further promoted due to the cation/anion balancing reaction.

Pits typically initiate at either a chemical or physical change in the material surface. These changes, such as the presence of inclusions, can alter the environment of the cation/anion reaction, which promotes the formation of pits. For example, MnS inclusions are common in stainless steels. Not only does the inclusion affect the ability to form the passive layer, but the MnS in contact with the aggressive anionic solution results in dissolution more readily than the surrounding material. This dissolution results in the production of cations, and promotes the autocatalytic reaction responsible for pitting corrosion [76].

5.3 Factors Affecting Pitting Corrosion

Due to the complex and random nature of pitting corrosion, it becomes increasingly difficult to determine how specific changes in factors, such as environmental conditions and material characteristics, have on the initiation of pitting corrosion. Many studies have been conducted that attempt to determine these factors. One such study conducted by Ezuber [77], was directed at establishing how temperature, presence of dissolved CO_2, and flow affected the pitting behavior of UNS S 32205 duplex stainless steel (DSS) in a chloride solution. Both mill annealed and heat-treated samples were tested during this experiment. Results are as follows:

- In 1 M NaCl solution, both samples showed considerable resistance to pitting corrosion at a temperature of 23°C. Evidence of pitting corrosion is first noticeable after increasing the temperature

to 50°C and resistance of the samples decreases as the temperature value and/or duration increases beyond this point.

- The introduction of the CO_2-saturated chloride solution into the experiment resulted in affecting the stability of the passive film. The CO_2 lowers the pH of the solution, increases the rate of dissolution, and decreases the possibility of repassivation. Therefore, this increase in breakdown of the passive film increases the initiation of pitting corrosion.
- Upon increasing the flow of the system, a reduction in pit growth was observed. The increase in flow served to disrupt the chemistry within the formed pits and hindered further growth. This also resulted in an increase in pit repassivation, which also hindered pit growth.

Conclusions drawn from these results indicate that each parameter played a major role in the initiation or disruption of pitting corrosion. Increases in temperature and decreases in pH due to CO_2 concentration resulted in an increase in pitting, while an increase in flow resulted in hindering further pit growth and stability. These characteristics are highly important when evaluating the pitting corrosion potential of a system.

6. PREDICTIVE MODELING OF EROSION

6.1 Predictive Modeling of Cavitation Erosion

The current study reports the use of various data-driven models for the study and prediction of corrosion-erosion in NPPs and about the available first principle and models that could be useful in predicting the remaining useful life of NPPs.

M. Dular and O. Coutier-Delgosha [78] in their numerical modeling study using computational fluid dynamics arrived at interesting conclusions. In their study, they developed an erosion model and blending it with CFD, helped reduce the time requirement for conducting the analysis and the process involved in the design. It was also noticed that determining a predictive idea about the long-term cavitation erosion in the early stages of the design gave scope for developing optimized hydraulic shapes. They proposed a global model accompanied by CFD simulation results on a two-dimensional (2-D) foil section. Parameters like pressure and velocities of the flow close to the hydrofoil was measured and used for validation of CFD results. Cavitation erosion can be correctly predicted owing to the accuracy in the measurement of the intensity and duration of pressure waves.

At the 13th International LS-DYNA Users Conference, Souli et al. [79] presented their research on numerical modeling of phase changes and the effects of cavitation in NPP pipes. Their work developed an equation of state for the change in phase in the applications involving fluid structure interactions. This model has been verified and validated for problems due to hammering of water against a surface. This process involves a change in phase from liquid to vapor and vice-versa. When shock pressure at the closed valve is reflected, the phase change occurs. The authors have done a commendable job as they have studied 3-D problems. The analyses have been performed for both the fluid and the structure under impact or attack. Fluid structure coupling along with contact algorithm have been instrumental in solving problems in NPP pipes. Experimental observation establishes a strong correlation with pressure time history and peak pressure. Generally, some major and important parameters that must be considered for designing a model for cavitation predictions include density, pressure, temperature, mixture, and volume fraction of vapor inside the element. The combinations of these factors can be altered depending on large-scale or small-scale phenomenon.

In a study on modeling cavitation and boiling bubbly flows, S. Mimouni et al. [80] performed numerical simulations using NEPTUNE_CFD code. The simulations presented by the authors were in resolution of balance of mass, momentum and energy balance accounted for turbulent, and compressible and unsteady flows for both vapor and fluid phases. Initiation of cavitation is observed at the wall due to nucleation or by the pre-existing germs of cavitation. When $H_l < H_{sat}$ (H_l is the total enthalpy in liquid

state and H_{sat} is total enthalpy in saturation state) micro bubbles travel through the flow and eventually grow in size. However, when $H_l > H_{sat}$, void fraction condenses in a symmetric manner. The turbulent model is responsible for the creation and characterization of the vortex formed in the flow. The vortex causes the slug bubbles to break into smaller bubbles. When $H_l - H_{sat}$ is maximum, the vertical structure entraps the small bubbles at regions of low pressure. Furthermore, it has been found that the presence of non-condensable gas can definitely improve the predictions of cavitation by manifold. This is because the non-condensable gas can cause nucleation even at temperatures less than saturation state at the local liquid pressure.

A. Peters et al. [81] presented a new approach to predict cavitation erosion. They investigated and proposed a model for 3-D Euler-Euler flow simulations. This modeling technique involved prediction of the areas affected by erosion and it helped analyzing the erosion potential in those areas. In the same lines as Dular and Coutier-Delgosha [78], this model evaluated the generation of micro jets near the surfaces based on factors affecting the surrounding flow field. This model used dimensionless coefficients that helped in the qualitative prediction of erosion. This qualitative approach was based on the quantity and intensity of impacts in a particular area. The proposed erosion model gave distinct relationships between the cavitation cycles and the erosion impacts.

While studying cavitation erosion in the throttling devices in NPPs, Tomarov et al. [24] discovered that nearly 30% of the throttling devices in the condensate feed channel suffer from erosion due to cavitation. Hence, in their study they proposed using erosion-corrosion computational code called RAMEK, which is essentially beneficial and helpful in evaluating the primary process of wall thinning and the corresponding causes responsible for the damage of components and pipelines in NPPs, which operate on single-phase water flows. Continuing studies and research in the field of modeling for cavitation, P. Zima et al. [82] conducted experiments and suggested a model for the collapsing of cavitation bubbles in hydro machinery. Their work gave an efficient computational quantified analysis of the energy involved when the cavitating bubbles collapse. Numerical prediction of actual erosion becomes optimally feasible to evaluate the position and intensity of the initial collapses; it considers the scattering of the points of impact arising out of fluctuations in the rate of flow. They also concluded that this model was a good way of predicting the flow aggressiveness of the propagating cavitation bubble at steady state or even at near steady state flow even with low intensities of cavitation, for example; near the design point in the hydraulic machines.

S. Hattori et al. [83] conducted research and while performing experiments for modeling cavitation erosion from the bubble collapse impact loads, they came up with the parameter:

$$\sum(F_i^{\alpha} \times n_i) \tag{5}$$

where F_i: impact load, n_i: number of impacts and α: constant, which was instrumental in determining the erosion life. They confirmed that Equation (5) is directly proportional to the incubation time of the cavitating liquid jet. Once the bubble collapse impact loads are known by measurements and the constants α and n are determined based on two separate conditions, the incubation time period can also be measured. These factors taken together can help predict the erosion life.

M. Dular et al. [84] studied erosion on single hydrofoils and its variation with visual cavitation structures. It was observed that the unsteadiness of cavitation could be elaborated from the standard deviation of gray level. Power law determined that a rise in pressure also increases the cavitation shedding frequency, which eventually with time also increases the bubble number density. Also, a higher attenuation of the pressure wave results in an increase in water gas content, which explains the fall in aggressiveness. The model proposed by them followed the idea that a series of processes at the initiation of separation and collapsing of cavitation cloud results in the formation of a single pit. Collapsing bubble creates a shock wave that becomes attenuated in the liquid by the distance it covers from the source. This predictive model takes data of visualization of cavitation structures as its input and evaluates the distribution and magnitude of the damage due to erosion. The effect of flow velocity and water gas content could be easily reproduced from this model. Also, due to less use of empirical relationships, this model could be used for predicting damage for different geometries. The researchers have assured that this model is good enough for cavitation erosion prediction and damage mitigation in real-life practical applications of hydro machinery.

Zi-ru Li et al. [85] made an experimental assessment of the erosion due to cavitation by implementing an unsteady Reynolds-averaged Navier-Stokes (URANS) method along with a post processing technique developed for NACA0015 and NACA0018-45 hydrofoils. Hence, they came up some important conclusions such as:

- Attenuation of the eddy viscosity in the region of higher vapor volume fractions in the multiphase URANS method in FLUENT generates a realistic dynamic shedding of the sheet cavitation.
- They developed a new erosion intensity function that had the mean of peak values of the time derivative of the local pressure $(\partial p/\partial t)$, which was greater than threshold as its underlying principle.

$$I_{Erosion} = \frac{1}{N}\sum I_i \ and \ I_i = \begin{cases} \partial p/\partial t\,;\ \partial p/\partial t \geq Threshold \\ 0;\ \partial p/\partial t < Threshold \end{cases} \quad (6)$$

- This function gives a clear correspondence between the locations with maximum risk of erosion from computational analysis to that obtained from the experimental investigations.
- It is presumed that the horseshoe-shaped cloudy cavity is generated due to the effect of the vertical side wall boundary layer.

Apart from the various predictive models discussed above, C. Pătrăşcoiu [86] suggested a new yet simple straightforward mathematical perspective for predicting cavitation erosion. He proposed theoretical models of cavitation erosion curves generating them from ordinary differential equations (ODE). ODE approach is beneficial because the parameters come up naturally in the solutions, therefore, there is no necessity for any assumption of these parameters. Curve fitting of the erosion curve to the experimental data that is obtained from numerical methods help to retrieve the parameters. It has been stated that for materials normally the initial rate (speed) of erosion is in equilibrium with the ultimate value of volume loss rate. In this case, to make the study simpler and to simplify the determination of parameters, the study could be focused on the one phase only (either initial or final).

E. Shams and S. V. Apte [87] at the Computational Flow Physics Lab at Oregon State University conducted research on small-scale cavitation and initiation using two different methods. First, a bubble model for gaseous cavitation where the dynamics and the motion of the bubble was obtained by solving the Rayleigh-Plesset and adaptive time-stepping procedure, respectively. Secondly, a scalar transport model with liquid volume fraction with source and sink for phase change in vaporous cavitation.

The scalar transport method helps to get periodic growth and decay of the liquid vapor fraction near the trailing edge, by virtue of local differences in pressure minima. It was found to be helpful in predicting the origin of cavitation on the shear layer for a cavitation index of 0.1. On the other hand, the subgrid dynamics of the bubbles and the inception of cavitation above the trailing edge were captured by

the discrete bubble model. For very low cavitation indices, fast changes in the bubble sizes were seen inside the shear layer. This study confirms that scalar transport combined with discrete bubble model is significantly helpful in studying and predicting the necessary effects of phase transfer in small-scale cavitations, along with the pressure oscillations on the nuclei of the subgrid bubble.

Soyama and Kumano [88] in the quest of defining a quantifiable model for cavitation erosion prediction they measured the impacts due to cavitation with the help of a polyvinylidene fluoride (PVDF) transducer and the erosion tests were conducted using a cavitating jet experimental set up. This was in correspondence with that of the ASTM G 134. The materials on which the tests were performed were pure aluminum (JIS A1050), aluminum alloy casting (JIS FC250), stainless steel casting (JIS SCS1), aluminum alloy casting (JIS AC4A), bronze casting (JIS CAC402), iron casting (JIS FC250), pure copper (JIS C1100), ceramic (MACERiTETM HSP), acryl resin and dicyclopentadiene resin (DCPD). The test yielded the following interesting results:

- The energy per unit time was found to be directly proportional to the erosion rate under optimal threshold condition. This relationship was obtained when the energy due to the impact causing cavitation was compared with the rate of erosion. This was determined to be the fundamental threshold level of the material.
- Various cavitating conditions can be simulated by a single impinging jet causing cavitation.
- They also proposed a method to predict cavitation erosion in hydraulic machines by virtue of erosion tests and quantitative analysis of cavitation impact due to a jet causing cavitation.

Furthermore, Chahine and Hsiao [89] in their study on cavitation modeling found that the pitting of the material during the collapsing of the bubbles can be investigated by modeling the dynamics of growth and collapse of bubbles near the responding and deforming materials. The initial stand-off distance between the bubble and the nearby boundary characterize the impulsive pressure loading which occurs due to the collapsing of bubbles. The velocities of the jet are directly proportional to the stand-off distance. Ironically, the higher velocity of jet does not always result in higher impact pressure. This is because the impact pressure varies also with the distance travelled by the front of the jet for making an impact on the wall after it touches down on the opposite side of the bubble. It was observed from fluid-structure interaction simulations that material deformation dampens the load on the material. The interaction between the bubbles affects the loading pressure on the surface of the material and also the shape of the pit to a great extent.

R. Simoneau et al. [90] from Hydro-Quebec made a study to predict and model cavitation erosion basing on a study made on eighteen 200 MW Francis units, and the results are as follow:

- Powerhouses Satellite 21 and Ireca-Hydrology showed similar performance. There was a reduction factor of 4 for erosion rate over, 308 stainless steel.
- These two powerhouses successfully could achieve a reduction in the cavitation repair frequency by 3, while it also shows the possibility of a reduction factor of 4 as well.
- On certain occasions low-intensity cavitation erosion of carbon steel and very thin weld overlays have delayed the achievement of the above-mentioned goal.

A predictive method was proposed by Y. Ito et al. [91] on developed stage of cavitation erosion where they have assumed a typical flow in a 1/10 scale model of a jet-flow gate-valve. They made a comparative analysis of the rate of pitting nuclear energy (NE), the erosive pressure pulses PSC and the corresponding acoustic pulses. Quite interestingly, they came up with the following conclusions:

- A higher threshold noise level $(P_{sc})_{th}$ helps to detect the high-pulsive components from the cavitation noises (i.e., acoustic pulses P_s), which in turn helps to predict the rate of erosion and the developed stage under operational conditions.

- When $(P_{sc})_{th}$ is high, a direct proportionality linear relationship was found to exist between the pitting rate N_E and the number of acoustic pulses N_A.
- On comparison with the maximum acoustic pulses $(P_s)_{max}$ from a hydrophine and the erosive pressure pulses $(P_{sc})_{max}$ measured by a prescale on the eroded surface, it was found that there is a simple linear relation:

$$(P_{sc})_{max} = k_1(P_s)_{max} \tag{7}$$

where k_1 is a machine constant.

- The impulsive cavitation energy that is transferred into acoustic energy is very small.
- For pitting rate N_E that is obtained by a thin aluminum foil technique, the following velocity power law holds good:

$$N_E \propto U_T^{10} \tag{8}$$

where U_T is the mean throat velocity.

Matevz Dular et al. [92] presented a model that promised a better probability of prediction and damage control mechanism caused by cavitation erosion in real-life hydraulic machines. In a paper presented by them in 2005 at the American Society of Mechanical Engineers (ASME) Fluids Engineering Division Summer Meeting and Exhibition, they proposed the developing a of a cavitation erosion model that was capable of predicting the magnitude and distribution of damage caused due to cavitation erosion. It was so enabled that it could reproduce the effect of flow velocity and the water gas content.

On a study on cavitation performance tests on the primary pump model on an NPP, A.S.L.K. Rao et al. [93] conducted the performance testing of 1/3 geometrical scale pump in a closed circuit test rig. They tested for head power, efficiency, NPSHR3%, NPSHvis against the capacity at the rated speed. Hence, they made the following observations that were in agreement with the initial expectations. The prototype pump's predicted performance at design speed of 700 rpm meets the expected duties. As the head found to be higher by 7%, nearly 3% trimming of the impeller diameter is predicted for the prototype pump. This trimmed diameter results in a pressure pulsation, which is at a lower level as it makes optimal clearance between impeller outer diameter and diffuser inner diameter. Along those lines the NPSHR3% for the prototype pump is approximately half of the NPSHA and at operating NPSHA, there are no signs of visible cavitation. The prototype also had a stable head capacity, which was confirmed from the model test results.

Veerabhadra Rao and Buckley [47] conducted experimental analysis, came up with unified empirical relations for cavitation and liquid impingement erosion processes, and found the following conclusions:

- The average erosion rate and the volume of erosion have an empirical power-law relationship, which explained the acceleration and deceleration erosion zones.
- There exists a power-law relationship during the acceleration zone for the extensive erosion data from venturi, magnetostriction, and liquid impingement devices.
- Thus, the power-law relationship helps in the unification of data for various materials and cavitation erosion processes and in turn helps in the prediction of rates of erosion for longer hours of operation. It also helps in the construction of curves in case of missing experimental data points.

6.2 Predictive Modeling of Liquid Impingement Erosion

One of the primary types of erosion-corrosion that causes ruptures and leakage in piping systems of NPPs is liquid droplet impingement erosion. Any type of damaging effects in NPPs, either in the pipelines or valves, is unaffordable as it involves huge losses both financially and productivity wise. Also,

radioactive materials used in NPPs might get exposed to the atmosphere through a leakage causing some serious environmental hazards and loss of life.

Liquid droplets travelling at a certain high velocity when impacts a solid surface at an angle called the impact angle results in surface degradation leading to loss of surface material. This phenomenon of erosion of solid material due to an impinging jet of liquid is known as liquid impingement erosion.

Many researchers have been working on finding out the most accurate and optimal model for predicting the erosion mechanisms. Jun Ishimoto et al. [94] did numerical analysis on the structural 3-D aspect of a liquid droplet-vapor in two-phase pipe flow travelling at a very high velocity, and the LDI erosion characteristics was also predicted. This was done by means of integrated parallel CFD analysis. They obtained the following conclusions:

- Mathematical calculation of the vapor subcooling is done so as to enable the study of the generation of the micron-sized liquid droplet. Vapor condensation takes place when the outlet pressure is above 100 kPa.
- LDI primarily happens when the impinging liquid droplets have a diameter of 1.0 to 2.0 mm, which generally strikes the bent parts of the pipes.
- This model helped to reduce the LDI induced erosion for tapered-type orifices even at outlet pressures greater than 100 kPa.
- They found that the model has striking resemblance with the actual phenomenon in NPPs. There exists a significant similarity between the numerical and experimental results, thus making this model all the more suitable and appropriate for use.

Ryo Morita [95] performed experiments on steam to clear the diameter of the liquid droplet and its distribution. The following are major inferences from the steam flow calculations obtained for local flow conditions so as to establish a relationship with the droplet diameter:

- Computational code MATIS-SC was used to ensure that the computational wall pressure distribution matches qualitatively well with the experimental information. Flow velocity is also in reasonable good agreement both for computational and experimental data.
- Γ-distribution approximation could be used for the histogram of the droplet diameter. For 99% of the total value of droplet in experiments and Γ-distribution is less than 10% which reveals its accuracy.
- The author has proposed a new correlation that includes the effect from the variation of heat energy and it also include the latent heat as well. The variation is almost linear and hence it shows good coherency when compared to the liquid droplet under consideration and it does not diverges even on increasing the diameter.

Some computational fluid dynamics analysis calculations were conducted by R. Li et al. [96] to determine the kinetic energy attenuation characteristics of the fluid carrying the liquid droplets causing LDI erosion. The kinetic energy attenuation is calculated by introducing a damping function on the energy spectrum of the single-flow phase. The inter-phase effects (i.e., the dispersed phase and continuous phase) were investigated using a Eulerian-Lagrangian method by virtue of a two-way couple calculation system.

R, Li, et al. [97] conducted extensive research and proposed a calculation methodology for predicting LDI erosion. They found that by conducting CFD in a full-scale bent pipe by means of CFD calculations determines the damping characteristics of the carrier fluid turbulence kinetic energy and the rate of erosion. They came up with the following conclusions:

- An LDI erosion prediction procedure was conducted for bent pipe geometry over the existing CFD analysis with a new impact angle function.

- Two-way coupling, turbulence damping, and droplet impingement angle function were instrumental in predicting LDI by comparing with the velocity profile and erosion rate for adding a physical aspect to the calculations.
- The droplet velocity parameter calculations were evaluated based on the real NPP accident data, and a velocity prediction was made.

Fujisawa, N. et al. [42] suggested a model for experimental prediction of LDI based on the effect and behavior of liquid film on LDI. They studied LDI by means of high-speed conical spray where they made sure that spray diameter is greater than the circular specimen. The effect of the liquid film was adjudged by changing the diameter of the specimen and the distance from the nozzle. The droplets properties were characterized by using the PIV for droplet velocity, the local volume flux was determined by a sampling probe, and the droplet diameter was discovered by the shadowgraph method. Thus, by combining the experimental and theoretical considerations, it was found that the rate of erosion increases as the specimen diameter decreases, as the standoff distance increases, and eventually also as the liquid film thickness decreases. It was found that the predicted rate of erosion has a healthy correlation with the experimental data with a factor of 1.3.

Li. R., et al [35] carried out their great work in the field of LDI predictions forward when they conducted CFD calculations to evaluate the behavior of a single LDI with a much greater velocity under impact on a rigid wall. They came up with the following inferences:

- On solving the fluid dynamics and continuity and momentum equations, they learned the generation and propagation of the shock waves, which revealed the importance of compressibility of the liquid medium.
- Numerical analysis proves that the critical maximum pressure is highest at the point just before the jet eruption and after the angle of contact. They also suggested a droplet impact angle function for global LDI predictions.

Along those lines, they suggested that there is also scope for future work; also, there are limitations, such as all calculations should be based on 3-D space, as LDI is a 3-D phenomenon. They suggest that the future piece of work should be based on the fact that the wall damage is based on solid elasticity theory.

Fujisawa, N., et al. [37] carried out experimental study to determine the wall-thinning rate of deep erosion by LDI by means of a spray jet apparatus. The experiments were performed on the erosion surface contour, the rate of wall-thinning and the characterization of erosion surface was done by using SEM. Mostly the experiments were meant for the specimen with larger diameter than the spray size for different combinations of droplet velocities and the standoff distances. In case of surface contour, the higher rate of thinning on the center of the groove attributes to the sharp groove features penetrating into the wall. The damping effect of the film of liquid on the rate of wall thinning and the impact of side jet resulted in the decrease of the wall-thinning rate as the depth of erosion increases. They proposed a model with the attenuation factor along with a function of erosion depth. This introduction of attenuation factor gave a better relationship with experimental data, thus improving the correlation accuracy by a factor of 2.

Morita and Uchiyama [98] conducted research for better realistic evaluations of an LDI in the power plant. They carried out a series of experimental studies based on the wet steam flow for simulation of real-life plant conditions. They took into consideration the cushioning effect of the liquid film considering its formation by the droplet on material surface and then by putting it with the LDI model, a CRIEPI model was proposed. The CRIEPI model was instrumental in predicting and reproducing the measured experimental data within a good correlation factor of 2. It also throws light on the tendency arising due to the liquid film observed in experiments. The CRIEPI implements the cushioning effect of the liquid film and the following LDI mechanism could be obtained:

Thinning rate due to LDI = (impact force per droplet)*(frequency of droplet collision)*(resistance of material)*(cushioning effect of liquid film).

Investigation of the LDI tendency and the probability of prediction in Japanese Tokai-2 NPP were done by Ohira, T., et al. [45] and the wall thickness measurement data were considered from the fourth heater vent line in Tokai-2 NPP. They were well categorized and the LDI investigation was performed with the LDI evaluation system in CRIEPI. It was observed that the ratio of the maximum rate of thinning to the average rate of thinning might be related to the average rate of thinning. Hence, it was proven that the evaluated and measured rate gave the same result. The LDI evaluation system has a greater potential of successfully predicting the LDI management in actual NPPs.

Morita, R., et al. [99] proposed a method for LDI prediction in plan piping emphasizing on the elbow element in a steam piping flow. They used in house codes MATIS-SC (3-D) and MATIS-SP (1 dimensional [1-D]) for steam flow calculations to evaluate the flow. Furthermore, for evaluating LDI they used a user-defined function 'g' as LDI sensitivity. A steam piping system was used for calculations of the test results. The following inferences were obtained:

- 3-D and 1-D flow calculations are in agreement to each other with an exception in the region close to the orifice of the first (most upstream) elbow.
- It was observed that the jet from the orifice on collision with the first elbow downstream of the orifice. Therefore, the velocity of collision is significantly higher than the calculated section average obtained from 1-D codes.
- The LDI sensitivity is higher for the last elbow (most downstream) as the velocity of flow is much greater than other elbows.
- The first elbow has a higher LDI sensitivity for the reason that the flow from jet from orifice might collide with the elbow.
- Collision frequency has all of the plausible reasons to vary the order of the possibility of the occurrence of LDI.

6.3 Predictive Modeling of Solid Particle Erosion

In order to establish an effective mathematical model for predicting erosion rates of different materials due to solid particle erosion, Siddhartha et al. [58] developed the following model, Equation (9), which was found to be superior to previously attempted models.

$$E_r = \frac{1}{6H_v} * \eta * \rho * V^2 * \left(\frac{2a \sin\alpha \cos\theta + 3h \cos\alpha}{a \sin\alpha \cos\theta + h \cos\alpha}\right) \quad (9)$$

where α is impact angle in degrees, H_v is the hardness (N/m^2), η is erosion efficiency, V is the impact velocity (m/s), ρ is the density of the target material (kg/m^3), and E_r is the theoretical erosion wear rate (kg/kg). Reference values for erosion rates, as well as material properties, such as density, hardness, impact velocity, and impact angle, were taken from previous experimental results established by Arjula et al. [100]. A previous model developed by Biswas et al. [101] was used as a basis for comparison in overall acceptability in terms of percent error. Validation of the mathematical model was conducted using MATLAB under various conditions, such as dimension of erodent particle, impact velocity, angle of impact, and type of material. After validation and comparison to the experimental results of Arjula et al. [100], the theoretical rate of erosion wear for the proposed model was found to have an acceptable percent error range of 0 to 15% for the various operating conditions and material types. This is far more superior to that of the previous work of Biswaset al. [101], which was only able to achieve a constant percent error of 33%. Due to the fact that this model accounts for both vertical and horizontal impact velocities, as well as the ability to account for physical dimensions of the erodent particle, it makes this model an effective tool in predicting erosion rates due to solid particle erosion.

In an attempt to predict the erosion rates effectively within oilfield control valves due to solid particle erosion, Forder et al. [102] developed an erosion model using CFD. Due to the structure of these valves, the particle impact characteristics vary greatly, and it becomes extremely difficult to predict erosion rates using pre-established universal models. To overcome this, two separate mathematical models of erosion based on impact angle had to be incorporated into the new model: low-angle cutting and high-angle deformation. Low-angle cutting typically occurs at angles between 0 and 40 degrees and the model used in this study, Equation (10) developed by Hashish [103], is as follows:

$$W_c = \frac{100}{2\sqrt{29}} r_p^3 \left(\frac{u_p}{C_k}\right)^n \sin 2\alpha \sqrt{\sin \alpha} \tag{10}$$

where W_c is eroded volume due to cutting (m^3), r_p is particle radius (m), u_p is particle impact velocity (m/s), C_k is cutting characteristic velocity (m/s), and n is the characteristic velocity exponent (*value 2-3*). High-angle deformation typically occurs at angles between 30 and 90 degrees and the model used Equation (11) developed by Bitter [104,105] is as follows:

$$W_d = \frac{m_p \left(u_p \sin \alpha - D_k\right)^2}{2E_f} \tag{11}$$

where W_d is the eroded volume due to deformation (m^3), m_p is the mass of the particle (kg), D_k is deformation characteristic velocity (m/s), and E_f is the deformation erosion factor (J/m^3). By combining both of these models, given below in Equation (12):

$$W_t = W_c + W_d \tag{12}$$

where W_t is the total eroded volume (m^3), an accurate mathematical model for predicting erosion within these control valves was established. To validate this model, the data produced from the CFD erosion model was compared to that from experimental results under similar conditions. The results showed that the CFD erosion model had good correlation to the experimental results in terms of location and intensity of erosion. This model has the added benefit of utilizing different material types based on additional coding embedded within the model.

In a study to develop a probability model for solid particle erosion in a straight pipe, Zhang et al. [106] established a direct relation between the dispersion of particles within the flow and the points of impact on the pipe wall. This model focuses on the probability of two independent events occurring at the same time. The first being that a large vortex occurs in the flow field near the pipe wall, and the second being that a particle can enter this region. The final probability model is the result of combining these two events to predict the likelihood of a single particle impacting the pipe wall. Upon validation of this model by comparing several numerical studies, as well as physical experiments, the model predicts that penetration rates increase as pipe diameter decreases and flow velocity increases. Also due to this comparison to other studies, it was determined that this probability model can be effective in predicting erosion rates for particles ranging from 50 to 1000μm. However, it is important to note that this model does not factor particle shape into its predictions and is based solely on the primary factors that influence erosion caused by impacts of solid particles.

There exists many different models that serve to predict the rate at which solid particle erosion occurs within a flow system. Most of these erosion models are based on a certain type of erosion mechanism or are specific to a type of system, but very few studies aim to develop a model that applies to a range of applications. In a recent study, Peng et al. [107] conducted an analysis of several of these models utilizing CFD in an attempt to ascertain which of these models produced the best results in comparison to experimental results. Five different erosion models were selected and each was paired with two particle rebound models: the Ahlert [108] erosion model for AISI 1018 steel; the Det Norske Veritas (DNV) [109] erosion model designed to apply to various materials; the Erosion/Corrosion Research Center (E/CRC) at the University of Tulsa [110] developed an erosion model designed to apply to different physical pipe characteristics whose model is reported by Zhang et al. [111]; the Neilson and Gilchrist [112] erosion

model, which focused on impact angle of solid particles; and the Oka et al. [113,114] erosion model, which incorporates many different aspects that affect material erosion. The two particle rebound models used are: the Forder et al. [102] non-stochastic model and the Grant and Tabakoff [115] stochastic model. CFD data analysis of each of these models on an elbow can be seen in Figure 8, which compares the predictive models against experimental data compiled by Zeng et al. [116].

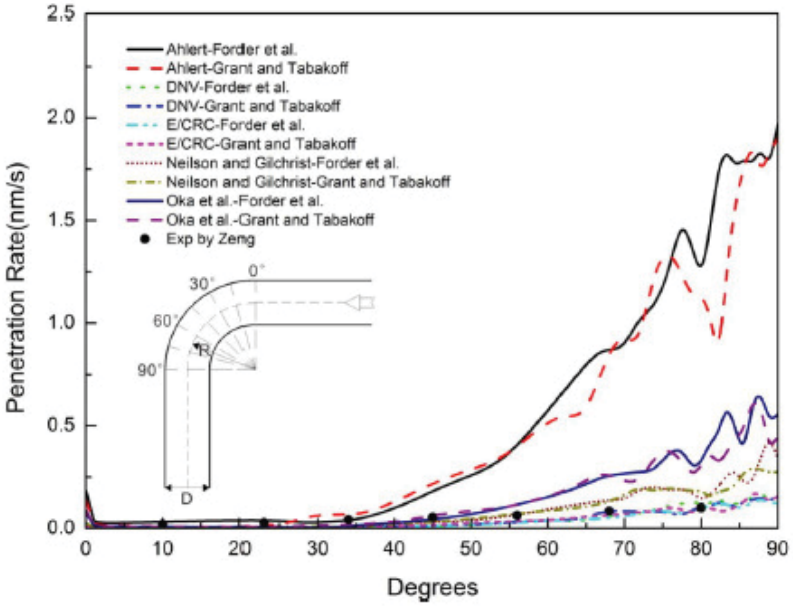

Figure 8. Data compilation from CFD analysis of predicted models and experimental results that compare penetration rates to varying degrees of elbow [107].

As can be seen in the figure, Peng et al. found that both the DNV erosion model as well as the E/CRC erosion model produced data points most similar to the experimental data. Due to the similarity between the two models, further testing was required to determine which one was best suited as an effective erosion prediction model. To accomplish this, more experimental data was needed. A study by Bourgoyne [117], which involved solid particle erosion in diverter systems, supplied the necessary experimental data. Ratios of predicted penetration to experimental penetration were calculated for both the DNV and E/CRC erosion models. The results can be seen in Figure 9.

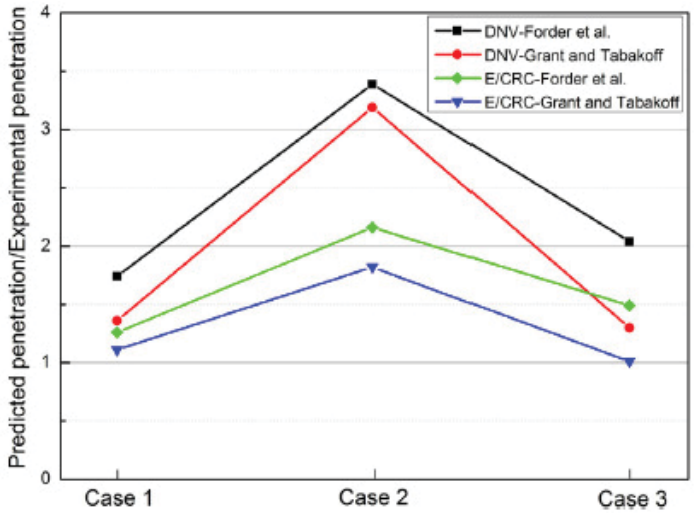

Figure 9. Ratio of predicted and experimental penetration [107].

This analysis concludes that the E/CRC erosion model, Equations (13 and 14) along with the Grant and Tabakoff particle rebound model, Equations (15 and 16) show the greatest compliance with the experimental data.

$$ER = C(BH)^{-0.59} F_s u_p^n f(\alpha) \tag{13}$$

$$f(\alpha) = \sum_{i=1}^{5} R_i \alpha^i \tag{14}$$

where C is a constant equal to 2.17×10^{-7} for carbon steel, BH is the Brinell hardness of the wall material, F_s is the particle shape coefficient, u_p is the particle impact speed (*m/s*), n is also a constant equal to 2.41, and α is the impact angle in radians.

$$e_n = 0.993 - 1.76\alpha + 1.56\alpha^2 - 0.49\alpha^3 \tag{15}$$

$$e_t = 0.988 - 1.66\alpha + 2.11\alpha^2 - 0.67\alpha^3 \tag{16}$$

where e_n is normal velocity component restitution coefficient, e_t tangential velocity component restitution coefficient, and α is the impact angle.

6.4 Predictive Modeling of Pitting Corrosion

In a study aimed at establishing an effective stochastic model capable of simulating pitting corrosion, Valor et al. [118] made the following conclusions:

- Using physical and statistical methods, the combination of two independent non-homogeneous in-time processes (pit initiation and pit growth) can be used to create a consolidated stochastic model of pitting corrosion.
- Using a non-homogeneous Poisson process, pit initiation can be modelled as a Weibull process to model a set of multiple pit nucleation events.
- Based on the corrosion rate of the material, pit growth can be modelled using a non-homogeneous Markov process, which in turn is guided by the Kolmogorov differential equation.
- Upon testing the model in comparison to experimental data, it was determined that the model is capable of simulating pitting corrosion depending on the material and environment. Also, in comparison to other models, the new proposed model was more accurate in recreating experimental results.

Such a model can be used to determine the susceptibility of a system based on such factors as material composition and environmental conditions to which the system is exposed.

In another study, this time aimed at establishing a predictive fitness-for-service (FFS) assessment of pitting corrosion, authors Shekari, Khan, and Ahmed [119] developed a new model also relying on a non-homogeneous Markov system. This process is commonly utilized in pitting corrosion modeling due to the random nature of its initiation. The model proposed by the authors uses pit density, maximum pit depth, and maximum allowable pressure of the defected component to predict a failure time of the system due to pitting corrosion. The model was then tested on a piping case study to validate its effectiveness. Results from the case study concluded that choosing remaining thickness and failure probability threshold limits are of high importance in determining remaining life of the system. In particular, it also stresses the importance of periodic inspections to allow adjustments of the model to be made based on maximum pit depths currently present in the system.

Another Markov stochastic model developed by Fontes, Frutuoso e Melo, and De Martin Alves [120] was specifically directed at determining time evolution of NPP piping replacement due to pitting corrosion. The proposed model was tested against data received from regular inspections of a section of pipe at the Angra I NPP in Rio de Janeiro, Brazil, to determine its effectiveness at predicting the time it takes for the pit corrosion depth to reach a maximum before replacement is required. Conclusions drawn

from this study include an advancement of the effectiveness and applicability of the model in comparison to previous models. Because model coefficients are not based on the material composition or the corrosive environment, it means the model can be used for a range of systems without the need to alter the parameters of the model. Authors also note that utilization of this model could potentially reduce or eliminate the need for routine pipe inspections resulting in a reduction of both maintenance time and costs.

6.5 Prediction of Remaining Useful Life in NPPs

Bond, L. J., et al. [121] made a study on NPPs from an economic perspective for management of NPPs. They found that the nuclear power community has now adopted advanced online monitoring (OLM) and advanced diagnostics that can help in reduction in mandated surveillances, more accurate cost-benefit analysis, timely maintenance, analysis, and having adequate knowledge of maintenance tasks, minimizing failure probability. After analyzing the 104 U.S. legacy systems, it has been found that usage of online monitoring and diagnostics have the ability to save over $1B per year in the U.S. alone. Deployment of condition-based maintenance (CBM) in the NPPs has essentially boosted and improved the economic impact. Also the adoption of digital instrumentation and control (I&C) creates a window for addition of improved functionality and the possibility to add prognostics for key system elements. The target is to implement these approaches and ideas successfully to monitor cavitation erosion in the next generation GEN-IV reactors.

In a modeling study for estimating remaining useful life of electric cables in NPPs, Shumaker, B. D. et al. [122] suggested a prognostic model approach for remaining useful life (RUL) estimation. The current data in the Cable Polymer Aging Database (CPAD) shows the application probability of the condition of the cable for data monitoring for prognostics. With a collection of run-to-failure data, it was seen that RUL predicting models could be built with reasonable accuracy. When a cable gets closer to its end of life, General Path Model (GPM) estimation helps to provide accurate results. Hence, based on this modeling approach, condition monitoring programs will be able to carve a better maintenance plan and avoid unwanted failures.

Saarela, O., and Hulsund, J. E., [123] made some experimental study and suggested certain technique for lifetime modeling of equipment at NPPs. They proposed gamma process for estimation of remaining useful life. Models based on gamma process are suitable for modeling gradual lifetime expenditure, specifically due to its ability to adapt to the steeper rise of degradation towards the end of life. In this approach, each application has independent shape functions denoting the functional form of the damage development and values for the model parameters. This modeling technique using gamma process is useful for long predictions, especially in CBM application. Moreover, usable flexibility of various data mining methods like Bog Data can also enhance the CBM modeling techniques in the future. Hence, higher the reliability of RUL estimated, higher will be the acceptance of these ways and means for predicting deterioration of equipment in NPPs.

In predicting the remaining life of pipes in NPPs, M. D. Pandey et al. [124] conducted research and suggested a model for predicting useful remaining life in the primary heat transfer piping system that undergoes serious damage from flow-assisted corrosion. They suggested a couple of probabilistic approach known as the random variable (RV) rate and the random gamma process (GP) model. The optimistic sides of these two approaches are they are substantially helpful in to obtain the lifetime probability distribution and they help in predicting the expected number of substandard pipes. The RV model is instrumental in figuring out the variability in the corrosion rate across all of the pipes. The GP model takes into account the temporal uncertainty, whereas the RV model does not considers it. RV model gives a quadratic increase in the variation of wall thickness loss, where the GP model gives a linear variation. In a case study analysis of substandard pipes over a period of 10 years, it was revealed that the prediction of number of substandard pipes via a GP model is 34% less than the RV model.

Bakhtiari, S. et al. [125] conducted scooping studies on OLM - online prognostics (OLP) techniques and they observed that a practical OLM-OLP system could be effectively used for monitoring deterioration in systems, structures, and components (SSCs). The study was carried out at the Argonne National Laboratory (ANL) where an OLM system was used along with data to enable monitoring the development and growth of stress corrosion cracking by means of using a broadband active sensing technique. The researchers have suggested that further research and study are necessary, but they also found that for small-scale experiments, the usability of coupled OLM-OLP systems to predict probable SSCs are very much possible and viable.

An extensive study and analysis of various technical aspects of condition monitoring by Heo, G.Y. [126] gives the characterization by estimation of state and monitoring the state. Of lately, there has been acute interest in improvising the safety levels and efficiency of the secondary systems of NPPs. In 2004, the turbine accident in the Japanese Mihama NPP triggered an alarming wake up call for the regulatory authorities to consider the issues concerning secondary systems seriously. It has been found that a prototype condition monitoring system could be beneficial for use in secondary systems. Hence, condition monitoring, if put to effective use can be instrumental in significantly improving the overall competitiveness of NPPs.

Mansouri, A. et al. [127] carried out CFD simulations and they investigated and observed that in case of gas-solid flows, particles of solid have a tendency to cross the fluid streamlines, but on the contrary in case of solid-liquid flows it was found that the solid particles follow the liquid streamlines closely. As a result, U- and W-shaped cross-sectional wear patterns were produced for air and liquid testing, in geometry of direct impingement. A slurry erosion test was used to develop an approximate erosion equation for predicting the local wear depth. The erosion equation was developed by establishing a correlation between the erosion depths, which was measured from an impinging jet test at a normal angle with the particle impact data obtained from CFD simulations. The validation of erosion equation was done by oblique configurations. They found a healthy agreement from the profiles that were measured and the predictions made.

In a report prepared by Coble, J. B., et al. [128] at the Pacific Northwest National Laboratory for the U.S. Department of Energy, it was stated that in recent times, three major thrusts have been given to ensure the safety and economic stability of nuclear power generation in the United States: (1) increasing the longevity of the legacy fleet taking into account the operating lives of 60–80 years; (2) newer nuclear power plants with 60 years of design life; and (3) installation of small modular reactors, which will be using the light water reactor (LWR) technology.

Managing the life and monitoring the causes for deterioration of these reactors plays a key role. These developments are essential to address the purpose: (1) measurement by non-destructive techniques and the method of analysis for identifying the degradation; (2) special algorithms for characterization and to monitor the state of damage of the component; (3) the remaining useful life and the probability of failure of the component were determined by using a set of algorithms that use the information from the state of degradation. Furthermore, along those lines, the information obtained from probability of failure can be used to assess the risk significance by implementing a probabilistic risk assessment model. Prognostic algorithms, along with potential operational profiles, can be used together with predictions of growth rates of damage for enhancing the life of degraded SSCs until the next maintenance time. Component health information is also useful in optimization of operations and scheduling maintenance. Hence, these techniques cumulatively account for prognostics and health management (PHM) systems. However, in a real-world scenario, there are numerous challenges that pose a hindrance for implementing PHM techniques in actual NPPs. Most importantly, in the U.S. the licensing of using such PHM technologies in the evaluation and monitoring of plant life is based on the licensing that is regulated by the NRC. Implementation of PHM in NPP operations is essential. It provides significant improvisations in terms of safety, uptime, operations, and optimization of maintenance and the overall economics of plant. PHM is very instrumental for detection and characterization of degradation of light water reactors (LWRs), Gen

III/III+, Gen IV, and small modular reactor designs. Using PHM technologies for these reactors help monitor the needs arising out of extended fuel cycles and reduce access to critical components and remote siting with less maintenance staff. Thus, deployment of PHM technologies are beneficial for advanced monitoring, detection of fault, diagnostic, and prognostic infrastructure from the beginning of design until the end-of-life in actual NPPs.

In a technical report for suggesting prototypic prognostic technique for advanced small modular reactors (AdvSMRs), Meyer, R. M., et al [129] observed that using PHM technologies for determining RUL for AdvSMRs provides essentially better advantages than the stereotypical reactor design methods in terms of safety and reliability, sustainability, affordability, functionality, and resistance to proliferation. The basic requirements for using PHM in AdvSMR passive components were determined to be in the following areas:

- Sensors and instrumentation for condition assessment of passive components
- Fusion of measurement data from diverse sources
- The coupling between systems and across modules get addressed
- Implementing lifecycle prognostics
- Real-time risk assessment by integrating with risk monitors
- Having an interface with the plant supervisory control system.

Along with state-of-the-art PHM other measurements methods like stressors, global conditioning measurements and localized non-destructive evaluation (NDE) measurements can also be applied to diagnostic algorithms for evaluating the level of damage caused. Thus, the authors designed a research plan to address the shortcomings in research and technical needs, with intent to use a prototypic prognostics technology to mitigate the damage of AdvSMR components. The phase approach used corresponded to the following phases: (1) development and validation of prognostic algorithms by means of localized NDE and measurements by stressors, (2) component level development and validation of PHM, and (3) integration of local and component level prognostics to conduct PHM of a system. Prototypic degradation modes, such as high-temperature creep or creep-fatigue, need to be selected in each phase for showing prognostics methodology.

In a technical report by the International Atomic Energy Agency (IAEA) [130], several studies and experiments were conducted where in the first aspect of noise measurement there four primary benchmark that were studied in the report, namely the response time estimation, the coolant velocity estimation, the reactor transfer function determination and the moderator temperature coefficient estimation. Furthermore, the report also states methods like providing background and operational noise-reduction techniques, detecting the features of signals generated by loose parts by using discrimination techniques, implementing better localization methods and better mass estimation methods, working out a reliable loose parts monitoring system, evaluating the safety database, and displaying information on loose parts in the control room for monitoring the loose parts. Leakage was monitored by acoustic monitoring on the reactor vessel head. Also, it is important to monitor the leakage in the primary pressure boundary; the mitigation can be done by monitoring the leakage at valves. It is essential to keep a monitor on the vibration in the machine components undergoing rotation. This done by identifying the plant components and the different reasons for vibration, measuring vibrations, gathering optimum information from the measured vibrations, using hand-held devices for monitoring vibration on a periodic basis, continuous monitoring of online vibration, providing vibration surveillance and protection systems, and using wireless vibration sensors and transmission of signals.

Extensive research has been conducted for mitigating the aging and the eventual degradation of NPPs. The following methods have been put into effective use for monitoring and handling the deterioration of plant components:

- Target phenomenon
- Modeling degradation phenomenon
- Selection of materials
- Specimen materials
- Experimental methods
  - Fatigue test
  - Non-destructive testing (NDT).
    - Acoustic impedance method
    - Magnetic leakage flux method
    - Magneto-acoustoelasticity
    - Magnetic acoustic emission (AE)
    - Piezoelectric thin film
    - Thermal method
    - Electrical conductivity
    - Eddy current
    - Magnetic Barkhausen noise.

The trends that can be expected to be useful in monitoring and effective mitigation of degradation of components in NPPs are as follows:

- Providing cost-effective regular monitor of important components by implementing low-cost OLM systems and developing smart sensors for the needful.
- Facilitating the use of built in vibration sensors in motors, pumps, turbines, and other large equipment.
- Making extensive use of condition monitoring software with rapidly developing “expert” diagnosis abilities.
- Using condition monitoring within the “mainstream” operations and maintenance.
- Integrating and accepting common standards and establishing an interface between the condition monitoring software and process control software.
- Focusing on business implication and applications of condition-monitoring technologies.
- Reducing the cost per point of application of condition-monitoring techniques.
- Using more and more process control equipment—both hardware and software.

Eventually, it is suggested for better economic effects and for higher strategic importance, it is essentially beneficial to conduct periodic condition monitoring tasks in-house rather than giving contracts to third-party vendors. Moreover, as in insight in to the future technologies to be used in NPPs, the report suggests using wireless technology, data fusion, field bus technology, smart instrument, and power line data carrier.

Blatt, W., et al. [131] determined the velocity components of a particle with liquid by implementing laser Doppler anemometry. The turbulence due to the radial component of velocity was responsible for

the hydrodynamic activity in a tube having a constriction. Extensive study shows that the average flow velocity, the geometry of the flow, concentration and diameter of the particle can be directly correlated to the rate of mass loss by means of power laws. Radial kinetic energies are used for a better understanding of the results obtained from the mass-loss measurements. They are derived from the measurements from laser Doppler anemometry by considering the particle rate and the square of the radial fluctuation velocity.

In a report by EPRI [132], it has been investigated and suggested that there are not many models available to predict cavitation erosion. However, there are quite accurate and accepted models for the prediction of cavitation mechanisms happening in valves, downstream of orifices, and other known geometries. The occurrence of noise or any kind of vibration can be used as a method to screen the plausibility of cavitation erosion. Along those lines, CHECWORKS™ (Version 4.0 and later) can also be applied for determining the probable chance of susceptibility. Even though no models exist for predicting flashing erosion, there is a direct method to figure out the chances of flashing to occur downstream in a valve or orifice. The location that needs investigation can be evaluated by using the downstream velocity. CHECWORKS™ (Version 4.0 and later) can be used to determine the probability of occurrence of flashing. Also along those lines for LDI erosion, CHECWORKS™ (Version 4.0 and later) can be effectively used to evaluate the rate of LDI. Another approach is to use the "rule-of-thumb" values for critical velocity. Alternatively, the predicted velocity of the liquid can help identifying the locations that needs investigation.

As far as solid particle erosion is concerned, the existing current modeling methods cannot be used for power plants, as they need data regarding the size of the particle and its density. Also CHECWORKS™ (Version 4.0) is not designed for predicting solid particle erosion. Normally components in a power plant are inspected by ultrasonic techniques, radiographic techniques (RT) or by visual inspection methods. Presence of wear can be known from both UT and RT methods. Large bore piping systems are inspected using RT techniques. Generally, valves inspections are performed by visual technique (VT) and RT. Small-bore piping systems in BWRs have been investigated using pulsed X-Ray equipment that performs radiography.

The remaining service life of various components in a power plant can be calculated by using the following correlation:

$$T_{life} = \frac{t_c - t_{accpt}}{R \times SF} \tag{17}$$

where T_{life} is remaining service life, t_c is current thickness, t_{accpt} minimum acceptable thickness, R is current wear rate, and SF is a safety factor.

Improvement in materials or selection of materials and changes in the local design on components of a power plant are very effective and essentially instrumental in shaping the reduction of the rates due to erosion wear to a great extent.

6.6 Conclusion

In concluding lines, some suggestions were made based on experience of Simoneau, R. [90] from the observations from Hydro-Quebec, which would be beneficial and essentially helpful in mitigating the overall cost of cavitation damage in hydro machinery. Using high-resistance alloys or steels like Ireca at all times for cavitation repairs concerning high intensity is a better way to handle cavitation-related issues. The thickness should be at the maximum level spot and the area needs to be enlarged to provide the essential service life. Secondly, better-detailed cavitation damage reports, stating the size, location, and nature of the eroded metal with photographs need to be prepared at least some time before going for the repair work. Another option for minimizing the cost of cavitation repairs is to have data management and damage modeling software keeping in mind the higher resistance materials. Monitoring the vibration due

to cavitation should be done in conjunction with the modeling software to facilitate the operation at low-cavitation intensity and to obtain a more streamlines and exclusive prediction model.

There is an insatiable quest for energy and hence keeping that in mind, the United States nuclear industry has taken up steps and means to figure out ways so as to improve and increase the life of existing NPPs. In a study conducted by Lybeck, N., et al. [133] suggested that using methods like CBM for monitoring the active components in NPPs ensures a better understanding and management of the hindrances received from aging NPPs. Incorporating PHM demands the implementation of integrated health management for fully functional and usable OLM and prognostics. They researched and found out that there are 14 commercially available PHM software products and they have been categorized as research tools, PHM system development tools, deployable architectures and peripheral tools. For a complete monitoring and handling the situation of aging NPPs, a PHM system consists of various modules like data acquisition, modeling of the system, detection of faults and their diagnostics, system prognostics and operations and maintenance planning. Hence, all of these aspects when combined and cumulatively applied together help in monitoring and analyzing the aging NPPs, and thus create opportunities for generating preparedness for an effective and sustainable management in inducing an extension to the life of NPPs.

7. EROSION/CORROSION MONITORING TECHNIQUES

7.1 Introduction

Stress corrosion and fatigue arising out of corrosion are responsible for creating significant setbacks in several industrial facilities resulting in severe economic degradation because of lesser available plants and component repair or the need for replacement. In NPPs, cracks due to environmental factors are seen in a wide range of components, which also cover reactor piping and steam generator tubing, bolting materials, and pressure vessels. As it is believed that cracking is almost irreproducible, it ends up in making life assessment of these components of NPPs really tedious with increased levels of difficulty and complications [134].

7.2 Online Monitoring for Environmental Factors

Anderson et al. [134] have inferred that some greatly modified and advanced monitoring and modeling for prediction of cracking due to environmental factors in high-temperature water have been studied such as:

- Developing sensors and monitors
- Quantitative modeling like SMART
- Verification and validation of design and life prediction codes
- Mathematical approach for prediction of the cracking of Type 304 piping.

7.3 Online Monitoring Using FPGA/RT Technique

Bajic, B. [135], in a study regarding multidimensional cavitation monitor in Field-Programmable-Gate-Array/Real-Time (FPGA/RT) technology, inferred that the multidimensional technique for predicting cavitation erosion and monitoring gives an estimate that is based on a good amount of reliability. The estimation gives a better understanding of the intensity of cavitation and results in a detailed diagnostic of the damage caused due to cavitation. Such a technology can be very helpful for optimization of turbine or the operation of the plant for minimizing the rate of erosion. These approaches contribute significantly for conducting predictive maintenance for cavitation, and for identifying the turbine parts that need improvement.

The intensity of cavitation obtained from simple monitoring techniques of cavitation comes with a high-bias error and it does not yield the complete details of cavitation.

The cavitation monitoring technique, based on FPGA/RT technology, could be used as an independent entity as well as provide a channel for cavitation of the general monitoring system of the plant. Moreover, it has been found that model tests cannot replace prototype cavitation or even its monitoring.

According to Bajic, there are three major objectives in the diagnostics or monitoring of turbine cavitation:

- Operation optimization
- Predictive maintenance
- Diagnostics.

There are two methods to achieve these objectives:

- Diagnostic test
- Permanent monitoring.

While studying about the development of various software tools for calculating erosion-corrosion wear (ECW) of pipelines in NPPs Baranenko, V. I. et al. [136] suggested there is a need for developing software tools and proper documentation with the right certification for predicting the ECW rate, the rate of thinning of walls of pipes, and the life span of an operational pipeline.

ECW can be calculated form the following parameters:

- Thermo- and hydrodynamic characteristics, such as fluid temperature and velocity
- pH, concentration of oxygen, and amine being used
- Chemical composition (i.e., the contents of chromium, copper, and molybdenum in the metal)
- Characteristics defining geometry like the pipeline diameter, and Keller's coefficient
- Time elapsed when the equipment is in operation, which may be in years or hours
- Moisture content of steam.

One of the most widely used computer software tool CHEC used these days for prediction of ECW was developed by EPRI of the United States back in 1987.

Since 1995, CHECWORKS™ have been implemented in almost all of the NPPs in the U.S. to predict erosion rate. CHECWORKS™ helps calculate the following entities, such as:

- The mean ECW rate when the power unit is in operation
- The current ECW rate as a function of the conditions of operational power unit and the water chemistry being used at the station.
- The total wear of metal from the time when the power unit was made operational until the time of inspection.
- Time for which equipment items can operate until their repair or replacement.

7.4 Self-Diagnostic Monitoring System

In a report published by the Pacific Northwest National Laboratory based on online intelligent self-diagnostic monitoring system (SDMS) for next generation NPPs authored by Bond, L. J., et al. [137], it was observed that the main reasons or plausible circumstantial conditions responsible for degradation of

power plants in terms of sudden shut downs, extensive maintenance, and operational inefficiency were characterized by constant irregular vibration in moving/hanging parts, bio-fouling, and erosion-corrosion wear and the consequential degradation of the system as a whole. SDMS provides a platform of proof-of-principle where a de-centralized and uniformly distributed suite of sensors is very articulately integrated with both the active and passive components, which could be used in the next generation NPPs. SDMS was equipped with the state of the art operational sensors, advanced stressor-based instrumentation and distributed computing, data network modules, and signal processing for advancement of the monitoring and assessment of the power reactor system.

The major technical guidelines of SDMS include the following;

- Developing, designing, and demonstrating SDMS architecture that utilizes distributed artificial intelligence agents at plant, system, and even component levels.
- Using the SDMS technology on a computer.
- Making condition monitoring plausible by developing advanced radio-frequency tag/multi-sensors units.
- Creating a self-explanatory descriptive design for and fabrication of a demonstration system for SDMS.
- Conducting validation tests through baseline verification testing, and performing degradation trials on a pilot-scale service water system
- Potential economic impact of SDMS data analysis and software tools for safety and efficiency, potential for enabling reduced unscheduled outages, and reducing maintenance and extending the life span of the reactor needs a regular and periodic assessment for keeping things under control.

DOE-NE induced a cable monitoring technology (i.e., the “Shortwatch” cable stressor monitoring technology) in to a SDMS. This enabled the idea of the degradation of air-operated valves. The pioneering ideology (i.e., the Decision Support for Operations and Maintenance) has been applauded and rewarded with a Research and Development (R&D) 100 award.

- Designing the system architecture and demonstration system for SDMS
- Establishing wireless communications via radio-frequency modules and sensors
- Developing a demonstration system for SDMS
- Designing a test-bed preparation and baseline for SDMS with low-temperature process loop and specialized instrumentation
- Developing a computational system for SDMS
- Creating a demonstration system trails series for SDMS
- Developing a test-bed analysis and preparation module for high-temperature process loop
- Designing a demonstration system for data integration in SDMS
- Evaluating economic impact analysis due to SDMS by means of calculating the cost of ownership
- Following a healthy and efficient project management system.

Hence, implementing the SDMS technology toward OLM of NPPs is major progress in the field of risk-informed operations and maintenance of current and future commercial nuclear power reactors.

7.5 Data Handling Technique for Non-Destructive Evaluation

Data handling methods for reliable NDE by Bridgeman, J. and Shankar, R. [138] suggested that periodic inspection and condition monitoring of NPPs can help in an effective erosion-corrosion monitoring of various components of the power plants, resulting in cost-effective management and maintenance. The pivotal areas for consideration are the knowledge of the components requiring inspection and the analysis and management of the huge amounts of NDE data arising from the measurements. The researchers inferred that a utility approach toward the technique of creating a well-organized database of wall thickness measurements will help to analyze the trends in the data for differentiating the erosion-corrosion degraded components. The ability of determining degraded elbows and reducers resulting from analysis of certain specific regions is essentially of great importance. When the authors plotted the distribution of wall thickness normalized by the nominal value the graph showed that most of the differences are found in the regions that are most prone to erosion-corrosion damage. However, for T-sections the trends tough to analyze due to insufficient data and manufacturing differences in the wall thickness. Hence, organizing such data in the database will create a robust statistical conclusion. Therefore, for minimizing the degradation of NPPs, data analysis technologies should be integrated into the planned expert system for component selection and the status should be found for the component-based inspection data. Along those lines, an expert system is always useful in determining the components that need inspection and for disposing NDE data.

7.6 Erosion-Corrosion Management System

Butter L. M. and A. G. L. Zeijseink [139] made a study on Erosion-Corrosion Management System (ECMS) for secondary circuits of the South Ukrainian Nuclear Power Plant (SUNPP). The ECMS developed by KEMA in Netherlands served the following purposes:

- Objects and grid of pipelines that were to be inspected and measured could be selected and stored in each characteristic area
- Ultrasonic equipment was used to manual and semi-automatic loading of the measured thickness
- Based on the quality of the material, water chemistry and operating conditions, minimum thickness, erosion-corrosion rate, and the lifetime area can be calculated.

The secondary unit VVER-1000 at SUNPP has been installed with an ECMS aimed at tackling the erosion-corrosion problems for the following outcomes:

- Enhancing the availability, reliability, safety, and choice of materials, etc.
- Successfully mitigating erosion corrosion by optimizing the selection of water chemistry
- Reducing the times and efforts for inspection and eventually reducing maintenance cost and efforts.

The major goal of installing the ECMS in the three VVER-1000 reactors from SUNPP is to enhance control on erosion-corrosion phenomena in the secondary circuit of the VVER-1000. Controlling corrosion in SUNPP would result in:

- Improved safety
- Reduced cost of repairs of steam generators
- Reduced inspection efforts and time.

7.7 Ultrasonic Intelligent Sensors from CLAMPON

ClampOn Ultrasonic Intelligent Sensors [140] has developed a ClampOn Topside Corrosion-Erosion Monitor (CEM), which is an ultrasonic instrument developed for measurement of wall thickness loss in pipes for a defined area of cross section. The properties of Acoustic Guided Lamb Waves are exploited by

using active ultrasound for detection of any variation in the wall thickness in reference to the values obtained while installation of the system. Nearly 32 transducers generate a grid of signal paths that detect the changes occurred in the wall thickness. Monitoring of the actual and minimum wall thickness is done by tomography, which creates a 3-D visualization of the monitored section. ClampOn topside CEM can be advantageous in the following ways:

- It helps in real-time data collection and measurement of wall thickness
- This system is non-intrusive
- Retrofit installable
- This system has a quite large coverage area
- It provides accurate and high resolution.

7.8 Non-Destructive Technique from General Electric

The NDT technologies from General Electric (GE) [141] provides important data that can be collected and converted into useful information. Along with historical plant data, intelligent software, image enhancement, database management, applicable codes, and additional knowledge help in making informative decisions concerning treatment, mitigation, remainder life, component replacement, or plant operating conditions.

Various monitoring and sensors technologies have been implemented by GE in current industrial applications and are listed below:

- Rightrax installed-sensor system
- Digital radiography
- Ultrasonic phased-array inspection
- Remote visual inspection (RVI)
- Phasor XS
- Apollo, multi-channel, multi-frequency eddy current instrument
- Remote visual inspection with Menu Directed Inspection (MDI)
- USM Go
- Rotating equipment inspection.

The RVI technique used by GE is instrumental in capturing real-time views and images from inside of tubes, pipes, rotating machinery, engines, heat exchangers, tray towers, refractory-lines vessels, etc. The various technologies of RVI are as follows:

- Video borescopes
- Onsite remote visual inspection service
- Pan-tilt-zoom cameras
- NDT equipment rental
- Menu-directed inspection
- Rhythm software.

The UT technology used by GE has been widely accepted as a major non-destructive testing for almost 50 years now and it is used to determine a wide range of defects within a solid material. The various UT techniques are:

- Conventional flaw detectors
- Corrosion flaw detectors
- Phased array flaw detectors
- Corrosion thickness gauges
- Transducers
- Rhythm UT- DICONDE image management platform.

RT is considered to be one of the oldest, a very reliable and proven non-destructive testing methods and it helps in determination of changes in thickness, internal and surface defects, etc. The different techniques of radiography testing are:

- Film radiography
- Computed radiography
- Direct radiography
- Industrial X-Ray tubes & Generators
- 3-D computed tomography
- Rhythm software can acquire image data from computed radiography and direct radiography sources from film digitizers.

GE also pioneers in eddy-current testing (ET), which is a fast, accurate and cost-effective electromagnetic NDT method used for the detection of surface or near-surface flow like metal loss due to corrosion or erosion.

ET testing involves the following techniques:

- Multi-channel/multi-frequency instrument
- Probes
- Special eddy current array probe technology renders wide-area coverage.

GE Inspection Technologies also offer advanced and user-friendly software tools that help in improving the efficiency of decision making processes. The various software tools are:

- Menu-mirected Inspection
- Rhythm-remote expert
- Rhythm-data management.

Furthermore, the installed ultrasonic sensors like Rightrax LT and Rightrax HT from GE have some great advantages such as:

- They provide non-intrusive inspection
- They can be used easily in remote locations
- They need no scaffolding or rigging costs
- They have early warning systems to make the user aware of any potential data on demand

- They have high accuracy
- They ensure the safety of the operator to a much higher level
- They ensure enhanced integrity of asset.

Davies, L. M. et al. [142] made an extensive detailed study about various roles of NDT in CBM of NPP components. Non-destructive testing is widely considered a reliable and viable means of monitoring material degradation in NPPs. Materials degradation if they exhibit characteristics such as:

- Irradiation embrittlement
- Thermal aging
- Fatigue
- Plastic deformation
- Residual or applied stress
- Creep
- Stress corrosion cracking.

NDT technologies have proved to be fruitful and essentially extremely reliable and helpful in determining the condition of the material, thus predicting the degradation in advance, which in turn results in a greater possibility of reduction in the amounts of material loss and the costs of testing the materials. The following considerations are taken into account while monitoring material degradation by NDT:

- The state of the material of the component or the structure that might be affected by the manufacturing processes
- Loads existing outside the normal and transient conditions that needs to be summed up with the initial state of stress and ambient conditions
- Shape, size, and density of the defects that can be predicted by the manufacturing processes and environmental attack
- Building safety margins with respect to the sensitivity of the applied NDT method.

As per the author, the current state of the NDT monitoring material degradation lies mainly on experimental solutions. Hence, in case of an event in the real NPPs, the situation needs to be replicated in a laboratory condition so it can be studied and experimented with using various probable parameters and issue a prediction based on the experimental analysis over a number of years.

GE's System 1 Extender Rightrax corrosion and erosion monitor [143] helps in detecting and reporting wall thickness, thus enabling trending and mitigation of degradation from corrosion and erosion. A CBM system helps in the integration of the most critical piping and other assets. This would minimize the time-based inspection costs due to the development of an online condition monitoring system. This solution technique is currently implemented by the Bently Nevada Asset Condition Monitoring System 1 platform. The System 1 Extender/Rightrax has the following advantages:

- Enhanced reliability
- Optimum availability
- Reduction in lost production revenue.

A typical Rightrax system is a combination of the following features:

- Visit to the site for inspection of piping and/or vessel infrastructure

- Selecting of locations for Rightrax sensors and reviewing of the plot plan drawings and piping and instrumentation diagrams
- The scope, design and the installation plan of the hardware needs to be in alignment with the Environmental Health and Safety and condition-monitoring requirements
- Factory acceptance testing at the S&IT manufacturing plant; sensor-to-software integration test
- Rightrax measurements and System 1 software needs to be installed at a site, commissioned, and integrated.

Hashemian, H. M. [144] made an extensive study on several OLM applications in NPPs and made the following observations:

- By the availability and introduction of fast and reliable data acquisition technologies coupled with proliferation of computers and superior algorithms for processing tons of data and latest advanced software packages, condition monitoring in NPPs can be conducted regularly and efficiently using dedicated equipment installed in power plants.
- The author provides and insight into the review of a class of condition monitoring technologies that are relevant and directly dependent on the existing process sensors while being operational in all modes of the plant functioning including start up, normal operating periods, and shutdown conditions.
- The type of application defines the way in which the data should be sampled, whether periodically or continuously. The steady-state direct current (DC) component of the data is processed for pointing out gradually developing anomalies like calibration changes in process sensors.
- The frequently changing alternating current (AC) component of the data was analyzed for determining the response time of pressure sensors or for measuring the vibrational characteristics of the internals of the reactor, checking blockages inside the coolant system of the reactor and the identify flow anomalies, and rendering other diagnostics.
- The AC and DC components have been integrated together to create an OLM system for the NPPs, and here the author has cited the following OLM implications:
  - Online detection of sensing-line blockages
  - Response-time testing of pressure transmitters
  - Online calibration monitoring of pressure transmitters
  - In-situ cross calibration of temperature sensors
  - Equipment condition assessment
  - Predictive maintenance of reactor internals
  - Fluid flow monitoring.

7.9 Acoustic Emission Technique

He, Y. and Shen, Z. [145] conducted detailed research for predicting cavitation erosion in NPPs using an AE technique. The following inference could be drawn out of the research:

- The author applied acoustic emission technology in a direct manner for determination of cavitation erosion rate.
- While conducting the cavitation erosion experiments, the surface topography of the A-36 sample was observed. The characteristic feature of the surface topography helped in identifying the stages of development of the cavitation erosion processes with respect to the rate of loss of mass of the sample.
- Characterization of the acoustic emissions caused by virtue of the cavitation erosion was given by higher amplitudes, high frequency, and impulse.

- The AE signals obtained can be de-noised by implementing the wavelet-based de-noise mechanism that is achieved by reducing the disturbance from the environment.
- By inducing the parameter analysis method, the root mean square and the mean energy of the acoustic emissions were analyzed.
- It was observed that even though the acoustic emissions caused by cavitation erosion exhibit equivalent strength root mean square, the mean energy showed a strong positive correlation with the rate of loss of mass due to cavitation erosion, which evidenced the plausibility of the procedure for detection of cavitation erosion by administering acoustic emission as a technique.

7.10 Ultrasonic Monitoring

Ultrasonic monitoring has been successfully implemented in many industrial pipelines and pressure vessels for detecting corrosion erosion phenomena. Corrosion erosion phenomena result in gradual loss of wall thickness and thus results in decreased life span of piping systems. F. Honarvar et al. [146] in their study on ultrasonic monitoring have pronounced three major outcomes arising out of wall thickness they are (1) it affects directly the cost of replacement of the component, (2) it also hampers the rate of production during the replacement work, and (3) it might also lead to catastrophic failure, which eventually raises the risks due to the safety and environmental factors.

The authors have implemented two signal processing techniques namely, cross-correlation technique and model-based estimation technique for evaluation of the rate of thinning in the wall of the piping systems in NPPs due to erosion-corrosion. These two techniques were instrumental in estimating the thinning rate change as small as 10 μm/year within 15 days with a confidence interval of 95% of ±1.5 =μm/year. The results obtained from model-based estimation technique are marginally more precise than those derived from cross-correlation algorithms. Due to the simplicity in the algorithm, being numerically more stable and being less expensive in terms of computation time, the cross-correlation technique is preferred over the model-based estimation method for many industrial application.

7.11 An Approach by IAEA

According to a report by IAEA [147], there are three basic functional requirements of light water and heavy water nuclear power reactors:

- There must be assurance about the structural integrity and operational status of the plant at all times
- Considering the radioactivity, the design of the plant must have optimal permission for access into operation and maintenance
- Controlling and safe disposal of the wastes from the plants must be done in compliance with the established regulations.

IAEA carried out a coordinated research project from 1986 to 1991 on water chemistry known as WACOLIN (Investigations on Water Chemistry Control and Coolant Interaction with Fuel and Primary Circuit Materials in Water Cooled Power Reactors), which distinctly revealed the impact of water chemistry on corrosion. IAEA concluded that monitoring water chemistry parameters was essentially necessary in real time, with utmost reliability and the monitoring needed to be done to maximum precision. OLM of the plant operation are necessary so as to make sure that the plant is fully operational within its technical specifications, the plant is responding accurately to the actions undertaken by the staff operating the plant and also long-term trends might lead to operational malfunctions, thus helping in early detection of any potential risk or problem.

The broader perspective of such detailed information of the behavior and performance of the plant results in getting data for adequate and sufficient control of the plant operation and for getting data for performing mathematical modeling, eventually leading to the design of expert systems.

The current methods of water chemistry monitoring and sampling has certain drawback such as:

- A non-standardized sampling procedure might lead to probable changes in the properties and composition of water
- There might be a time delay in collecting valuable information
- The obtained information might not be fully complete.

These problems can be and have been effectively mitigated to certain extent by implementing high temperature monitoring devices that have been well tested in pilot plants and test reactors and even commercial reactors.

The major essential features of the WACOL (High-temperature On-line Monitoring of Water Chemistry and Corrosion) program are as follows:

- Identifying the critical parameters
- Maintaining a consistent database inventory of the current OLM techniques
- Suggesting new monitoring techniques with the potential of being used in operational plant conditions
- Gathering recommendation an expert ideas and comments regarding the preferred location of sensors and equipment
- Getting advised on the calibration of the instrument and the verification and validation
- Assessing relevant data.

The first Research Coordination Meeting on WACOL suggested eight specific types of OLM technique, such as measuring:

- Electrochemical potential
- Conductivity at high temperature
- pH values at high temperature
- Chemical species and dissolved gases
- Particles via optical methods
- The rate of growth of crack
- The electrochemical noise
- Impedance.

The second Research Coordination Meeting decided to implement the OLM techniques on the four different types of plant namely:

- Primary side of PWRs
- Secondary circuit of PWRs
- BWRs
- Research reactors.

The final WACOL report talks about the state of the art OLM techniques of water chemistry and corrosion in operating reactors and the technical details of important contributions made by participants towards the development and qualification of new monitoring techniques.

Another IAEA report [148] regarding OLM for enhancing the performance of NPPs via instrument channel monitoring, OLM could be defined as and method run by automation for monitoring the output signals of an instrument and assessment of the calibration of such an instrument while the plant is still operational without causing any hindrance to the monitored channels. In simple terms, an OLM system can be rightly referred as a signal validation or data validation system. Technically, the OLM system has no idea regarding the layout of the channel. A digitized signal is sent, which is received by the OLM system from a computer from the plant, a historical file, or from a real-time data acquisition system. Even though the instrument channel on the OLM system produces milliamps of or voltage output, the signal at the receiver end is scaled up to probable process units like pressure, temperature, or percentage.

Nuclear power industry focuses on OLM system technology so that the time based calibrations can be replaced with condition-based calibrations. This results in reduction of personnel radiation exposure, as low as reasonably achievable, save costs due to calibration and enhance the safety of the plant and the reliability of the instruments.

Generally, the conventional calibration of an instrument follows two steps such as:

- Calibration status of the instrument is established. This step is achieved by applying a series of known inputs covering the operating range of the instrument.
- If there is a necessity for calibration, then it needs to be done. When an instrument does not meet the acceptance criteria, then the calibration is done by applying the same series of input signals as in Step 1 while adjustments are done on the output signals for compliance with the acceptance criteria.

OLM tracks the output of the instrument channels for determining drift, bias errors, noise, and other anomalies while functioning over the fuel cycle. OLM system has the following advantages:

- Eliminating unnecessary calibrations leads to reduction of radiation exposure
- Reducing the probability of damage to the instrument while calibrating it
- Helping during outages in plant to reduce the time required and the associated costs of major sensor calibration activities
- Providing continuous availability of assessment data of the calibration status of important sensors
- Monitoring sensor interrelationships to identify the abnormal plant conditions
- Helping during the early warning of sensor or component degradation and assessing the condition of plan components
- Compressing the information regarding sensors to ensure they receive attention
- Providing faster reactions due to implementation of OLM systems in case of anomalies in plant components
- Constantly monitoring sensors, systems, and components of the plant in a real-time condition
- Validating and verifying signals for other computerized tools.

OLM systems are efficient when used with data acquisition and transient data analysis systems that help obtain online capability for performing reactor diagnostics, measure core barrel vibration frequency, estimate flow rates of fluids, and detect flow blockages and anomalies in the flow in the reactor coolant system. It also helps in the measurement of the response time of sensors and the moderator temperature coefficient while the plant is still operational. OLM systems are instrumental in monitoring vibrational and loose parts of the plant components and help in detection and determination of line blockages, leaks, and voids.

7.12 Wall Thinning Evaluation Method

W. Kastner et al. [149] in his study on establishing a calculation code for prediction of erosion corrosion mechanisms in NPP piping systems came up with certain inferences:

- Wall Thinning due to Erosion Corrosion (WATHEC) model was used for predicting such erosion corrosion phenomena in NPPs. But it has been cited by the author that after the failures at Surry 2 and Trojan, the WATHEC model was used in a number of NPPs, and the verification and validation of the results have been performed by means of NDE.
- These observations gave the confirmation that the computer program was reliable and also the piping systems in plants built Siemens/KU were less susceptible to erosion corrosion.
- The susceptibility is low because of the continuous feedback that is received from the design, construction, and operation, and during this process no material loss was detected.
- This kind of model is quite handy and useful to use in plants where all of the vital parameters have not been taken into account, like flow conditions or pH levels.
- Using such a model helps in minimizing the measurement and monitoring efforts and time and also it helps in enhancing the life expectancy of the components of the piping systems as a whole.

7.13 Condition-Based Maintenance Technique

CBM had been observed as an upcoming trend that is being implemented in the information technology (IT) environment of NPPs for monitoring erosion-corrosion mechanisms. H. Kim et al. [150] suggested a CBM framework that has already been successfully implemented in NPPs of Korea and fossil-fueled plants. The most important aspect of CBM methodologies is to make sure that an optimum amount of superior quality sensors are used for precise management and data collection. Furthermore, they suggested that such a framework and techniques could be efficiently used for in-situ thermal efficiency management. The authors have talked about specifically ways and means for determining performance degradation and techniques for diagnosis, prognosis, and operator-friendly decision making modules.

As the idea of in-situ thermal efficiency management has not yet been internationally accepted and also its accuracy varies depending upon the proficiency of development, hence it has been suggested to take a preparative measure of creating an administrative back up so that the in-situ efficiency management can imbibe into routine operation.

Lai, H. -C. et al. [151] in their research paper described that the various online corrosion monitoring techniques that are currently used in the NPPs in Taiwan. Those monitoring techniques respond and conduct applications ranging from water chemistry control to monitoring processes and optimizing the behavior of material in BWR and PWR environments. Along those lines, simulating crevices in steam generator tubing, electrochemical potential monitoring in PWR primary water, and detecting corrosion in service water loops are still in the preliminary stages of their inceptions.

By virtue of continuous online corrosion monitoring systems, electrochemical interactions contributing to material degradation can be constantly scrutinized thus minimizing its impact, and the structural and functional integrity of the properties of the plant and its components can be maintained.

7.14 Using RAMEK Code as an Online Monitoring Approach

V. N. Lovchev et al. [152] made a detailed thorough research about various improvements and optimization techniques for monitoring erosion corrosion where they stated that the main focus for implementing the Comprehensive Program is to find solutions to provide optimum safety to nuclear

power systems (NPSs) that encounter sudden failure of their components and equipment. The Comprehensive Program ensured the following advantages towards monitoring:

- Improved safety features of NPSs as it helps in prevention of accidents due to erosion corrosion
- Cost effective monitoring, diagnostics, and prognosis activities
- Enhanced economic gain due to lesser number of forced disconnections and outages of the equipment, leading to a higher capacity utilization factor because of erosion corrosion-induced failures and accidents
- Minimum costs for repairs on preventing and removing consequences
- Improved and better life expectancy of NPS piping systems and equipment in the NPS secondary circuit coolant system.

Along those lines, certain calculated-analytical substantiation and correction of standard programs have been developed for ensuring a reduction of excessive volumes of operational surveillance of the elements used in NPPs. These remedial and mitigating measures must be done with qualification of the RAMEK computation code.

An informational-analytical database of array have been designed that comprises of results from operational surveillance of metal, operating factors, properties of the metal, and 3-D computer models for simulation of the configuration and geometry of the flow.

These data have helped in creating a computer atlas of identification maps that assist in determining the location, dimensions, and the identification number of each element entered in the general list.

S. S. Palusamy et al. [153] invented a corrosion-erosion trend monitoring and diagnostic system, which has been patented under United States Patent. Their invention was basically a system that would help analyze the containment and integrity of a containment system, which comprises of storage of data for inspection, characteristic data, and a processor for evaluating the inspected data. The invention also has a data acquisition system, which continuously records data about the wall thickness on a regular basis. The wall thickness data after validation is stored as inspection data in the data storage location. The current pipe wall integrity is evaluated by means of the stress calculated from the characteristic data under operational conditions and material properties by help of the data evaluation processor. Furthermore, the data evaluation processor also lays the foundation of future prediction of wall thickness by analyzing the trend in change of wall thickness. Therefore, this trend in the change of wall thickness is most likely to be used for creating a high-priority indication of maintenance for the inspected component.

7.15 Impedance Monitoring Approach

J. Ryl and F. Darowicki [154] carried out research on impedance monitoring of carbon steel under exposure to cavitation erosion for predicting the mechanism. The researchers found that joint erosion-corrosion in samples exposed cavitation coupled with corrosion degradation contributed to nearly 70% of the net loss of mass of the steel sample. From the experiments the authors found a small shift of current i_{cav} flowing through the system could be correlated with a mass loss function mean depth of penetration rate. The early stages of exposure with subsequent stabilization with time revealed a great variation of these factors. Microscopic characterization revealed that the cavities were produced after initial cavitation exposure. Subsequently, a uniform surface sample failure was observed when the cavities got enlarged.

Dynamic electrochemical impedance spectroscopy technique gives a scope for a creative approach towards the evaluation and monitoring of cavitation erosion-corrosion degradation. Along those lines, there is evidence of the impact due to cavitation exposure on the factors responsible for impedance and also the rate of failure of the surface of the sample. Reversible outcomes due to the degradation of the corrosion product layer and an increased mass flow rate have been observed due to impedance.

7.16 Equipotential Switching Direct Current Potential Drop Approach

K. H. Ryu et al. [155] suggested the implementation of an Equipotential Switching Direct Current Potential Drop (ES-DCPD) system, which could be used effectively for predicting the rate of loss of thickness of the walls in the piping systems. The inspection from Ultrasonic Testing appeared to be in good agreement with the ES-DCPD. It has been observed that the ES-DCPD technique can be applied to a wide range of area for identifying the thinned location. The Narrow Range Monitoring (NaRM) can be utilized for a localized area. When it comes to precise prediction of the location of maximum wall thinning, NaRM is a better and more-advisable method than online UT method. The ES-DCPD NaRM has a better resolution and sensitivity. Its performance is quite stable and reliable under different temperature and radiation environments.

Simulation of the FAC environment with greater acceleration was made possible by constructing The Seoul National University FAC Accelerated Simulation Loop (SFASL). SFASL was instrumental in controlling and monitoring the factors responsible for causing FAC. Electrodes were developed that could be used for verification of the electrochemical conditions in SFASL. The FAC trend and the simulation of the wall thinning were done by implementing online ES-DCPD. By implementing the current focusing technique, ES-DCPD causes less peripheral interferences. There is a need for a compact fixture for ES-DCPD probes to avoid vibration in the pipes in case of long time applications. Once the ES-DCPD is successfully deployed, the ES-DCPD can be used in Canada Deuterium Uranium feeders, buried piping systems, and in the secondary circuits of NPPs.

The loss of material (i.e., the thickness of the wall) is usually a result of corrosion erosion phenomena occurring inside the piping systems. A. Saluja, et al. [156] observed from monitoring and inspection experiences that at a point when the thickness reaches a critical level, the tensions are no longer supported and leakage or rupture can be found. This makes monitoring inevitable for ensuring reliability and functionality of the pipeline system. Online corrosion monitoring technique being a direct measurement method, is known for its reliability and precision. Nowadays, UT sensors capable for withstanding high temperatures are used for measuring corrosion rates very accurately. Database management systems and data storage have made transmission, storage, and evaluation of data essentially possible. This metamorphosis of reactive into proactive means of maintenance through non-intrusive OLM has resulted in remarkable cut down on operational costs and it ensures better and safe environment to work in NPPs.

S. Uchida et al. [157] worked on various evaluation methods for corrosion in cooling systems in NPPs and hence they came up with the following conclusions:

- As one out of the five step FAC evaluation procedures, a method of calculation was proposed based on the static electrochemical and dynamic double oxide layer analysis.
- The static electrochemistry model paved the way for calculating anodic and cathodic current densities, as well as the electrochemical potentials.
- An electrochemistry model was established based on the thickness of the oxide film and its behavior. Furthermore, the electrochemical model obtained was used to determine the cathodic current resistances from the bulk to the surface and vice versa by using anodic current.
- Under different corrosive conditions, the two models were combined to obtain the electrochemical potentials and the rate of local corrosion.
- Iit was observed that there was a good agreement between the coupled and measured models.

7.17 Electromagnetic Acoustic Resonance Technique

In their study, R. Urayama et al. [158] applied electromagnetic acoustic resonance (EMAR) for OLM of thinning of the wall of the pipe within a real-world high-temperature environment and the probability of quantification of the wall thinning was discussed. They made the following inferences form the study:

- Within the couple of tests conducted using pipe wall-thinning test equipment, the progressive growth of wall thinning was observed at 165°C and a difference in the rate of thinning under various fluid flow conditions was observed.
- The difference between the EMAR measurement and the microscopic measurement resulted in 0.06 nm.
- Superposition of the n^{th} compression (SNC) analysis of the wall thinning process led to waveforms that showed attenuation at SNC peak intensities and multiple peaks hinting at a change in the shape of the bottom surface.
- It was quite possible to take measurements without peeling off the pipe coating and probes could be easily held by probe magnets at the measurement location.

Using EMAR and SNC analysis techniques yielded the following advantages:

- As wall thinning could be measured to the order of 0.01 nm, the evaluation of wall thinning can be made to precision.
- These methods can be used quite effectively for verification, clarification, and the verification of adequateness of representative locations for measurement of wall-thinning mechanisms in the piping systems.

7.18 Condition-Based Inspections of Passive Components Enabled through Smart Online Monitoring

The Light Water Reactor Sustainability (LWRS) Program, funded by the U.S. Department of Energy's Office of Nuclear Energy, aims to provide scientific, engineering, and technological foundations for extending the life of operating LWRs. This program involves several goals, one of which is ensuring safe operation of NPPs' passive components, such as concrete, piping, steam generators, heat exchangers, and cabling [159].

Within the LWRS Program, the Advanced Instrumentation, Information, and Control (II&C) Systems Technologies Pathway conducts targeted research and development to address aging and reliability concerns with the legacy analog instrumentation SSC and related information systems of the U.S. operating LWR fleet. This work involves two major goals: (1) ensuring legacy analog II&C systems are not life-limiting issues for the LWR fleet, and (2) to implementing digital II&C technology in a manner that enables broad innovation and business improvement in the NPP operating model. Resolving long-term operational concerns with II&C systems contributes to long-term sustainability of the LWR fleet, which is vital to the nation's energy and environmental security [160].

At the same time, EPRI has established a separate and complimentary research Long Term Operations (LTO) program to address roughly the same issues of aging and degradation of existing nuclear fleet. One of the working areas of the LTO program is I&C and IT (including OLM of critical equipment) [161]. The R&D scopes and objectives of this working area are to develop a highly automated condition monitoring and assets management system designed to detect anomalies, automate diagnostics, maintain a repository of equipment failure signatures, forecast remaining useful life of the nuclear plants assets, and provide guidance for optimized maintenance and investment decisions.

To coordinate the collaboration between the programs, DOE-NE and EPRI executed a memorandum of understanding to "establish guiding principles under which research activities (between the LWRS and LTO Programs) could be coordinated to the benefit of both parties." [161]

Both programs rely on a series of pilot projects, which are being a part of the larger strategy, yet small enough to be implemented within one utility to demonstrate and validate the underlying principles of the

proposed technology. The technology implemented within a pilot project is scalable to the whole industry.

Operations and maintenance costs comprise approximately 60 to 70% of the overall generating cost in legacy NPPs [162]. Replacing inspection-based maintenance with condition-based maintenance has the potential to reduce operating cost and advance safety. The current practice involves performing maintenance of active components through maintenance rules and passive components through aging management programs [163].

The Generic Aging Lessons Learned report [163] lists around 50 AMPs, with the overwhelming majority relying on periodic inspections during planned downtime. The periodic inspections are usually performed using NDE techniques, which require extensive logistic.

It is widely recognized in nuclear industry that the cost of NDE logistic is higher than the cost of NDE. For example, to perform NDE on piping systems, insulation removal and scaffolding often require access to bare piping. For buried piping, pipe's excavation is often the only option to get access. After all of these efforts, very small number of inspections produce something that requires action. Unnecessary maintenance is one of the major cost drivers in operation of nuclear power plants and is a major motivator behind the industry's initiative —"Delivering the Nuclear Promise: Advancing Safety, Reliability and Economic Performance" [164].

Acknowledging that the current situation in market regime is unsustainable [164], the initiative aims to achieve 30% reduction in nuclear power plants operating cost while maintaining the highest standards of safety. It is also acknowledged [164] that the industry needs to rethink operating practices, make bold efficiency improvements and innovation, and redesign their maintenance practices to improve efficiency and effectiveness while continuing to advance safety and reliability. Solving these problems will require paradigm shift from periodic inspections of sample locations to continuous OLM of some components and need-based inspections.

Development of such OLM systems for piping components along with an information integration framework is the goal of the coordinated pilot project pursued by Idaho National Laboratory (INL) and EPRI. This pilot project aims to develop and validate an integrated multi-sensor OLM system capable of inspecting large piping components in secondary systems and providing a pathway to move from inspection-based maintenance to condition-based maintenance. The OLM system is expected to provide current estimate of pipe wall thickness along with the remaining useful life estimate. Such a system could provide the following benefits:

- Improved capacity factor by reducing unplanned and planned outages
- Improved safety through fewer unexpected failures and less repairs
- Optimized equipment operation and maintenance through early identification of faults
- Improved fault diagnostics through increased availability of data relating to faults and shared knowledge of fault behavior based on case studies and expertise
- Extended lifetime of existing NPPs by having an increased understanding of the current health of the plant components and remaining useful life estimation
- Minimized human factors effects on non-destructive testing.

The OLM system will have a larger area of coverage than the current NDE techniques and will aim to answer the question that current aging management programs are facing—where to inspect or identify inspection locations. There is no technology currently available that would pinpoint which piping component need to be inspected. This is the major reason for redundant inspections.

The idea of condition-based maintenance has been embraced by many industries since 1980s. A classic example is an introduction of tire-pressure monitoring system in automotive industry in

mid-1980s, which is mandated now in U.S. since 2007. As shown in Figure 10, the old practice of regularly checking the tire pressure once a month is currently replaced with tire-pressure sensors that alert the driver when the tire in under or over inflated, thus replacing periodic checks and adding to safety and time savings. As shown in Figure 10, more advanced tire pressure monitoring systems also identify the location that needs to be inspected in addition to identifying the presence of the problem.

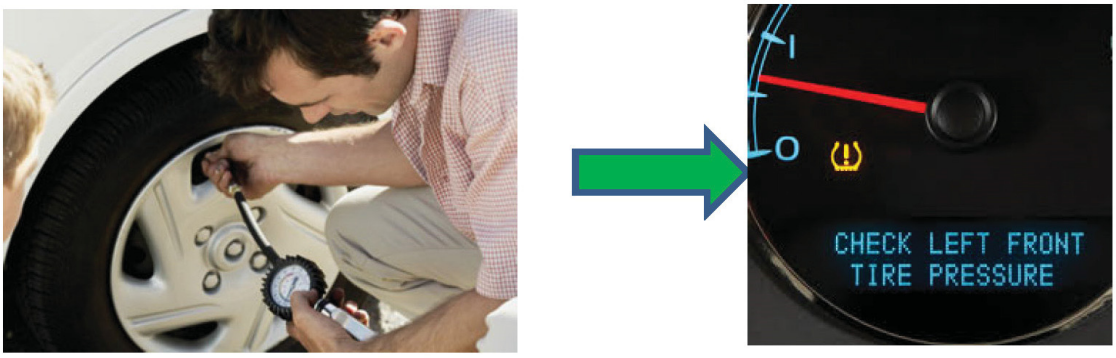

Figure 10. From periodic maintenance to condition-based maintenance.

The proposed joint research project seeks to develop an online piping wall thickness monitoring system that will be able to replace and/or complement periodic inspections alerting maintenance personnel about significant changes in pipes wall thickness and identifying locations where that change occurred.

The project time line is expected to be 2016–2020 with the whole project divided into four phases: definition phase, development phase, benchmark testing phase, and utility testing phase. The expected outcome is a prototype of online piping wall thickness monitoring system, guidelines, and technology transfer.

The proposed project will involve collaboration between INL, EPRI, and utilities. INL will play a major role in this project, leading design and development of the integrated OLM system, performing technical projects, and completing project deliverables. EPRI will participate in development of technologies for this project as a technical advisor. They will provide expert review of project plans, project results, and project reports. EPRI will also perform the development of their own technical approaches and share data collected from existing OLM technologies. In addition, EPRI will facilitate utility and industry engagement through their network of utility contacts and sponsored industry meetings. EPRI will also form a Utilities Technical Advisory Group specifically for this project to leverage utilities' feedback and participation.

A flowchart of the proposed joint project, which is called "Condition-based inspections of passive components enabled through smart online monitoring," is shown in Figure 11. The project has four phases: definition phase, development phase, demonstration phase, and utility-scale testing phase.

During the whole project, EPRI and INL will participate on a technical advisory working group that will oversee these studies. If successful, the OLM system is expected to be adapted to other piping components in existing LWR. Also, the developed system may serve as a prototype system to be adopted for future generations of LWRs.

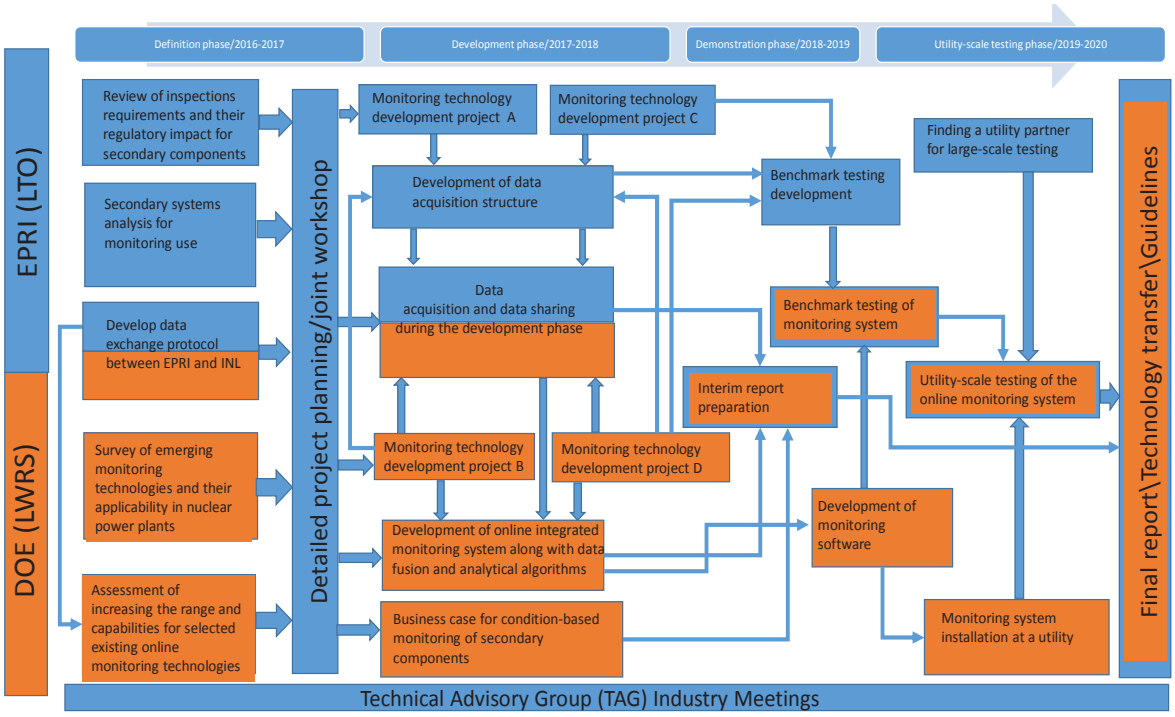

Figure 11. Development of condition-based inspections of passive components enabled through smart online monitoring.

7.18.1 Definition Phase

The definition phase, which will last about 6 months, include five activities denoted by five different boxes in Figure 11. EPRI and INL each have two activities in this phase in addition to one shared activity.

During the definition phase, EPRI will perform a survey to review inspection requirements for some specific piping components, such as raw water piping, and their regulatory and potential long-terms operations impacts for commercial LWRs. This survey will identify the most labor-intensive and costly aging management programs that can benefit from OLM by optimizing the number of scheduled inspection or by performing condition-based inspections. The survey will also identify compelling issues and needs for R&D activities. The ultimate goal of this survey is to identify major cost drivers in raw water piping inspections and root causes of cost drivers in periodic inspections.

EPRI's second activity during the definition phase is performing analysis of piping geometries and how they lend themselves to OLM techniques. This information will be used to identify technology and research gaps as well as components that will benefit most from OLM and condition-based inspections. Different piping geometries require different monitoring techniques and the goal of this activity will be to identify the number of different piping geometries that will require different monitoring approaches,

At the same time, during the definition phase, INL will conduct a survey of emerging measures, sensors, and algorithms for new OLM technologies, to complement or replace currently used NDE techniques.

Along with the new emerging technologies, INL will determine the potential to extend the range of established OLM technologies, such as guided waves (GW) in NPP piping systems. This activity will be performed in close collaboration with EPRI's NDE department, which has extensive experience in applying GW technology and collecting numerous data sets on piping components subjected to different degradation mechanisms. Some of these data sets will be transferred to INL to develop advanced signal

processing and noise cancellation algorithms that can extend the range of GW technology applicability, for example in situations when there are multiple pipe pitting and reflections from complex geometries.

To conduct effective data exchange between EPRI and INL, both organizations will be involved in a joint activity to develop a data exchange protocol. This data exchange protocol will be used throughout the whole project to share data, results, and software.

The development phase will culminate in a multi-day project planning workshop where INL, EPRI, and utilities define specific piping components that would benefit from OLM. The information collected during the definition phase will also be used to develop a business case for online health monitoring for presentation to interested utilities. The workshop will also define specific monitoring development technology projects that will be pursued by INL and EPRI.

7.18.2 Development Phase

Having defined the system's components, the project will move into development phase that will last for 2 years. During this phase, INL and EPRI each will develop two OLM techniques that would address the technology gaps identified during the definition phase. These monitoring technology development projects are designated as A, B, C, and D in Figure 11. Since the NPP's piping has complex geometries, it is impossible to offer a single-sensor modality that would be able to collect data from the whole piping component. Taking this into account, the complete coverage of the piping system with OLM sensing will require several sensor modalities applied to different geometries, such as elbows, flanges, valves, and tees. This justifies the need for multiple monitoring development projects that will draw ideas from reviews performed during the development phase. The exact number of these technology development projects will be defined after the development phase is complete; however, the current thinking is that four new monitoring technologies, combined with already existing technologies such as GW, will be sufficient to monitor the entire piping system.

During the development phase, EPRI will establish data acquisition structure that would be able to collect data from different sensor modalities. Currently, different OLM technologies collect data in different formats, with different sampling rates, and with different accuracy. A common data acquisition structure will be needed to reconcile these data streams and make them usable in the OLM system.

INL will be responsible for developing an online integrated monitoring system, which will perform data processing, data fusion, and decision making to provide end users the status of the piping system, specifically evaluation of wall thickness and the remaining useful life of pipes. INL has extensive experience in developing data fusion algorithms that combine time series, visual, and categorical data to provide an overall index of system's health. INL also has experience in developing pattern recognition-based decision-making algorithms, which allow identification of equipment failures or precursors to failures. The integrated OLM system will interface with the data acquisition structure by accessing reconciled data files created by the latter.

During the development phase, both organizations will acquire and share data collected from the developing technology. This data exchange will be a critical part of the INL work on integrated OLM system.

Also, during the development phase INL will develop a business case condition-based monitoring system, describing the economic benefits for the targeted piping systems. A utility partner will be enlisted to provide actual activity and cost data as a baseline, as well as to validate the projected savings. A report will be developed that will present generalized benefits for a range of typical industry piping inspection scopes.

At the end of the development phase, a milestone report will be published detailing the prototype of OLM system structure and functions.

7.18.3 Demonstration Phase

The demonstration phase will test and validate the underlying principles of the OLM system, such as integration of new sensor modalities and existing technologies, the data acquisition system, data fusion and decision-making algorithms.

During the demonstration phase, the prototype system and software will be jointly tested by EPRI and INL using different piping configurations and conditions. The prototype of OLM system will be tested at EPRI's piping mock-up, located in Charlotte, North Carolina. EPRI has both above ground and buried piping mockups that can be used to test different monitoring technologies. During this phase, EPRI will be responsible for developing benchmark testing structure and protocols, such as different piping configurations and operating conditions.

INL will be responsible for development of monitoring software that will be used to collect and process data from the prototype monitoring system. The deliverable for this phase will be a prototype OLM system.

7.18.4 Utility-Scale Testing Phase

EPRI's role will be to establish the host relationship with a utility partner and manage the overall testing activity. INL will be responsible for installing the OLM system at a utility partner. Both organizations will jointly test the system. Both organizations will develop guidelines, publish final milestone report, and participate in technology transfer. The conceptual representation of the system's output is shown in Figure 12. A detailed description of the Structural Health Monitoring Framework is available in Joint Research Plan on Structural Health Monitoring with the Electric Power Research Institute, INL/INT-16-38821, Revision 0 [219].

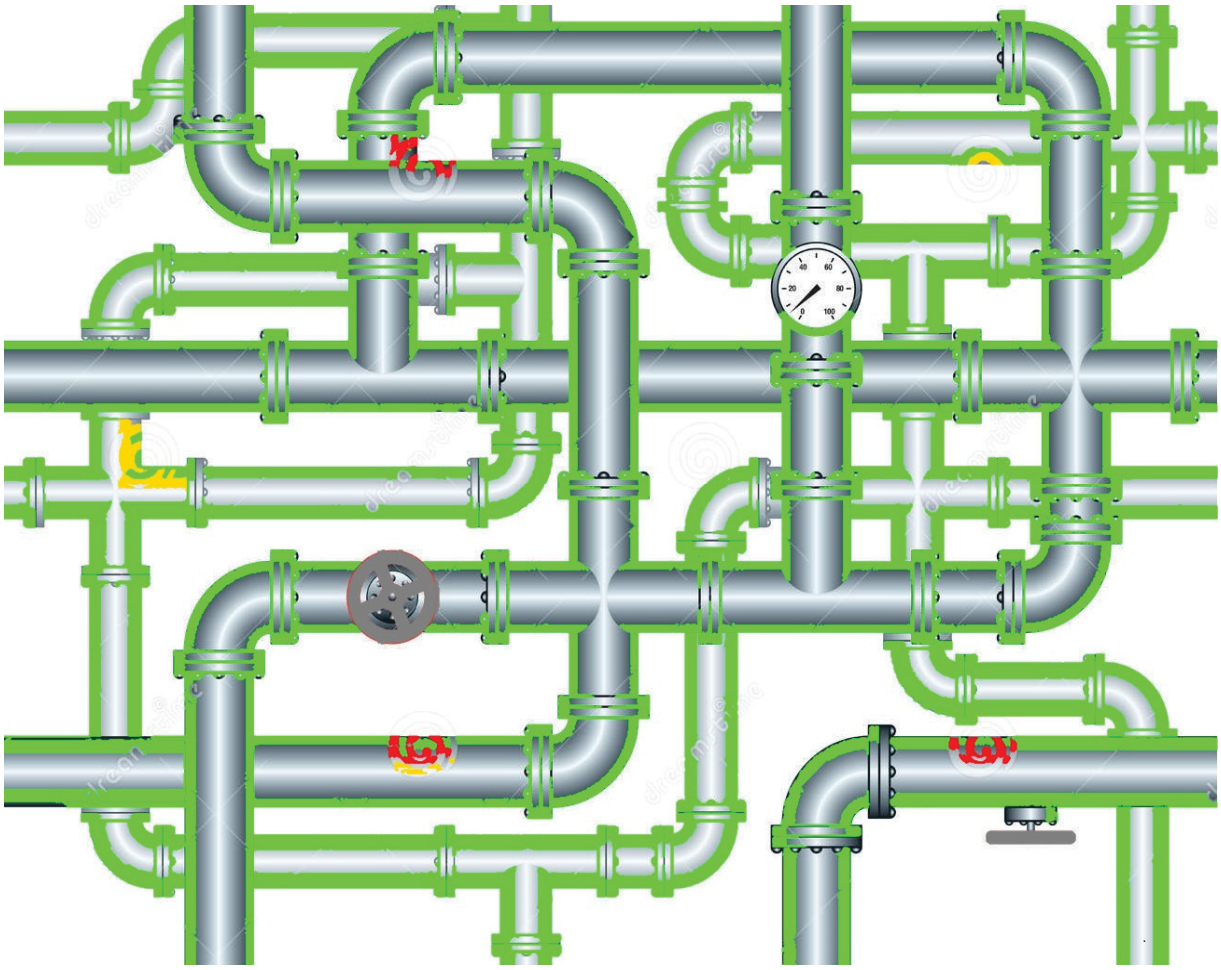

Figure 12. Conceptual representation of the online monitoring system's output. The wall thickness is color coded with green representing the safe thickness, yellow-borderline thickness, and red representing the wall thickness close to safety threshold, which requires immediate attention.

8. GUIDED WAVE TESTING

8.1 Introduction

As a means of defect detection technology, guided waves testing have been successfully implemented in the field of non-destructive for several years now [165]. The velocity of the guided waves is directly dependent on the thickness of the material that are characterized by the dispersion behavior of the modes of the guided waves. Hence, the difference in the thickness of the component will give a variation in the time of arrival of the guided wave. The test conducted by the Imperial College in London has proved the applicability of the utilization of shear horizontal waves for finding out the average thickness of a plate along a line between the two transducers. The work done helped generating a methodology for extraction of the value of the thickness measured by shear horizontal-guided wave signals, which were characterized by temperature.

8.2 Guided Waves Used as an NDT Method

Guided waves testing technology is a signal-processing tool for non-destructive testing of piping systems in power plants. F. Cau et al. [166] conducted extensive research and came up with the following conclusions:

- They conducted the research in case of inaccessible pipes by implementing a diagnostic system that was based on neural networks for NDT with ultrasonic waves
- Finite element method was deployed for obtaining desired dataset for training, validation, and testing of the signals,
- Preprocessing of the signals were done to make the signals suitable as input for the neural networks. This was performed by means of fast Fourier transform and principal component analysis methods.
- The affected region on the pipe had been torsional wave mode excited by means of realistic, non-symmetric faults with a variation in the parameters, such as axial position, axial length, angular amplitude, and thickness,
- Under numerical simulation of defects, the preliminary analyses reveal that the time taken by the reflected signals is proportional to the position of the defect but independent of the entity of the fault. This idea of the time value helps to determine the location of the notch.
- The classification error distribution of various parameters, like defect angular amplitude, thickness of defect and the axial length of defect, was good and the future research demands the need of developing a signal processing package for the NDT instrument.

8.3 Guided Waves Used as Ultrasonic Echoes

G. Acciani, et al. [167] investigated and suggested an automation technique for detecting the sizes of defects caused by corrosion in non-accessible piping systems. Such an approach is characterized by the analysis of the reflection of the ultrasonic echoes by superficial flaws present in the pipes. The ultrasonic reflected signals are processed to obtain a set of reliable features, which are eventually extracted by wavelets transformation and the selection is done by means of a filter method with subsequent genetic algorithm. These set of selected features are then fed into a couple of multi-layer perceptron, which provides the angular and axial dimensions of the flaws. Making use of ultrasound waves yields the following advantages:

- It helps analyzing long piping systems
- There is a significant reduction of human efforts via automatic diagnosis
- The selection of mother wavelet helps in the selection of features suitable for representing signals in the problem under consideration. The selection methods are also fruitful in storing information about the sizes of the defects and it leads to an initial reduction that helps in retaining the most significant coefficient obtained from the signals.

This approach is instrumental in the detection and evaluation of the dimensions of superficial defects in pipes whose shapes do not have a specific dimension. Moreover, this approach is automated thereby, reducing human efforts and obtaining the defect dimensions by using the adaptive algorithms from neural networks.

8.4 Ultrasonic Guided Waves Used for Structural Health Monitoring

An optical fiber guided laser ultrasonic system was developed by H. Lee, et al. [168] for creating a baseline-free method for detection of damage for the structural health monitoring (SHM) of insulted piping systems under high temperature conditions in NPPs. This method employs an optical fiber with a specially designed lens for focusing and a fixture set up for delivering a Nd:YAG pulse laser to a target excitation point which is embedded for generating ultrasonic wave. A second optical fiber is connected between a fiber vibrometer and a point for measurement of ultrasonic wave sensing. The performance of the system was tested at varying temperatures of up to 300°C. Using the axisymmetric behavior of multiple wave propagation paths in pipelines a baseline-free damage detection algorithm was designed. The baseline-free damage evaluation system has been tested in case of intact as well damage situations of pipe specimens in NPPs.

8.5 Cylindrical Guided Waves Approach

Preliminary and early prediction of the degradation process in the pipeline systems in NPPs can help prevent several catastrophic accidents. Structural health monitoring of piping systems is one of the major challenges in the current scenario in NPPs.

Ahmad and Kundu [169] conducted extensive research on a new technique for detecting damage in pipes, by propagation of cylindrical guided waves through piping systems. They employed continuous wavelet analysis for identification of defects in the pipe networks when the pipes are free in air or vacuum as well as when they are embedded in the soil. They made the following conclusions:

- Detection of anomalies can be done properly by the right selection of wavelet functions and scaling aspects
- Efficient study of the integrity of underground piping systems can be achieved by implementing daubechies, symlet, and meyer wavelet functions.

8.6 Ultrasonic Wave Propagation Imaging Technique

C. Lee and S. Park [170] investigated the visualization of damage of pipeline structures by using laser induced ultrasonic waves. Ultrasonic wave propagation imaging technique was used that uses a Q-switched Nd:YAG pulsed laser system and a galvanometer-based laser scanner. The dispersion characteristics of the Lamb modes of the pipes were studied where the fundamental principle was based on the group velocity dispersion curves in the frequency range of 0 to 500 kHz. The A0 mode was dispersive while the S0 mode was constant under 250 kHz. The two frequency ranges were separated using digital filters. The authors investigated the notches and the decrease in thickness for simulation of cracks and erosion, respectively. Irrespective of the shape and geometry of the piping systems, the ultrasonic wave propagation imaging images were obtained successfully. Three cases were investigated. They are:

- The notch at the site of the welded joint between the two straight pipes were examined at ambient temperature conditions
- The notch on the welded joint between the straight and curved pipes were investigated
- The reduction in the thickness on the curved pipe was investigated, which showed that the thickness reduction was produced on a specific area while detecting the notch was dependent on a specific time.
- The notch on the welded joints between the two straight pipes was examined under high-temperature conditions.

Futuristic research work is being carried on for obtaining the flaw images with different damage sizes. The angular effect between the damage and the wave front of forward waves are planned to be studied. These NDT methodologies combines together shall be implemented for investigation of composite plates and railway tracks, etc.

8.7 Guided Waves Focusing Technique for Circumferential Sizing

The area of circumferential sizing of defects in piping systems by implementing guided waves focusing techniques was investigated by Mu et al. [171]. They found out that by means one circumferential scan of the pipes, multiple locations of defects could be located accurately. If the size of the defects was found to be less than the width of the focal beam then then good circumferential sizing results can be obtained by correlating the experimental reflection profile to the theoretical ones. Circumferential sizing of non-uniform defects and defects having bigger circumferential length could be done from the experimental profile directly. The authors have concluded that the prediction of the results of the sizes of defects is impacted by the shape of the defect as well as the shape of the angular profile. They also suggested that it is better to avoid using angular profiles that have bigger side lobes for better and accurate sizing.

8.8 Guided Waves Arrangement for Pipe Bends

Ni et al. [172] studied the various experimental methods to investigate the impact of pipe bend arrangement on guided waves-based detection of defects. They conducted research to figure out the sensitivity of detection at various crack locations using finite element simulation and experiments. The following inferences were drawn:

- Simulation analyses reveal that the characteristics of travelling guided waves through the first elbow were not affected by the difference in the configuration of pipe bends.
- At points where the pipes have more than one bend, the energy of the guided waves was focused on the extrados of space-Z and plane-Z pipe, but intrados of U pipe.
- The highest penetration rate was found to be in space-Z pipes when the guided waves traverse across it without any defects.
- Along those lines, it was determined that in these pipes the inspection of cracks in the straight pipe beyond two elbows was most sensitive.
- Location of defects and the pipe configurations characterize the sensitivity of detection.

8.9 Guided Waves for Determining Axial Length of Defects

X. Wang et al. [173] proposed a technique for evaluation of the characteristic axial length of defects occurring in the pipelines. The basic underlying principle was the consideration of the fact that the net reflection single produced at the defect is the interference between the two primary reflection components, which are one getting reflected form the front edge of the defect and the other from the back edge of the defect. The axial length under evaluation was found to be directly proportional to the distance between the reflection positions at the two edges of the defect. Decomposition and identification of the two reflection signals helps in evaluating the axial length of the defect.

This method has an added advantage as it can be used for investigating more defect parameters and also enable comprehensive defect characterization once the two primary edge locations were identified. Respective edge of the defect yields geometric information which can be obtained from the identified edge signal. Employing proper component analysis methods would help in the assessment of radial depth, circumferential extent and other factors of the defect. This proposed research can be applied to circumferential defects in straight, empty piping systems. A generalized implementation of this methods can be deployed in case of real complex situations like arbitrary shaped localized corrosion defects in different operating circumstances.

8.10 Using Shear Horizontal Guided Waves Testing for Estimating Depth of Flaws

Estimation and evaluation of the depth of flaws using guided wave testing with shear horizontal-guided waves is a modern method that has been investigated by A. C. Cobb and J. L. Fisher [174]. The basic principle defining this method if that the different wave modes exhibit different particle motion in the direction of thickness of the material. For the fundamental SH0 mode, the particle motion is constant throughout the thickness whereas for SH1 mode it is higher near the boundaries. The ratio of the response for different modes is used in this approach. The advantage of such technique is that it enables an estimation of depth without using any field portable calibration specimens, which is rare in case of guided wave testing. The authors designed a model that could be used for prediction of the ratio of the amplitude of the signals returning from the flaws. This model has been implemented in plate specimens where a wide range of notch flaws is detected.

In an experiment to test the application and effectiveness of an ultrasonic guided wave system, Otero et al. [175] developed two different transducer arrays. The first, seen in Figure 13, is a circular collar containing 14 elements to be placed around a 6-inch-diameter steel pipe, and the second, seen in Figure 14, is a linear array of 12 elements for use in steel plate.

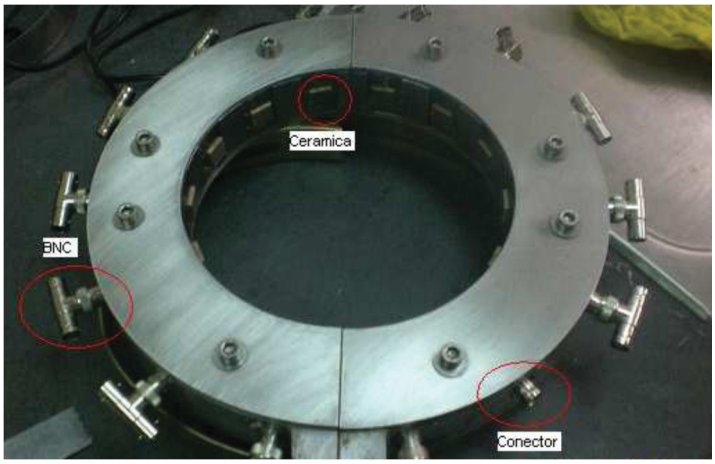

Figure 13. Circular collar transducer array applicable to 6 inch diameter steel pipe [175].

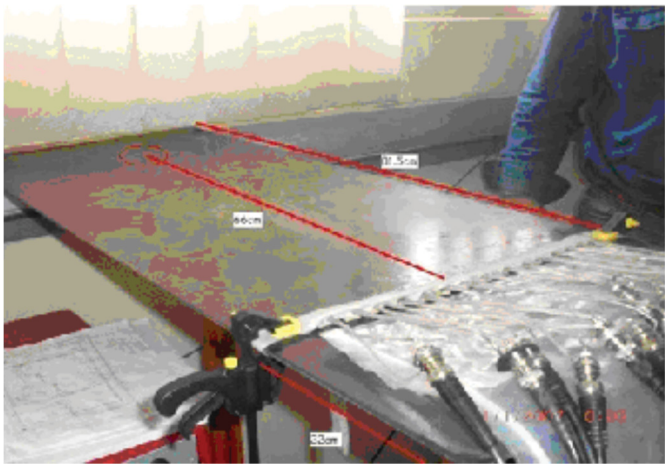

Figure 14. Linear transducer array applicable to steel plate [175].

Experiments of both systems were carried out using a LabVIEW interface program, which included the ability to change parameters of the ultrasonic signal such as frequency, transmitting voltage, and number of cycles. Other parameters in terms of receiving the signal could also be altered independently and included filters range and number of channels. Experimental results of both transducers were able to effectively detect artificial defects in both the pipe and plate.

While the use of ultrasonic Guided Wave Testing (GWT) is a highly effective method of detecting corrosion and other defects in long sections of pipe, this method becomes less efficient when dealing with pipe that is either buried in the ground or has been coated to prevent external corrosion. Loss of available range of ultrasonic GWT is significantly reduced in these situations due to the attenuation of the acoustic signal. This is primarily due to two mechanisms: energy-absorbing materials of the waveguide system cause signal dampening, and signal energy travels through the embedded material and not just the section of pipe being tested. The severity of signal loss from both of these mechanisms is highly influenced by the embedded or coating material.

J. -W. Cheng, et al. [176] in their study have revealed that there exist a better agreement between the experiments and the predictions for the attenuation of guided waves in viscous fluid-filled piping. It was observed that liquid with low viscosity have zero impact on the torsional mode T(0,1) mode whereas, the fluids having higher viscosity, which gets deposited in the pipe causes the reflected signal to attenuate by about 25%. Thus, such a study by the researchers can be implemented in refineries and petrochemical industrial plants for testing of piping systems as a large number of industrial pipelines carry fluids for various manufacturing processes.

8.11 Application of Electromagnetic Acoustic Transducers

M. Gori et al. [177] developed a non-destructive testing method having higher speed and better detecting capability for inspection and monitoring of heat exchangers and boiler tubes. In their research they designed a rapid non-destructive inspection technique to detect and find the location of the defects in heat exchanger tubes (inner diameter = l0–20mm) and boiler tubes (external diameter = 25–100mm). They used non-contact Electro Magnetic Acoustic Transducers (EMATs), which were controlled from a remote position and were operated by shear horizontal-guided waves.

The tube geometry is instrumental in defining the type of probe that can be designed for detecting both transverse and longitudinal waves. This can be achieved by operating the EMATs either from the inner or outer surface. Laboratory tests on heat exchangers and super heater tubes have confirmed that defects having depths up to 1 mm have the ability for localization and remote detection.

8.12 Transient Signal Analysis of Steam Generator

Using transient acoustic signals for analysis of the structural integrity of steam generator tubing was performed by B. Lu et al. [178]. They made the following conclusions out of their research:

- They used Lamb waves in their study and found that they were very sensitive towards the structural defects seen in brass tubes. Along those lines they also observed that the defect size, location, shape, and the surrounding media in the structure directly impact the Lamb wave propagation along the guided structures.
- According to their research, the smallest defect measured was around 1 mm. The smaller micro-structural defects could also be monitored easily, as the propagation of elastic waves depend on the microstructure of the materials.
- It is observed that there are four different types of Lamb waves in tubular structures. The Lamb nodes are found to be very complex because of the combination of multi-mode waves in plate or tubular structures. Each mode is characterized by the non-linear decrease in speed with increase in the product of thickness and frequency.
- Hilbert-Huang transform has been deployed for easy adaptation and separation of sensitive wave modes. This also helps in reduction of unwanted noise in the signals.
- They also used a multi-sensor suite that is comprised of two diametrically opposite sensors for separation of single mode Lamb waves. Anti-symmetric mode signals yielded great results as windows were moved and zoomed towards the signals.
- The researchers figured out that the increase in the leakage of energy in the Lamb waves was an outcome of submerging the test specimens in water.

These methodologies proposed by this study shall be beneficial for online and in-situ monitoring of critical equipment for ensuring safety and reliability of the system as a whole.

8.13 Signal Attenuation in Embedded Pipe

In an attempt to determine the amount of attenuation of the signal in embedded pipe, Leinov et al. [179] conducted an experiment to determine the different factors that have the greatest influence on signal attenuation in terms of embedded material. A 5.67-m-long, 8-in.-diameter carbon steel pipe was used as the test specimen, 3 m of which was embedded in a specifically designed container to simulate the embedded section of pipe. A drawing of the apparatus can be seen in Figure 15(a) and 15(b).

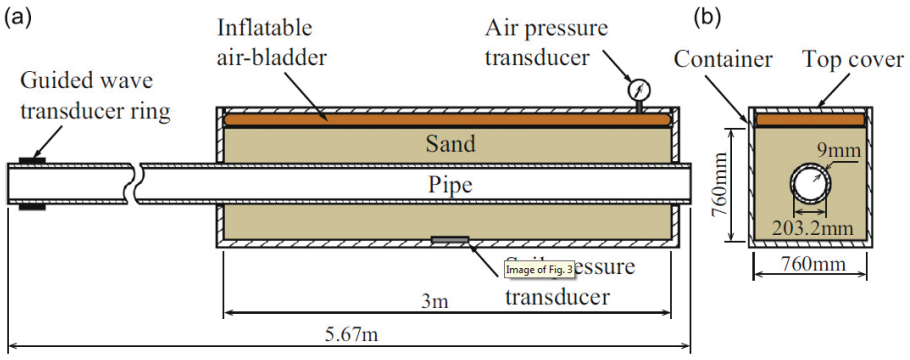

Figure 15. Experimental apparatus: (a) side view, (b) front view [179].

This experiment consisted of five different embedded material characteristics which are: dry loose sand, dry compacted sand, dry mechanically compacted sand, water saturated sand, and drained sand. An inflatable air-bladder was also used to apply pressure on the section of pipe to simulate several different depths of the buried pipe. The experiment concluded that increased pressure and compaction of the sand resulted in an increase in the attenuation of the signal; therefore, it can be assumed that an increase of buried depth and compacted material will cause of significant decrease in the applicable range of ultrasonic GWT.

8.14 Impact of Fusion-Bonded Epoxy Coating on Pipe

In a different but very similar experiment using the same experimental apparatus, Leinov et al. [180] attempted to determine the effect of a fusion-bonded epoxy (FBE) coating on a similarly sized section of pipe under similar conditions. The thin coating of FBE was determined to slightly increase the amount of attenuation in comparison to the previous study. Due to the increased benefits of the coating in terms of external corrosion, ultrasonic isolation of the section of pipe was then demonstrated using a polyethylene (PE)-foam layer between the coated pipe and the sand. Due to the PE-foam layer having a smaller impedance than both the pipe and the sand, this caused a reduction in the leakage of the ultrasonic signal into the surrounding sand. Without this isolation, it was estimated that propagation distances on the coated pipe were approximately 10 m, while isolating the pipe using the PE-foam increased this distance to approximately 15–30 m.

In another similar experiment, but on a much smaller scale, Ahmad [181] attempted to determine propagation effect of a buried pipe with active flow. Typically, when a section of pipe needs to be inspected, the pipe is excavated and the coating is removed if present. It is also important to note that the flow of the pipe is typically shut down prior to any testing. Both of these procedures require time and money. Ahmed's experiment was aimed at discovering what effects this active flow had on guided wave propagation. It was discovered that the overall strength of the signal in a pipe with active flow is reduced compared to that with no flow. However, on several occasions enhanced propagation was observed and proved to help in the identification of defects.

8.15 Signal Attenuation in Guided Wave Testing

In a paper aimed to explain methods, application, and current research being conducted in the field of GWT, Lowe & Cawley [182] discuss the mechanisms that cause signal attenuation in GWT. These mechanisms are:

- Attenuation due to type of material, including any coating present
- Scattering caused by a rough surface produced by corrosion
- Reflections from features in the pipe, such as welds or supports
- Mode conversion of the signal caused by bends, which causes a reduction in applicable range
- Leakage in instances of embedded pipe.

They go on further to discuss how bends in a pipe can affect the applicability of GWT as most systems will contain bends. They state that typical pulled bends in pipe do not present a high level of difficulty in assessing test readouts for defects using GWT. The problem arises when the pipe contains sharp bends created by two sections of pipe welded to an elbow. The bend causes a mode conversion of the signal and it requires a technician with a high skill level to differentiate between the reflected signal of the welds surrounding the bend and between defects present in the pipe. They also note that while it is possible to test sections of pipe with multiple bends, it is recommended to limit testing to sections containing only one bend and to place the bend at the far end of the test range to alleviate complications of interpreting the reflected signal.

An issue when testing sections of pipe using GWT is the fact that signals are not only reflected from defects present but from welds and other features of the pipe as well. In a paper discussing the application of GWT, Cawley [183] describes a method to eliminate this misinterpretation. He suggests that by using an axially symmetric mode when utilizing GWT, any reflected signals from uniform welds or flanges will only reflect an axially symmetric mode. In a vast majority of cases, corrosion defects will not form in a uniform fashion, only reflecting non-axially symmetric signals. The graphs in Figure 16(a) and 16(b) represent this difference.

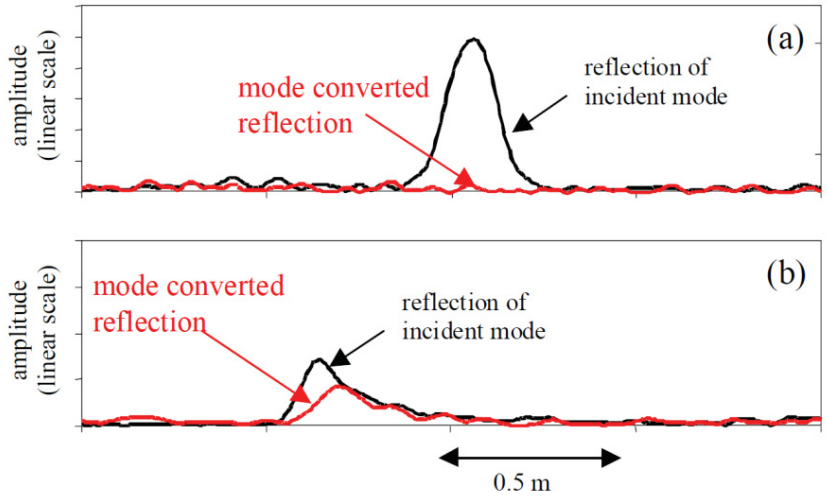

Figure 16. (a) Uniform feature (weld), (b) corrosion [184].

As can be seen in the figure, the mode converted reflection of the uniform weld does not reflect a non-axially symmetric mode, while in the case of the corrosion it does. This is a fairly basic concept to avoid the common misinterpretation of welds in a pipe as corrosion, especially when sections of the pipe are not visible.

8.16 Axisymmetric and Focused Pipe Inspection Approach in GWT

In a study aimed to provide an overview of the wide range of applications for GWT, Rose [184] provided details on two prominent concepts of utilizing GWT to inspect pipes. These concepts are axisymmetric inspection and focused pipe inspection. In an axisymmetric inspection, the individual sensors within the collar, similar to that in Figure 13, are pulsed in phase to produce an axisymmetric wave that uniformly moves along the pipe. In a focused pipe inspection, a focused beam revolves around the circumference and down the pipe using a prescribed time delay profile. Graphical representations of the axisymmetric and focused pipe inspection concepts can be seen in Figures 17 and 18, respectively.

Figure 17. Axisymmetric guided wave inspection displaying wave propagation at specific times along the length of pipe [184].

Figure 18. Focused guided wave inspection displaying focused beam at specific times as it moves around and along the length of pipe [184].

Also in this study, Rose provides detailed lists of the accomplishments and obstacles of using GWT to inspect pipes. Some mentioned successes in the field are:

- Knowledge of axisymmetric and non-axisymmetric modes
- Produce great penetration power with the use of specialized sensors
- Defect size detection to less than 5% cross sectional area
- Location and length of defect estimations with focusing
- Ability to test pipes with insulation or coatings.

Some mentioned obstacles are:

- Inspections on sections of pipe with numerous tees, elbows, and bends, and the ability to inspect beyond an elbow
- Pipes with active fluid flow

- Reliability and difficulty in correctly identifying defects compared to other pipe features, such as welds
- Ability to reliably detect defects beyond the first major defect.

8.17 Guided Waves Testing in a Crude Oil Pipeline

In an experiment to study the relationship between received signal parameters and pipe wall integrity, Mokhles et al. [185] performed GWT on sections of a crude oil pipeline. Most of the pipeline system had not been used in over 40 years. However, the sections that have been replaced recently provided a healthy comparison between the old and new sections of the piping system. Out of the total 527 locations tested, only 35 (25 from the old pipe and 10 from the new pipe) were selected for the purpose of comparison. In each test location, pipe wall thickness was measured in four locations around the circumference of the pipe. In the new sections of pipe, the variance between these four measurements is relatively low due to the lack of internal corrosion, whereas the variance in the sections of old pipe were much higher due to the presence of corrosion. This is called the variance factor and was used as the basis of comparison to the signal parameters in those specific locations. To obtain an enhanced comparison, the signal/noise value was divided into the attenuation value for each locations results, which they call the comparison factor. A graph of this relationship can be seen in Figure 19.

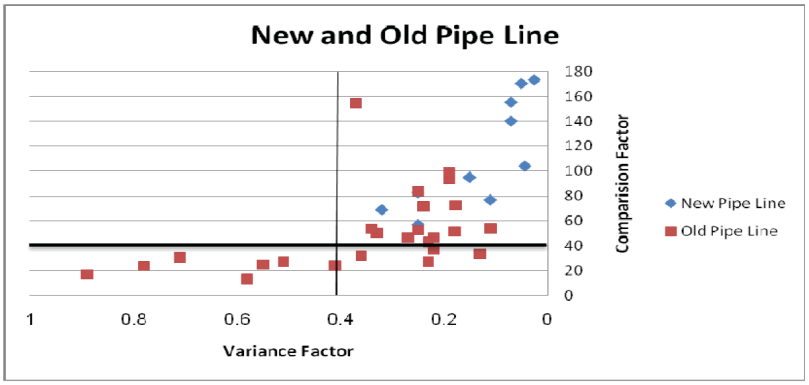

Figure 19. Relationship between variance factor and comparison factor in 35 test locations of crude oil piping [185].

As can be seen in the figure, all of the points for the new pipe have a low-variance factor and relatively high-comparison factor due to the lack of corrosion. It was determined that anything with a variance factor greater than 0.4, and a comparison factor less than 40, should be considered a high-risk location. The use of this relationship is a much faster approach than other methods as it allows a quick analysis of long sections of pipe to determine the areas that pose the greatest risk.

8.18 GWT on Under Water Piping Systems

Won-Bae Na and T. Kundu [186] in their research regarding under water piping systems using guided waves came up with the following conclusions:

- They developed a new advanced coupler mechanism so as to study the plausibility of flexural cylindrical guided waves for detecting defects in underwater piping systems.
- Guided waves were generated, propagated, and received by the help of incident angle adjustment and frequency sweep techniques. The new coupler method and guided waves proved to be an efficient device and an effective tool respectively, for structural health monitoring of underwater piping systems.

- Analytical study of the dispersion curves of aluminium surrounded by water showed the presence of number of modes. It was observed that the flexural guided wave modes closer to the asymptotes of the dispersion curves have a higher sensitivity than those which are far away from the asymptotes.

This research has proved that the new transducer holder and its coupling mechanism can be used for underwater pipeline monitoring by using ultrasonic guided waves.

8.19 GWT as an NDE Technique for SHM of Water and Waste Water Piping Systems

In a technical review, P. Rizzo [187] made an extensive study on various non-destructive evaluation methods for structural health monitoring of water and wastewater piping systems. The author has explored and suggested the following NDE techniques for inspection of the water mains and waste water piping networks:

- Electromagnetic methods:
  - Eddy current
  - Ground penetrating radar
  - Magnetic flux leakage
- Mechanical methods:
  - Acoustic emission
  - Ultrasonic testing
  - Impact echo method
  - Acoustic leak detection
  - Sonar
- Visual inspection methods:
  - Using closed-circuit television (CCTV).

Surface anomalies in the wastewater pipes inspected by means of CCTV, laser scanning, or sonar could be improved by enhancing the resolution of images obtained from the CCTVs. The author proposed a trenchless un-tethered system can probe the structures from inside without disrupting the service can be highly beneficial. The structural health monitoring techniques for pipelines also comprises of various other important issues like modeling of damages, establishing criteria and the process for setting up indices for evaluation of damage or defects.

8.20 Guided Waves Testing by EMAT

In another study about detection of pipe wall damage, M. Vasiljevic et al. [188] proposed the use of guided waves generated by EMAT system. Cylindrical guided waves having longitudinal modes L(0,1) and L(0,2) were created and they were found in a metal pipe by means of EMATs. The authors in their study analyzed the signal before as well after multiple propagations of different wave modes inside the pipe. This helped in overcoming the problems associated with the identification of the small signal from the defect and the truncation of the signal after the defect signal but much prior to the arrival of the reflected signal from the end of the pipe.

The signal could be stabilized by multiple reflections and scattering of the traversing wave modes by the pipe ends and the defects that help in generating consistent spectral plots. These plots provide substantial evidence for differentiation of defective pipe and defect-free piping systems. For precise prediction of location of the defect, the signal from the defect must be identified in the time history plots.

8.21 Other Signal Processing Techniques Using Guided Waves

R. Ahmad and T. Kundu [189], investigated the significance of various signal processing methodologies in guided wave applications for detection of defects in pipelines networks. Here the authors have talked about two different techniques such as:

- Fourier transformation of experimental signals provides information regarding the modes of propagation and helps identifying the modes that are more sensitive towards defects.
- Comparison of different wavelet coefficients for pipes under various boundary conditions helped in finding the defective pipes via continuous wavelet analysis method.
- They also suggested that mother wavelet functions might be used for differentiating defective pipe from defect-free pipe.

A. Demma et al. [190] made a comparative study for investigation of the effects of defect size on the reflection of guided waves in piping systems. They presented the following parameters in their work:

- They maps denote the reflection coefficient as a function of the depth and circumferential extent of the defect.
- T(0,1) incident at 35 kHz
- A correction factor for different pipe sizes
- Location of the defect in the cross-section
- Ultrasonic guided wave mode
- The frequency of excitation.

Practical testing knowledge helped in getting information regarding circumferential extent of the defect from mode conversion by means of the flexural/axisymmetric ratio.

An estimation of the defect could be easily made by implementing maps defining the minimum and maximum reflection coefficient denoted as a function of circumferential extent and depth of defect. The maximum reflection coefficient map is used in case of a wide frequency range, whereas the minimum reflection coefficient map is used in case of a narrow frequency bandwidth.

Pengfei Sun et al. [191] in their work on guided waves based pipe inspection proposed a new EMAT system to evaluate the stainless steel heat exchanger tubes in the shell of a heat exchanger. They further improved the structure of the EMAT and worked on suppressing the unwanted mode formed during the experiment. The EMATs for guided wave inspection of pipes are generally placed on the outer surface of the pipes. But in case of heat exchangers most of the area within consists of the space enclosed by the shell and the tube surfaces, thus not allowing outer surface placement of the transducers. Existing methods involve inserting a probe into the heat exchanger tube from one end to inspect the tubes. Specially developed EMATs have been long used to generate and receive torsional waves, but these are again affected by the plates supporting the tubes.

Recently, using guided waves to inspect the heat exchanger tubes have gained particular interest as the transducer need not be pulled across the length of the entire tubing for inspection. Rather, guided wave sensors, both contact and non-contact type, are used. This method has a very high efficiency of defect detection and is thus, of primary importance when the number of tubes to be inspected is very large. EMATs are used to produce guided waves in the heat exchanger tubes using electromagnetic coupling without any requirement of physical contact with the tubes.

EMATs based on Lorentz force were used to inspect stainless steel pipes with weak magnetostrictive force. Torsional waves were excited by the Lorentz force within the heat exchanger tube. These waves are essential in detecting both circumferential and longitudinal cracks. In their work, they developed an EMAT to evaluate heat exchanger tubes made of stainless steel with the help of the L(0,2) mode, which can be operated at higher frequencies and is non-dispersive. This EMAT works on the principle of radial and axial non-uniform static magnetic fields.

The conclusions of the work done in the paper can be summarised as follows:

- Unlike conventional EMATs, the new design works with static magnetic fields consisting of both axial and radial components.
- Experimental and simulation results suggest that the EMAT can transmit and receive L(0,2) mode guided waves.
- An unwanted L(0,1) mode is also received in the signal that has to be suppressed. Mode control is achieved by using two repelling permanent magnets at a spacing of L, within the receiver structure.
- With the improved transmitter and receiver structures, mode control is achieved and the amplitude of the unwanted L(0,1) mode is significantly reduced.
- This kind of mode control only works in the longitudinal +Z direction and not for –Z direction. For the latter, damping substances need to be used at the other end to reduce the effect of elastic waves.

Mode conversion is also seen in case of non-axially symmetric defects.

8.22 Guided Waves as a Means of NDE for SHM of Steam Generators

K. Sinding et al. [192] have explained about the successful and effective means of utilizing non-destructive evaluation and structural health monitoring techniques for steam generators where ultrasonic transducers having the ability of withstanding high temperatures can be implemented. This approach also demands a stronger coupling of the transducers to the complex geometries of the heat exchangers at elevated temperatures. Their purpose was to make use of piezo-electrics for deposition of comb transducers on to the curved surface topography.

They concluded that spray on transducer deposition method enabled them to have a better strength in coupling of composite transducers to the pipe substrates. It was observed that the PZT/Bismuth Titanate were able to transmit and receive the second harmonic waves. They also have the capacity to withstand thermal ratcheting at high temperatures of about 400°. They also plan to perform these tests with bismuth titanate and lithium niobate composite material.

8.23 Dispersion Analysis Approach

Dispersion analysis of multi-layered structures were done by M. Bezdek et al. [193] where they used two different modeling techniques; hence, they made the following inferences:

- They used matrix methods theory with special attention given to multi-layered waveguides having liquid layers.
- They also found a numerical approach for generating dispersion curves, which were characterized by the matrix methods.
- Finite-element method approach was implemented for simulation of the waveguide set-up inclusive of the real-world wedge transducers.
- They also used a 2-D model of the setup and a post-processing technique for procuring the group velocity dispersion diagrams.

- The verification and validation of the model was done by using the theoretical and experimental results.
- Furthermore, the authors introduced sample dispersion diagrams for couple of various other wedge angles α and thus eventually they were compared to the modal solutions of the matrix methods. Finally, these finite element method simulation results were used for depiction of the displacement profiles across the waveguide.

8.24 Long Range Guided Wave Probe for Heat Exchanger Bore Testing

H. Kwun et al. [194] conducted a detailed research regarding bore testing of heat exchanger tubing by using a long-range guided wave probe in a torsional mode. The probe design comprises of a hollow cylinder waveguide, which is attached with a magnetostrictive sensor. The magnetostrictive sensor helps in the generation and detection of torsional waves in the waveguide. The experimental set up consisted of the waveguide that was inserted at one end of the tube and the tip of the waveguide was expanded to make close contact with the inner surface of the tube. This results in mechanical coupling of the torsional waves from the waveguide to the tube and vice versa. Data were obtained from tubes made of different materials like ferrous and non-ferrous tubes and different geometry like U-bend tubes and finned tube, etc. The long-range testing plausibility of the probe was studied. Field evaluation, verification, validation, and robustness of the probe have ensured its enhanced performance and it can be used in the industry quite soon.

8.25 Circumferential Guided Wave Approach for Crack Detection

Implementation of circumferential guided wave for detection of crack has been a topic of interest to material scientists. Y. -M. Cheong et al. [195] made some research using the technique for studying axial crack in feeder piping systems. A circumferential guided wave technique was applied for detecting axial cracks on the bent parts of feeder pipe. Dispersion curves generated from circumferential guided waves were calculated as a function of the curvature. For infinite curvature (i.e., in case of thin plates with increase in frequency), the S_0 and A_0 coincide eventually with the Rayleigh wave mode. However, in the case of pipes, with increase in curvature even at higher frequencies the lowest modes do not coincide. After reviewing the acoustic velocity and dispersion curves, it was found that the surface waves propagating along the inner and outer surface were ultrasonic waves generated by the rocking technique. The authors observed that it is ideal to use a long-range axial guided wave technique for general investigation of the pipe, whereas circumferential guided wave techniques should be used for quantitative analysis of the location and size of the defects. They also inferred that the application of circumferential guided wave technique for investigating a feeder pipe was limited for the following reasons:

- High-radiation exposure for the ultrasonic experts who examine the pipe
- Less accessibility to the bent region.

9. PIEZOELECTRIC PAINT SENSORS

9.1 Introduction

Klein et al. [196] first coined the term “Piezoelectric paint” in 1986 to define 0–3 composites that they had then prepared by suspending electro-ceramics and polymer in a water. A conventional paint base was used and was filled with lead zirconate titanate (PZT) and $PbTiO_3$ in various concentrations. This was followed by applying the paint on to a surface, drying it, and then, electroding and polling the same to be used for sensing purposes. Further research led to improvement in the characteristic properties of the paint as well as making it more economical and easier to implement for various purposes. Several developments led the sensor from being painted on to a surface to being sprayed on to one, thereby providing with a uniform layer of paint on the surface.

9.2 Application of Piezoelectric Paint Sensors for Defect Monitoring

9.2.1 Piezoelectric Paint Sensors Used as AE Sensors

In their work on non-destructive evaluation using piezoelectric paint sensors X. Li and Y. Zhang [197] have used a suitable distributed acoustic emission sensing method for defect monitoring. They further analyse the use of piezoelectric substances for ultrasonic signal measurements to determine the sensing capability of the piezoelectric paint. The mechanism for crack initiation detection is analysed using a finite element simulation model calibrated using experimental data. Using finite element simulation and experimental analysis the effect of connecting multiple sensors in an array on the output was investigated.

Based on the study, the following conclusions were reached.

- The piezoelectric paint sensor is a potential candidate for determination and monitoring of cracks in metal structures caused by fatigues.
- With increase in the number of piezoelectric sensors connected in parallel, AE signal amplitude increases.
- When the piezoelectric paint sensors are connected in parallel, capacitance of the array of sensors increases compared to a single sensor.
- Information on the detection of the AE signal is contained within the initial many microseconds of the AE signals.

X. Li and Y. Zhang [198] in their study of piezoelectric paint sensors in acoustic emission-based monitoring of fracture, give an insight on the sensor's material behaviour in ultrasonic sensing. A composite piezoelectric material consisting of very small piezoelectric particles randomly dispersed in a polymer matrix phase is what we call piezoelectric paint. Fracture monitoring, crack detection in metal, concrete and composite structures can be done via non-destructive evaluation methods based on acoustic emission. Effect of piezoelectric ceramic volume fraction is studied. They have carried out an electro-mechanical analysis of piezoelectric paint sensor based on a finite element model and based on the experimental data, a simulation model was calibrated.

To summarise the feasibility of such sensors, and the work done during the period of study of the paper, we have the following:

- Material properties of piezoelectric paint for ultrasonic sensing were modelled and analysed. These were further used to find out the effect of the various factors that can affect the sensor's performance.
- The piezoelectric paint sensor sensitivity was significantly affected by the particle volume fraction of the PZT.
- Piezoelectric activity, comparable to that of PVDF, can be achieved by 40 to 70% PZT volume fraction piezoelectric paint.
- A 2-D coupled field finite element model was designed to validate the performance of the paint sensor and was used to further study the interaction of the subject and the sensor.
- For ultrasonic sensing in fibre-reinforced polymer composite structures, piezoelectric paint sensors are suitable with better acoustic impedance matching.
- It is seen that judicious selection of piezoelectric ceramic and polymer as well as the volume fraction, to optimise the material properties of the paint is a feasible method for AE-based fracture monitoring.

9.2.2 Piezoelectric Paint Sensors for Surface Fatigue Detection

In his paper on in situ fatigue crack detection [199], Yunfeng Zhang reports the use of surface mounted piezoelectric paint sensor and its applications in surface fatigue crack detection. These polymer-based piezoelectric paints can be directly applied on to the surface of the subject to detect and monitor surface level cracks. Voltage is generated by the sensor when any form of mechanical strain is applied in it the plane of the paint. Upon the inclusion of a special electrode design based on the recent developments, a new effective method can be potentially obtained for the purpose of in situ fatigue crack detection.

Detection and monitoring of fatigues can lead to a longer lifespan and better reliability of the structural systems. Most of the processes in use today for the purpose of fatigue detection are manual and involve high costs, intensive labor, and produce variable results. There are also non-destructive evaluation techniques that include eddy currents, dye penetrants, AE, magnetic particle inspection, etc. In real-time usage, all of the NDE techniques mentioned have certain limitations due to various different factors.

Continuous detection and monitoring can be achieved by advanced sensors; piezoelectric paint sensors are proposed to provide a simple yet effective technique to achieve this.

- Through a series of vibration test, including harmonic loading and free vibration tests, the dynamic strain sensing capacity of piezoelectric paint sensors was validated.
- These sensors may not provide a competitive method, in case of ordinary sensing applications, when compared to conventional techniques. This is because the new sensors cannot differentiate between the two in-plain strains, thus measuring only dynamic strain.
- However, special applications like real-time monitoring of surface cracks can be performed using piezoelectric sensors.
- One shortcoming of this technique could be the generation of misleading information in case the existing cracks do not cross the sensor electrodes. However, this limitation can be alleviated using complex patterned electrodes or covering a relatively smaller area.

9.2.3 Piezoelectric Paints Used for Structural Monitoring

Since the discovery of piezoelectric materials in 1880, they have gained widespread popularity in various fields. Of late, these materials have found various uses in the field of structural monitoring. C. Yang and C. -P. Fritzen [200], in their work, study the applications of these new piezoelectric paint sensors as spatially distributed modal sensors, one that measures a single mode while filtering the other modes of the structure. These distributed sensors are evenly and continuously distributed on the host structure, compared to conventional ones. In cases where high-frequency un-modelled modes affect the closed loop stability, piezoelectric sensors are useful for active control due to reduced spill-over problems. The authors in this work fabricate a piezoelectric paint sensor, one that is flexible and can be tailored to any shape and applied on to any surface. These sensors are much easier to control based on the applications, as compared to traditional PVDFs.

Their work can be summarised by the following points.

- Piezoelectric paint, when cut by hand, has many inaccuracies. Cutting the edge of the modal sensor as smooth as the theoretical design is very difficult and the tip is too tiny to handle and can be damaged easily.
- Piezoelectric paint is flexible, distributable, and easy to shape.
- By placing it upside down, the polarisation profile of the sensor can be easily changed.
- Even with the existence of mode leak, the paint is still a potential composite for spatially distributed modal sensors.

9.2.4 Piezoelectric Paints Used as 2-D Phased Arrays

Byungseok Yoo et al. [201] in their work, have proposed a new damage detection method based on a 2-D phased array made of piezo-electric paint to find the interaction of guided Lamb waves and various defect types. During the development of the process, they have used the transverse mode of guided Lamb waves. The damage detection in isotropic thin plates is achieved by the transmission of these waves and their interaction with the boundaries and discontinuities. The group has also demonstrated the ability to detect the approaching wave-fronts' directionality, using 1-D phased sensor arrays. To detect the location and extent of damage on the plate, the filtering properties of various 2-D sensor arrays and signal processing techniques were employed.

The aforesaid research can be summarized as follows:

- Threshold setting and damage index calculation are proposed as new damage detection algorithms. These are then evaluated for detection of simulated defects.
- Detection of simulated damages in a 2024-T3 aluminium plate is done using a newly fabricated 2-D phased sensor array with spiral configuration.
- Based on calculations, it was seen that the damage indices are directly proportional to the size of the damages.
- The limitations of the 1-D phased sensor arrays were overcome by using the proposed 2-D phased sensor arrays.
- Transient responses due to the guided Lamb waves were analysed by applying 2-D phased array based signal processing techniques. These methods are generally used in antenna theory applications.
- Directional filtering abilities were demonstrated using sensor measurements. By eliminating any unwanted signals from the experimental signal, array responses can be improved during empirical mode decomposition.
- Noticeable wave reflections were observed from damaged regions and estimated damage locations, in the resultant array responses.
- Additional information for damage location and extent was provided by the variation of the Hilbert-Huang transform amplitude with increase in damage size.

Along those lines, Byungseok Yoo et al. [202] conducted a research on structural health monitoring based on 2-D phased sensor arrays using piezoelectric-paint and they also obtained similar conclusions.

9.2.5 Piezoelectric Paint Sensor Fabrication Method

Lae-Hyong Kang and Jyung-Ryul Lee [203] present a piezoelectric paint sensor fabrication method. They further demonstrate its application to impact and vibration monitoring. Composed of $Pb(Nb,Ni)O_3$-$Pb(Zr,Ti)O_3$ (PNN/PZT) powder and epoxy resin, this paint is applied on to a aluminium beam and the electrode is made on its surface using silver paste. With the application of a field voltage of 4 kV/mm for about 30 minutes at room temperature, and by using the aluminium beam as the second electrode, poling of the fabricated paint is done. The vibration response of the cantilevered aluminium beam under resonance was monitored based on the output of the piezopaint sensor. Displacement strain transformation method was used to obtain the out-of-plane strain of the beam structure. This was compared with the strain measured by laser displacement sensors at a constant beam positon. Along those lines, the signal from the impact can be monitored by using the fabricated paint, which is sensitive to higher frequencies.

Their work on the fabrication method of the paint sensor and its applications on impact and vibration monitoring can be concluded in the following points:

- The results from the displacement strain method when compared to the out-of-plane deformation measured from the laser displacement sensors match. The position of the various defects along the length of the beam can be determined using this method.
- Impacts were made on the beam using an impact hammer. It was seen that impact forces over 10 N could be captured by using the piezo paint sensor.
- PNN-PZT used in this study is a soft type piezoelectric ceramic, which makes the paint sensor highly sensitive with easy poling characteristics.
- Displacement-strain transformation matrix was used to estimate the displacement by multiplying the strain data to it. Hence, maximum number of mode shapes used could be equal to the number of sensors used.
- The whole structural vibration was also calculated in addition to the one point measurements and the data was analysed versus two measurement data.

9.2.6 Piezoelectric Paint Used as a Strain Sensor

I. Payo and J. M. Hale [204], have designed a piezoelectric paint to be used as a strain sensor. Milled PZT powder is suspended in a lacquer to make the piezo paint. The charge generated by the sensor per electrode area relative to the strain experienced by the substrate gave the sensor's sensitivity. This value of the sensitivity was based on the hypothesis that the sum of principal strains is proportional to the charge generated. Unlike previous works where the sensitivity was calculated based on the relation between the uniaxial substrate strain and the generated charge, this work also takes into account the biaxial strain.

Based on the experimental results, the following conclusions were reached:

- From the biaxial positive bending experiments the sensor sensitivity was calculated to be about 0.0187 $(C/m^2)/(m/m)$ with a tolerance of 0.0015.
- In case of uniaxial bending, the sensitivity was found to be 0.0183 $(C/m^2)/(m/m)$ with a similar tolerance value.
- When subject to equal and opposite strains, the output of the piezoelectric sensor was negligible, thus confirming the hypothesis that the sum of principal strains and electrical displacements are proportional.
- Analysis of the frequency response of the strain sensor places the sensitivity of the sensor within a ±2Db range over 5–500 Hz frequency range.

J. R. White and team [205] have developed a piezoelectric ceramic-polymer composite for use as a thick film strain sensor to be used for vibration monitoring. This paint can be applied onto various substances by using traditional spraying methods. The morphology of the composite and the electrodes used affected the sensor properties, thus various electrodes were tested where it was seen that the electrodes interacted with the piezo paint at times. To study the effect of different compositions and processing conditions, SEM and light optical microscopy were performed and the material morphologies were analysed. Heat treatment is done to anneal out the defects produced during the milling process and was followed by X-ray analysis and particle size analysis to characterize any changes during the process. X-Ray diffractometry was done to study the effect of polling. The following inferences were made based on this study,

- A potential coating system was developed with piezoelectric properties for use as a sensor for vibration monitoring in structures.

- The piezo paint sensors were found to have a very dynamic range with a bandwidth of 1–2 kHz and a microstrain range of 40–4000.
- The piezoelectric coefficient was found to be 20 pC/N approximately for d_{31}.
- The field trial results were successful, thus, showing that the sensors are resistant to outdoor exposure.
- All of the trials and measurements were performed within the above mentioned bandwidth and not outside. Expected bandwidth values are significantly broader.

9.2.7 Piezoelectric Paint used as Thick Film Sensors

In his work, J. M. Hale [206] describes the development of thick film sensors made of piezo paint for shock and vibration monitoring in structures. Characterization of properties of the thick-film sensor is done to show the dynamic range and bandwidth necessary for structural monitoring and robustness of the sensor. The new sensor, even if not ideal, is an improvement over the earlier type such that it can be sprayed on to instead of scraping on with a blade. Piezoelectric sensors are conventionally fabricated by screen printing inks on a substrate. Using paints instead of inks make it advantageous as it is suitable for uneven and curved surfaces as well, while also being able to be cured at room temperature. Thus, with the advantages of thick-film sensors, these piezo paint sensors can be used on large complex surfaces as well as temperature sensitive materials.

Based on the study and field work, the following conclusions were drawn:

- The newly developed paint allows a greater concentration of piezoelectric ceramic powder, which is easy to spray on to surfaces and is curable at room temperatures.
- Electrodes and wire connections for signal transmission can be made out of compatible materials.
- Reliable sensors can be made in bulk commercially based on established spraying and poling conditions.
- The dynamic range and bandwidth were found to be in a range suitable for structural monitoring of shocks and vibrations.
- A field test was performed by placing a sensor on a footbridge and monitoring it over a period of 3 years. It is seen that there is no much deterioration other than a slight loss in sensitivity over the years.

9.2.8 Other Applications of Piezoelectric Paint Sensors for Detection of Damage under Strain and Environmental Conditions

Yunfeng Zhang [207] in his work talks about crack monitoring and damage detection in complex structures by using piezoelectric paint sensors. Real-time continuous online structural health monitoring requires the use of advanced sensors. Traditionally available ceramics are not ideal for use in such applications, which leads to the development of polymer-based piezo paint sensor. By constantly measuring the output voltage signals from the piezo sensors, one can monitor the dynamic responses of the host subject. These sensors hold great potential since their properties can be easily calibrated, they are economical, easy to implement and can be used on a multitude of surfaces. The various characteristics of this particular sensor include the ability to measure dynamic strain and not static load; it is used as a surface-mounted sensor and the paint can be applied on rough and curved surfaces; it is self-powered and needs no external excitation; and it can be used to measure strain in one direction from the output voltage value. The output of the sensor is AC voltage, which can be given into any data acquisition system, eliminating the need for synchronisation.

Summarizing the work presented in the paper, we have:

- Through a series of preliminary studies, a new method of piezoelectric paint application on to surfaces was developed.
- Vibration tests, impact hammer tests, and harmonic loading tests were performed and the damage index was calculated.
- As an active sensor, the piezoelectric paint sensor can be used to monitor in real-time the dynamic 1-D strains, without the application of any external voltage.
- Using multi-electrode combinations along with the piezo sensor, a novel technique for surface crack detection was proposed and was experimentally validated.

To determine the effects posed to piezoelectric paint sensors when exposed to environmental conditions, such as rain, Raptis et al. [208] performed an experiment utilizing PZT particles in an acrylic lacquer. Samples coated with the piezoelectric paint were submerged in both water and potassium iodide solutions for different periods of time and then tested in terms of the potential sensitivity of the piezoelectric paint. They discovered that after a drying period, which was dependent on the time submerged, not only did the piezoelectric paint sensors recover to their original functioning state, they possessed an initial increase in sensitivity especially when submerged in the potassium iodide solution. While the cause of this phenomenon of enhanced sensitivity is not yet understood, it could lead to two different outcomes, either:

- These measurements will fail to be reproduced
- Enhanced sensitivity of piezoelectric paint will be obtained with further understanding and control

In a different study also aimed at determining the effects of weather on the capabilities and longevity of piezoelectric paint, Hale and Lahtinen [209] performed trials on two established bridges over a period of 2 and 6 years utilizing an acrylic based and epoxy piezoelectric paint, respectively. The results of these trials concluded that:

- Aging of piezoelectric paint is relatively unaltered when exposed to a wide range of environmental conditions such as sunlight, rain, snow, and frost
- Piezoelectric paint sensitivity drops within the first few months, but soon levels out to a stable and constant state
- After the test periods, the piezoelectric paint was determined to be nowhere near the end of its life cycle despite the exposure to harsh environmental conditions.

A large issue of utilizing piezoelectric paint is the fact that no standards exist in terms of fabrication. In an attempt to identify certain properties of piezoelectric paint such as microstructure, tensile strength, and sensitivity for the purpose of creating a standard fabrication procedure, Yang and Fritzen [210,211] performed a range of tests on samples of piezoelectric paint using the tape casting method. While other methods of utilizing piezoelectric paint exist, such as spraying or screen-printing, the tape casting method seems to be superior as it can be used in a wider range of applications. The spraying method can only be used in situations where the material to which the paint is applied is conductive, and the screen-printing method only produces thick films over a specific area. In terms of microstructure, it was determined that the maximum weight percentage is 60%, with 50% being ideal, before severe air voids become present. These voids reduce the strength of adhesion between the piezoelectric particles and can lead to dielectric breakdown during poling. Tensile strength tests confirmed that the piezoelectric paint produced by the tape casting method can be applied to a wide range of applications. Upon analysis of the sensitivity of the piezoelectric paint, it was determined that the piezoelectric charge constant was close to a published calculation, which concludes the overall effectiveness of the paint.

In several studies to determine the effects of film thickness, cure temperature, poling field, and volume fraction of PZT on the sensitivity of piezoelectric paint to be utilized as a vibration sensor or an AE sensor, Egusa and Iwasawa [212,213,214] made the following conclusions:

- Sensitivity was nearly identical for cure temperatures of 25°C and 150°C for a film thickness of less than 30μm
- As film thickness increases above 30μm, increases in sensitivity are greater at a cure temperature of 25°C versus 150°C
- Sensitivity increases with an increase in poling field and film thickness but is limited by eventual electrical breakdown at high levels of poling field
- Sensitivity increases with an increase in volume fraction from 30 to 53%.

In an attempt to determine the effectiveness at utilizing a piezoelectric film AE sensor to monitor fatigue crack growth in welded tubular structures, Zhang et al. [215] discovered the following relationships between frequency of AE signals and source mechanism:

- AE signals induced by friction of the fatigue crack surface were of relatively low frequency
- AE signals induced by fatigue crack propagation were of relatively high frequency
- This difference in induced frequency can be used to determine whether AE signals are due to friction between the crack surfaces or due to crack propagation, which aids in monitoring the lifespan of the structure.

Yoo et al. [216] utilized several 2-D phased sensor arrays each composed of 25 piezoelectric paint sensors on aluminum plate. The two arrays, cruciform and spiral, were specifically designed to allow not only the severity of damage to be determined, but also the damaged regions within the array based on the induced signal.

To determine the effectiveness of piezoelectric paint as dynamic strain measurement sensor, Zhang [217] performed both harmonic excitation and impact hammer tests on an aluminum beam coated with a piezoelectric paint composed of PZT-5A. Analysis of the impact hammer tests show that the piezoelectric paint sensor's output is proportional to the force of the impact and it was shown to have high repeatability with similar forces. Analysis of the harmonic excitation tests show that the piezoelectric paint sensor's output clearly matches that of the range of excitation frequencies used. The tests concluded that piezoelectric paint sensors are very effectively at monitoring dynamic strain on a system.

X. Li and Y. Zheng [218] conducted extensive research on a micro-mechanical constitutive model for flexible piezoelectric paint based on percolation property. They concluded:

- Piezoelectric paint was quite advantageous when used as smart sensing materials. This includes the flexible mechanical properties and its conformability to easily get surfaced with complicated geometries.
- The piezoelectric paints, which possess a ceramic volume fraction in the range of 35% to 65%, result in formation of 1-3 connectivity that further leads to higher piezoelectric activity in the composite material.
- Some of the special features, such as mixed connectivity and air void content have been addressed by means of a micromechanics constitutive model for piezoelectric paints. This is done by implementing the universal scaling law of percolation theory.
- The good agreement between the predicted electromagnetic characteristics of the piezoelectric composites and the experimental data obtained provides solid verification of the effectiveness of the percolation-based mixed connectivity model.

9.3 Conclusion

We can conclude that piezoelectric paint is a potential material that can be used to monitor structural shocks and vibrations. Characterization of the piezoelectric paint suggests that it is much more economical and easier to implement when compared to traditional sensors. The piezo-paint material possesses a dynamic range and has a much-higher bandwidth. With respect to conventional film sensors, piezo paint sensors have various advantages, such as greater area coverage, applicability on rough and complex surfaces, independent of external excitation voltage, and absence of binding adhesive between the host and the sensor. The dynamic strain of a structure can be monitored by real-time measurement of the output AC voltage of the sensor. It also finds applications in online damage monitoring and surface crack detection, and has been shown to resist environmental conditions when used over a long period of time.

10. REFERENCES

[1] Corrosionpedia, *Cavitation Erosion*, https://www.corrosionpedia.com/definition/244/cavitation-erosion, Web page visited April 5, 2016.

[2] Crockett, H. M., and J. S. Horowitz, "Erosion in nuclear piping systems," *Journal of Pressure Vessel Technology*, Vol. 132, No. 2, 2010.

[3] Fitch, E. C., *Cavitation Wear in Hydraulic Systems,* http://www.machinerylubrication.com/Read/380/cavitation-wear-hydraulic, Web page visited April 5, 2016.

[4] Laguna-Camacho, J. R., et al., "A study of cavitation erosion on engineering materials," *Wear*, Vol. 301, No. 1, 2013, pp. 467–476.

[5] Moeny, M., et al., 2008, "Cavitation Damage from an Induced Secondary Vortex," *FEDSM2008: ASME 2008 Fluids Engineering Division Summer Meeting, Jacksonville, Florida, U.S.A.,* American Society of Mechanical Engineers.

[6] Drozdz, D., R. K. Wunderlich, and H. -J. Fecht, "Cavitation erosion behaviour of Zr-based bulk metallic glasses," *Wear*, Vol. 262, No. 1, 2007, pp. 176–183.

[7] Hattori, S., and E. Nakao, "Cavitation erosion mechanisms and quantitative evaluation based on erosion particles," *Wear*, Vol. 249, No. 10, 2001, pp. 839–845.

[8] Yu-Kang, Z., H. Jiu-Gen, and F. G. Hammitt, "Cavitation erosion of cast iron diesel engine liners," *Wear*, Vol. 76, No. 3, 1982, pp. 329–335.

[9] Hattori, S., and T. Itoh, "Cavitation erosion resistance of plastics," *Wear*, Vol. 271, No. 7, 2011, pp. 1103–1108.

[10] Fairfield, C. A., "Cavitation damage to potential sewer and drain pipe materials," *Wear*, Vol. 317, No. 1, 2014, pp. 92–103.

[11] Karimi, A., and F. Avellan, "Comparison of erosion mechanisms in different types of cavitation," *Wear*, Vol. 113, No. 3, 1986, pp. 305–322.

[12] Howard, R. L., and A. Ball, "The solid particle and cavitation erosion of titanium aluminide intermetallic alloys," *Wear*, Vol. 186, 1995, pp. 123–128.

[13] Liu, X. W., et al., "Vibration cavitation behaviour of selected Ni–Mn–Ga alloys," *Wear*, Vol. 258, No. 9, 2005, pp. 1364–1371.

[14] Li, Z., et al., "Cavitation erosion behavior of Hastelloy C-276 nickel-based alloy," *Journal of Alloys and Compounds*, Vol. 619, 2015, pp. 754–759.

[15] Hong, S. M., et al., "Cavitation erosion behavior of SA 106B carbon steel after treatment of the melt with nano-sized TiC particles," *Tribology International*, Vol. 92, 2015, pp. 585–594.

[16] Dong, F., et al., "Cavitation erosion mechanism of titanium alloy radiation rods in aluminum melt," *Ultrasonics Sonochemistry*, Vol. 31, 2016, pp. 150–156.

[17] Tanarro, A., et al., 1994, "Erosion-Corrosion in Wet Steam and Single Phase Lines in Nuclear Power Plants," *Specialist Meeting on Erosion and Corrosion of Nuclear Power Plant Materials, Kiev, Ukraine,* International Atomic Energy Agency.

[18] Zhimin, Z., L. Jinsong, and Z. Hui, 2012, "Nuclear Power Plants Secondary Circuit Piping Wall-Thinning Management in China," *3rd International Conference on Nuclear Power Plant Life Management, Salt Lake City, Utah, U.S.A.,* International Atomic Energy Agency.

[19] Wu, P.C., 1989, *Erosion/Corrosion-Induced Pipe Wall Thinning in US Nuclear Power Plants,* NUREG-1344, Washington, D.C., U.S.A., U.S. Nuclear Regulatory Commission.

[20] Hu, H.X., Y.G. Zheng, and C.P. Qin, "Comparison of Inconel 625 and Inconel 600 in resistance to cavitation erosion and jet impingement erosion," *Nuclear Engineering and Design*, Vol. 240, No. 10, 2010, pp. 2721–2730.

[21] Liu, C. B., S. L. Jiang, and Y. G. Zheng, "Experimental and computational failure analysis of a valve in a nuclear power plant," *Engineering Failure Analysis*, Vol. 22, 2012, pp. 1–10.

[22] Chen, F .J., C. Yao, and Z. G. Yang, "Failure analysis on abnormal wall thinning of heat-transfer titanium tubes of condensers in nuclear power plant Part II: Erosion and cavitation corrosion," *Engineering Failure Analysis*, Vol. 37, 2014, pp. 42–52.

[23] Chen, F. J., C. Yao, and Z. G. Yang, "Failure analysis on abnormal wall thinning of heat-transfer titanium tubes of condensers in nuclear power plant Part I: Corrosion and wear," *Engineering Failure Analysis*, Vol. 37, 2014, pp. 29–41.

[24] Tomarov, G. V., A. A. Shipkov, and T. N. Golubeva, "Criterion-parametric prediction of cavitation erosion of metal for components of the condensate-feed channel of nuclear power plant power units," *Thermal Engineering*, Vol. 59, No. 4, 2012, pp. 325–331.

[25] Alley, D., and J. Gavula, 2014, "Nuclear Regulatory Commission Perspective Regarding Erosion and Erosion Corrosion in Piping Systems at Nuclear Power Plants," *CORROSION2014: Collaborate. Educate. Innovate. Mitigate, San Antonio, Texas, U.S.A.,* National Association of Corrosion Engineers International.

[26] Ozol, J., J. H. Kim, and J. Healzer, 1994, "Cavitation Experience with Control Valves in Nuclear Power Plants," *ASME 1994 Fluids Engineering Division Summer Meeting, Lake Tahoe, Nevada, U.S.A.,* American Society of Mechanical Engineers.

[27] Isaka, H., et al., 2002, "A Study of Cavitation Erosion," *ICONE10: 10th International Conference on Nuclear Engineering, Arlington, Virginia, U.S.A.,* American Society of Mechanical Engineers.

[28] Ma, N., L. Wang, and J. Qin, 2013, "Wall-Thinning Analysis of the Pipelines in the Secondary Section of NPP," *ICONE21: 21st International Conference on Nuclear Engineering, Chengdu, China,* American Society of Mechanical Engineers.

[29] Heymann, F. J., 1992, Liquid Impingement Erosion, *ASM Handbook: Friction, Lubrication, and Wear Technology,* Vol. 18, pp. 221–232, ASM International, Material Park, Ohio, U.S.A.

[30] TLV International, Inc., *Erosion in Steam and Condensate Piping*, http://www.tlv.com/global/TI/steam-theory/piping-erosion.html, Web page visited April 5, 2016.

[31] Foldyna, J., et al., "Erosion of metals by pulsating water jet," *Tehnicki Vjesnik*, Vol. 19, No. 2, 2012, pp. 381–386.

[32] Yao, J., et al., "Experimental investigation of erosion of stainless steel by liquid-solid flow jet impingement," *Procedia Engineering*, Vol. 102, 2015, pp. 1083–1091.

[33] Hattori, S., and M. Takinami, "Comparison of cavitation erosion rate with liquid impingement erosion rate," *Wear*, Vol. 269, No. 3, 2010, pp. 310–316.

[34] Ikohagi, T., et al., 2010, "Advanced Wall Thinning Prediction of Liquid Droplet Impingement Erosion," *ISaG2010: International Symposium on the Ageing Management & Maintenance of Nuclear Power Plants, Tokyo, Japan,* Mitsubishi Research Institute.

[35] Li, R., H. Ninokata, and M. Mori, "A numerical study of impact force caused by liquid droplet impingement onto a rigid wall," *Progress in Nuclear Energy*, Vol. 53, No. 7, 2011, pp. 881–885.

[36] Hwang, K. M., C. K. Lee, and C. R. Choi, "A study on the cause analysis for the wall thinning and leakage in small bore piping downstream of orifice," *World Journal of Nuclear Science and Technology*, Vol. 4, No. 1, 2014, pp. 1–6.

[37] Fujisawa, N., T. Yamagata, and K. Wada, "Attenuation of wall-thinning rate in deep erosion by liquid droplet impingement," *Annals of Nuclear Energy*, Vol. 88, 2016, pp. 151–157.

[38] Hattori, S., and G. Lin, 2012, "Effect of Droplet Diameter on Liquid Impingement Erosion," *7th International Symposium on Measurement Techniques for Multiphase Flows, Tianjin, China,* AIP Publishing.

[39] Hattori, S., and M. Kakuichi, "Effect of impact angle on liquid droplet impingement erosion," *Wear*, Vol. 298, 2013, pp. 1–7.

[40] Fujisawa, N., et al., "Experiments on liquid droplet impingement erosion by high-speed spray," *Nuclear Engineering and Design*, Vol. 250, 2012, pp. 101–107.

[41] Choi, D. H., K. H. Kim, and H. J. Kim, "Long-term investigation of erosion behaviors on metal surfaces by impingement of liquid droplet with high-speed," *Journal of Mechanical Science and Technology*, Vol. 29, No. 3, 2015, pp. 1085–1091.

[42] Fujisawa, N., et al., "The effect of liquid film on liquid droplet impingement erosion," *Nuclear Engineering and Design*, Vol. 265, 2013, pp. 909–917.

[43] Fujisawa, N., et al., "The influence of material hardness on liquid droplet impingement erosion," *Nuclear Engineering and Design*, Vol. 288, 2015, pp. 27–34.

[44] Fujisawa, N., et al., "Critical consideration on wall thinning rate by liquid droplet impingement erosion," *E-Journal of Advanced Maintenance*, Vol. 4, No. 2, 2012, pp. 79–97.

[45] Ohira, T., et al., 2009, "Prediction of Liquid Droplet Impingement Erosion (LDI) Trend in Actual NPP," *ASME 2009 Pressure Vessels and Piping Conference, Prague, Czech Republic,* American Society of Mechanical Engineers.

[46] Nicolici, S., I. Prisecaru, and P. Ghitescu, "Study of fluid-structure interaction in liquid droplet impingement phenomena," *University Politehnica of Bucharest Scientific Bulletin, Series D: Mechanical Engineering*, Vol. 74, No. 1, 2012, pp. 147–154.

[47] Rao, P. V., and D. H. Buckley, 1984, *Empirical Relations for Cavitation and Liquid Impingement Erosion Processes,* NASA-TP-2339, NASA Lewis Research Center, Cleveland, Ohio, U.S.A.

[48] Corrosionpedia, *Liquid Impingement Erosion*, https://www.corrosionpedia.com/definition/730/liquid-impingement-erosion, Web page visited April 5, 2016.

[49] Patnaik, A., et al., "Solid particle erosion wear characteristics of fiber and particulate filled polymer composites: A review," *Wear,* Vol. 268, No. 1, 2010, pp. 249–263.

[50] Bousser, E., 2013, *Solid Particle Erosion Mechanisms of Protective Coatings for Aerospace Applications,* Doctoral Dissertation: University of Montreal, Montreal, Canada.

[51] Branco, J.R.T., et al., "Solid particle erosion of plasma sprayed ceramic coatings," *Materials Research*, Vol. 7, No. 1, 2004, pp. 147–153.

[52] Satapathy, A., et al., 2004, "Resistance of Plasma Sprayed Redmud Coatings to Solid Particle Impingement," *DAE-BRNS Workshop on Plasma Surface Engineering, Mumbai, India,* Allied Publishers Pvt. Ltd.

[53] Levin, B. F., et al., "Modeling solid-particle erosion of ductile alloys," *Metallurgical and Materials Transactions A*, Vol. 30, No. 7, 1999, pp. 1763–1774.

[54] Laguna-Camacho, J. R., et al., "Solid particle erosion on different metallic materials," *Tribology in Engineering*, Vol. 5, 2013, pp. 63–78, InTech, Rijeka, Croatia.

[55] Arabnejad, H., et al., "Development of mechanistic erosion equation for solid particles," *Wear*, Vol. 332, 2015, pp. 1044–1050.

[56] Islam, M. A., et al., "Effect of microstructure on the erosion behavior of carbon steel," *Wear,* Vol. 332, 2015, pp. 1080–1089.

[57] Shimizu, K., Y. Xinba, and S. Araya, "Solid particle erosion and mechanical properties of stainless steels at elevated temperature," *Wear*, Vol. 271, No. 9, 2011, pp. 1357–1364.

[58] Siddhartha, and R. Bisht, "A modified approach for better prediction of erosion wear of materials: Redefining the paradigms," *Materials and Design*, Vol. 47, 2013, pp. 395–407.

[59] Andrews, D. R., "An analysis of solid particle erosion mechanisms," *Journal of Physics D: Applied Physics*, Vol. 14, No. 11, 1981, pp. 1979–1991.

[60] Finnie, I., "Erosion of surfaces by solid particles," *Wear*, Vol. 3, No. 2, 1960, pp. 87–103.

[61] Clark, H. M., "On the impact rate and impact energy of particles in a slurry pot erosion tester," *Wear*, Vol. 147, No. 1, 1991, pp. 165–183.

[62] Lynn, R. S., K. K. Wong, and H.M. Clark, "On the particle size effect in slurry erosion," *Wear*, Vol. 149, No. 1, 1991, pp. 55–71.

[63] Desale, G. R., B. K. Gandhi, and S. C. Jain, "Particle size effects on the slurry erosion of aluminium alloy (AA 6063)," *Wear*, Vol. 266, No. 11, 2009, pp. 1066–1071.

[64] Wada, S., and N. Watanabe, "Solid particle erosion of brittle materials (Part 3) - The interaction with material properties of target and that of impingement on erosive wear mechanism," *Journal of the Ceramic Society of Japan*, Vol. 95, No. 6, 1987, pp. 573–578.

[65] Liebhard, M., and A. Levy, "The effect of erodent particle characteristics on the erosion of metals," *Wear*, Vol. 151, No. (2), 1991, pp. 381–390.

[66] Jahanmir, S., "The mechanics of subsurface damage in solid particle erosion," *Wear*, Vol. 61, No. 2, 1980, pp. 309–324.

[67] Emerson Process Management, "A Newsletter from Emerson's Severe Service Team," *Severe Service Journal*, Vol. 11, No. 4, 2011.

[68] Emerson Process Management, "A Newsletter from Emerson's Severe Service Team," *Severe Service Journal*, Vol. 11, No. 2, 2011.

[69] Kiesbauer, J., "Control valves for critical applications," *Hydrocarbon Processing*, Vol. 80, No. 6, 2001, pp. 89–100.

[70] Grunenberg, D., *Effects of Valve Trim Geometry in Flashing Service,* Richards Industries Valve Group, Cincinnati, Ohio, U.S.A.

[71] Skousen, P. L., *9.3: Flashing*, http://www.globalspec.com/reference/80283/203279/9-3-flashing, Web page visited April 5, 2016.

[72] Fisher, *Control Valve Sourcebook, Pulp & Paper,* 2011, Fisher Controls International, LLC, Marshalltown, Iowa, U.S.A.

[73] Warren Controls, *Valve Sizing & Selection Technical Reference,* VSSTR-07/12, 2005, Bethlehem, Pennsylvania, U.S.A.

[74] Evans, B., and R.L. Ritter III, Flashing and Cavitation, *Valve Magazine*, August 18, 2015.

[75] NACE International, *Pitting Corrosion*, https://www.nace.org/Pitting-Corrosion/, Web page visited August 24, 2016.

[76] Frankel, G. S., "Pitting corrosion of metals a review of the critical factors," *Journal of the Electrochemical Society*, Vol. 145, No. 6, 1998, pp. 2186–2198.

[77] Ezuber, H. M., "Metallurgical and environmental factors affecting the pitting behavior of UNS S 32205 duplex stainless steel in chloride solutions," *Materials and Corrosion*, Vol. 63, No. 2, 2012, pp. 111–118.

[78] Dular, M., and O. Coutier-Delgosha, "Numerical modelling of cavitation erosion," *International Journal for Numerical Methods in Fluids*, Vol. 61, No. 12, 2009, pp. 1388–1410.

[79] Souli, M., et al., 2014, "Numerical Investigation of Phase Change and Cavitation Effects in Nuclear Power Plant Pipes," *13th International LS-DYNA Users Conference, Detroit, Michigan, U.S.A.,* Livermore Software Technology Corporation.

[80] Mimouni, S., et al., "Modelling and computation of cavitation and boiling bubbly flows with the NEPTUNE_CFD code," *Nuclear Engineering and Design*, Vol. 238, No. 3, 2008, pp. 680–692.

[81] Peters, A., et al., "Numerical modelling and prediction of cavitation erosion," *Wear*, Vol. 338, 2015, pp. 189–201.

[82] Zima, P., M. Sedlář, and M. Müller, 2009, "Modeling Collapse Aggressiveness of Cavitation Bubbles in Hydromachinery," *CAV2009: 7th International Symposium on Cavitation, Ann Arbor, Michigan, U.S.A.,* University of Michigan.

[83] Hattori, S., T. Hirose, and K. Sugiyama, "Prediction method for cavitation erosion based on measurement of bubble collapse impact loads," *Wear*, Vol. 269, No. 7, 2010, pp. 507–514.

[84] Dular, M., B. Stoffel, and B. Širok, "Development of a cavitation erosion model," *Wear*, Vol. 261, No. 5, 2006, pp. 642–655.

[85] Li, Z., M. Pourquie, and T. van Terwisga, "Assessment of cavitation erosion with a URANS method," *Journal of Fluids Engineering*, Vol. 136, No. 4, 2014.

[86] Pătrăşcoiu, C., "New analytical cavitation erosion models," *WSEAS Transactions on Mathematics*, Vol. 7, No. 8, 2008, pp. 528–538.

[87] Shams, E., and S. V. Apte, "Prediction of small-scale cavitation in a high speed flow over an open cavity using large-eddy simulation," *Journal of Fluids Engineering*, Vol. 132, No. 11, 2010.

[88] Soyama, H., and H. Kumano, "The fundamental threshold level—A new parameter for predicting cavitation erosion resistance," *Journal of Testing and Evaluation*, Vol. 30, No. 5, 2002, pp. 421–431.

[89] Chahine, G.L., and C. -T. Hsiao, "Modelling cavitation erosion using fluid–material interaction simulations," *Interface Focus*, Vol. 5, No. 5, 2015.

[90] Simoneau, R., M. -C. Petrin, and Y. Mossoba, "Modelling and predicting cavitation erosion," *The International Journal on Hydropower and Dams*, Vol. 2, No. 2, 1995, pp. 41–44.

[91] Ito, Y., et al., "A prediction method upon developed stage of cavitation erosion," *Reports of the Institute of High Speed Mechanics*, Vol. 54, 1987, pp. 71–78.

[92] Dular, M., B. Stoffel, and B. Širok, 2005, "Method for Cavitation Erosion Prediction: Model Development," *FEDSM2005: ASME 2005 Fluids Engineering Division Summer Meeting*, *Houston, Texas, U.S.A.,* American Society of Mechanical Engineers.

[93] Rao, A. S. L. K., et al., 1994, "Cavitation Performance Tests on the Primary Pump Model of a Nuclear Power Plant," *1994 ASME Fluids Engineering Division Summer Meeting*, *Lake Tahoe, Nevada, U.S.A.,* American Society of Mechanical Engineers.

[94] Ishimoto, J., et al., "Integrated super computational prediction of liquid droplet impingement erosion," *Progress in Nuclear Science Technology*, Vol. 2, 2011, pp. 498–502.

[95] Morita, R., 2008, "Droplet Diameter Measurements for the Prediction of Liquid Droplet Impingement Erosion," *ICONE16: 16th International Conference on Nuclear Engineering, Orlando, Florida, U.S.A.,* American Society of Mechanical Engineers.

[96] Li, R., et al., "A numerical study on turbulence attenuation model for liquid droplet impingement erosion," *Annals of Nuclear Energy*, Vol. 38, No. 6, 2011, pp. 1279–1287.

[97] Li, R., M. Mori, and H. Ninokata, "A calculation methodology proposed for liquid droplet impingement erosion," *Nuclear Engineering and Design*, Vol. 242, 2012, pp. 157–163.

[98] Morita, R., and Y. Uchiyama, 2012, "Development of a Wall Thinning Rate Model for Liquid Droplet Impingement Erosion," *ASME 2012 Pressure Vessels and Piping Conference, Toronto, Ontario, Canada,* American Society of Mechanical Engineers.

[99] Morita, R., F. Inada, and K. Yoneda, 2009, "Development of Evaluation System for Liquid Droplet Impingement Erosion (LDI)," *ASME 2009 Pressure Vessels and Piping Conference, Prague, Czech Republic,* American Society of Mechanical Engineers.

[100] Arjula, S., A. P. Harsha, and M. K. Ghosh, "Solid-particle erosion behavior of high-performance thermoplastic polymers," *Journal of Materials Science*, Vol. 43, No. 6, 2008, pp. 1757–1768.

[101] Biswas, S., and A. Satapathy, "Tribo-performance analysis of red mud filled glass-epoxy composites using Taguchi experimental design," *Materials and Design*, Vol. 30, No. 8, 2009, pp. 2841–2853.

[102] Forder, A., M. Thew, and D. Harrison, "A numerical investigation of solid particle erosion experienced within oilfield control valves," *Wear*, Vol. 216, No. 2, 1998, pp. 184–193.

[103] Hashish, M., 1987, "An Improved Model of Erosion by Solid Particle Impact," *7th International Conference on Erosion by Liquid and Solid Impact, Cambridge, United Kingdom*, Cavendish Laboratory, University of Cambridge.

[104] Bitter, J. G. A., "A study of erosion phenomena: Part I," *Wear*, Vol. 6, No. 1, 1963, pp. 5–21.

[105] Bitter, J. G. A., "A study of erosion phenomena: Part II," *Wear*, Vol. 6, No. 3, 1963, pp. 169–190.

[106] Zhang, R., H. Liu, and C. Zhao, "A probability model for solid particle erosion in a straight pipe," *Wear*, Vol. 308, No. 1, 2013, pp. 1–9.

[107] Peng, W., and X. Cao, "Numerical simulation of solid particle erosion in pipe bends for liquid–solid flow," *Powder Technology*, Vol. 294, 2016, pp. 266–279.

[108] Ahlert, K. R., 1994, *Effects of Particle Impingement Angle and Surface Wetting on Solid Particle Erosion of AISI 1018 Steel,* Doctoral Dissertation: University of Tulsa, Tulsa, Oklahoma, U.S.A.

[109] DNV, *Erosive Wear in Piping Systems,* DNV-RP-0501, 2005, Oslo, Norway: Det Norske Veritas.

[110] Parsi, M., et al., "A comprehensive review of solid particle erosion modeling for oil and gas wells and pipelines applications," *Journal of Natural Gas Science and Engineering*, Vol. 21, 2014, pp. 850–873.

[111] Zhang, Y., et al, "Comparison of computed and measured particle velocities and erosion in water and air flows," *Wear*, Vol. 263, No. 1, 2007, pp. 330–338.

[112] Neilson, J. H., and A. Gilchrist, "Erosion by a stream of solid particles," *Wear*, Vol. 11, No. 2, 1968, pp. 111–122.

[113] Oka, Y. I., K. Okamura, and T. Yoshida, "Practical estimation of erosion damage caused by solid particle impact: Part 1: Effects of impact parameters on a predictive equation," *Wear*, Vol. 259, No. 1, 2005, pp. 95–101.

[114] Oka, Y. I., and T. Yoshida, "Practical estimation of erosion damage caused by solid particle impact: Part 2: Mechanical properties of materials directly associated with erosion damage," *Wear*, Vol. 259, No. 1, 2005, pp. 102–109.

[115] Grant, G., and W. Tabakoff, "Erosion prediction in turbomachinery resulting from environmental solid particles," *Journal of Aircraft*, Vol. 12, No. 5, 1975, pp. 471–478.

[116] Zeng, L., G. A. Zhang, and X. P. Guo, "Erosion–corrosion at different locations of X65 carbon steel elbow," *Corrosion Science*, Vol. 85, 2014, pp. 318–330.

[117] Bourgoyne Jr., A. T., 1989, "Experimental Study of Erosion in Diverter Systems due to Sand Production," *SPE/IADC 1989 Drilling Conference*, *New Orleans, Louisiana, U.S.A.,* Society of Petroleum Engineers.

[118] Valor, A., et al., "Stochastic modeling of pitting corrosion: A new model for initiation and growth of multiple corrosion pits," *Corrosion Science*, Vol. 49, No. 2, 2007, pp. 559–579.

[119] Shekari, E., F. Khan, and S. Ahmed, "A predictive approach to fitness-for-service assessment of pitting corrosion," *International Journal of Pressure Vessels and Piping*, Vol. 137, 2016, pp. 13–21.

[120] Fontes, G. S., P. F. Frutuoso e Melo, and A. S. De Martin Alves, "An Itô model of pit corrosion in pipelines for evaluating risk-informed decision making," *Nuclear Engineering and Design*, Vol. 293, 2015, pp. 485–491.

[121] Bond, L. J., et al., 2007, "Improved Economics of Nuclear Plant Life Management," *2nd International Symposium on Nuclear Power Plant Life Management, Shanghai, China,* International Atomic Energy Agency.

[122] Shumaker, B. D., et al., "Remaining useful life estimation of electric cables in nuclear power plants," *Chemical Engineering Transactions*, Vol. 33, 2013, pp. 877–882.

[123] Saarela, O., and J. E. Hulsund, 2015, "Lifetime Modeling of Equipment at Nuclear Power Plants," *NPIC-HMIT2015: 9th International Topical Meeting on Nuclear Plant Instrumentation, Control,*

and Human-Machine Interface Technologies, Charlotte, North Carolina, U.S.A., American Nuclear Society.

[124] Pandey, M. D., D. Lu, and D. Komljenovic, 2009, "The Impact of Probabilistic Modelling on Predicting the Remaining Life of Pipes in Nuclear Plants," *ICONE17: 17th International Conference on Nuclear Engineering, Brussels, Belgium,* American Society of Mechanical Engineers.

[125] Bakhtiari, S., et al., 2012, "Condition Based Prognostics of Passive Components—A New Era for Nuclear Power Plant Life Management," *3rd International Conference on Nuclear Power Plant Life Management (PLiM) for Long Term Operations (LTO), Salt Lake City, Utah, U.S.A.,* International Atomic Energy Agency.

[126] Heo, G. Y., "Condition monitoring using empirical models: Technical review and prospects for nuclear applications," *Nuclear Engineering and Technology*, Vol. 40, No. 1, 2008, p. 49.

[127] Mansouri, A., et al., "A combined CFD/experimental methodology for erosion prediction," *Wear*, Vol. 332, 2015, pp. 1090–1097.

[128] Coble, J. B., Ramuhalli, P., Bond, L. J., Hines, J. W., & Upadhyaya, B.R. (2012). Prognostics and health management in nuclear power plants: A review of technologies and applications. (PNNL-21515). Richland, Washington, USA: Pacific Northwest National Laboratory.

[129] Meyer, R. M., et al., 2013, *Technical Needs for Prototypic Prognostic Technique Demonstration for Advanced Small Modular Reactor Passive Components,* PNNL-22488, Rev. 0, Pacific Northwest National Laboratory, Richland, Washington, U.S.A.

[130] *Advanced Surveillance, Diagnostic and Prognostic Techniques in Monitoring Structures, Systems and Components in Nuclear Power Plants,* NP-T-3.14, 2013, International Atomic Energy Agency, Vienna, Austria.

[131] Blatt, W., et al., "The influence of hydrodynamics on erosion-corrosion in two-phase liquid-particle flow," *Corrosion*, Vol. 45, No. 10, 1989, pp. 793–804.

[132] Horowitz, J., 2015, *Recommendations for an Effective Program against Erosive Attack*, 3002005530, Electric Power Research Institute, Palo Alto, California, U.S.A.

[133] Lybeck, N., et al., 2011, "An Assessment of Integrated Health Management (IHM) Frameworks," *3rd International Conference on Nuclear Power Plant Life Management (PLiM) for Long Term Operations (LTO), Salt Lake City, Utah, U.S.A.,* International Atomic Energy Agency.

[134] Andresen, P. L., et al., "Monitoring and modeling stress corrosion and corrosion fatigue damage in nuclear reactors," *The Journal of the Minerals*, Vol. 42, No. 12, 1990, pp. 7–11.

[135] Bajic, B., Multidimensional Cavitation Monitor in FPGA/RT Technology, *HydroVision International*, 2011, Korto Cavitation Services, Sacramento, California, U.S.A.

[136] Baranenko, V. I., et al., "Development of software tools for calculating corrosion-erosion wear of pipelines at nuclear power stations," *Thermal Engineering*, Vol. 54, No. 12, 2007, pp. 981–988.

[137] Bond, L. J., et al., 2003, *On-line Intelligent Self-Diagnostic Monitoring System for Next Generation Nuclear Power Plants,* PNNL-14304, Pacific Northwest National Laboratory, Richland, Washington, U.S.A.

[138] Bridgeman, J., and R. Shankar, "Erosion/corrosion data handling for reliable NDE," *Nuclear Engineering and Design*, Vol. 131, No. 3, 1991, pp. 285–297.

[139] Butter, L. M., and A.G.L. Zeijseink, 2000, "Erosion-Corrosion Management System for Secondary Circuits of Nuclear Power Plants," *8th International Conference of Water Chemistry of Nuclear Reactor Systems, Bournemouth, United Kingdom,* British Nuclear Energy Society.

[140] ClampOn, *Ultrasonic Intelligent Sensors - ClampOn Topside CEM Corrosion-Erosion Monitor - Digital Signal Processing*, 2016.

[141] GE Inspection Technologies, *Corrosion & Erosion - Inspection Solutions for Detection, Sizing & Monitoring*, 2010.

[142] Davies, L. M., B. Gueorguiev, and P. Trampus, 2000, "Role of NDT in Condition Based Maintenance of Nuclear Power Plant Components," *WCNDT15: 15th World Conference on Non-Destructive Testing, Rome, Italy,* NDT.net.

[143] GE Measurement & Control, *System 1* Extender Rightrax Corrosion and Erosion Monitoring*, 2015.

[144] Hashemian, H. M., "On-line monitoring applications in nuclear power plants," *Progress in Nuclear Energy*, Vol. 53, No. 2, 2011, pp. 167–181.

[145] He, Y., and Z. Shen, 2012, "Experimental Research on Cavitation Erosion Detection Based on Acoustic Emission Technique," *EWGAE30-ICAE7: 30th European Conference on Acoustic Emission Testing & 7th International Conference on Acoustic Emission, Granada, Spain,* NDT.net.

[146] Honarvar, F., et al., "Ultrasonic monitoring of erosion/corrosion thinning rates in industrial piping systems," *Ultrasonics*, Vol. 53, No. 7, 2013, pp. 1251–1258.

[147] IAEA, *High Temperature On-line Monitoring of Water Chemistry and Corrosion Control in Water Cooled Power Reactors,* IAEA-TECDOC-1303, 2002, International Atomic Energy Agency, Vienna, Austria.

[148] IAEA, *On-line Monitoring for Improving Performance of Nuclear Power Plants Part 1: Instrument Channel Monitoring*, NP-T-1.1, 2008, International Atomic Energy Agency, Vienna, Austria.

[149] Kastner, W., et al., "Calculation code for erosion corrosion induced wall thinning in piping systems," *Nuclear Engineering and Design*, Vol. 119, No. 2, 1990, pp. 431–438.

[150] Kim, H., M. G. Na, and G. Heo, "Application of monitoring, diagnosis, and prognosis in thermal performance analysis for nuclear power plants," *Nuclear Engineering and Technology*, Vol. 46, No. 6, 2014, pp. 737–752.

[151] Lai, H. -C., W. -Y. Mao, and C.F. Chu, "Corrosion monitoring application in Taiwan's nuclear power plants," *Energy Materials*, Vol. 3, No. 2, 2008, pp. 91–98.

[152] Lovchev, V. N., et al., "Improvement and optimization of techniques for monitoring erosion-corrosion wear of equipment and pipelines at nuclear power stations," *Thermal Engineering*, Vol. 56, No. 2, 2009, pp. 134–141.

[153] Palusamy, S. S., J. C. Schmertz, and D. H. Roarty, 1990, "Corrosion-erosion Trend Monitoring and Diagnostic System," U.S. Patent No. 4,935,195, Assignee: Westinghouse Electric Corp.

[154] Ryl, J., and K. Darowicki, "Impedance monitoring of carbon steel cavitation erosion under the influence of corrosive factors," *Journal of the Electrochemical Society*, Vol. 155, No. 4, 2008, pp. 44–49.

[155] Ryu, K. H., et al., "Online monitoring method using equipotential switching direct current potential drop for piping wall loss by flow accelerated corrosion," *Nuclear Engineering and Design*, Vol. 240, No. 3, 2010, pp. 468–472.

[156] Saluja, A., J. Costain, and E. Van der Leden, 2009, "Non-Intrusive Online Corrosion Monitoring," *NDE2009: National Seminar & Exhibition on Non-Destructive Evaluation*, *Tiruchirappalli, India,* NDT.net.

[157] Uchida, S., et al., "Evaluation methods for corrosion damage of components in cooling systems of nuclear power plants by coupling analysis of corrosion and flow dynamics (III)," *Journal of Nuclear Science and Technology*, Vol. 46, No. 1, 2009, pp. 31–40.

[158] Urayama, R., et al., "Online monitoring of pipe wall thinning by electromagnetic acoustic resonance method," *E-Journal of Advanced Maintenance*, Vol. 5, 2015, pp. 155–164.

[159] Hallbert, B., and K. Thomas, 2015, *Advanced Instrumentation, Information, and Control Systems Technologies Technical Program Plan for FY 2016,* INL/EXT-13-28055, Rev. 4, Idaho National Laboratory, Idaho Falls, Idaho, U.S.A.

[160] IAEA, "Material Degradation and Related Managerial Issues of Nuclear Power Plants," 2005, *Technical Meeting, Vienna, Austria,* International Atomic Energy Agency.

[161] Wacker, J. F., et al., 2007, *FY06 Annual Report on the Progress and Path Forward for the NA-22 Funded Project PL06-AUT308-PD01: Automation of Ultra-trace and Radiochemical Methods,* PNNL-16527, Pacific Northwest National Laboratory, Richland, Washington, U.S.A.

[162] INL, 2015, *DOE-NE Light Water Reactor Sustainability Program and EPRI Long Term Operations Program – Joint Research and Development Plan*, INL/EXT-12-24562, Rev. 4, Idaho National Laboratory, Idaho Falls, Idaho, U.S.A.

[163] U.S. Nuclear Regulatory Commission, *Generic Aging Lessons Learned (GALL) Report,* NUREG-1801, Rev. 2, 2010, Washington D.C., U.S.A.

[164] Levis, W., *Delivering the Nuclear Promise: Advanced Safety, Reliability and Economic Performance,* 2016, Nuclear Energy Institute, Washington D.C., U.S.A.

[165] Imperial College London, *Area Monitoring Using Ultrasonic Guided Wave*, http://www.imperial.ac.uk/non-destructive-evaluation/research/inspection-and-monitoring/area-monitoring-using-ultrasonic-guided-wave/, Web page visited April 27, 2016.

[166] Cau, F., et al., "A signal-processing tool for non-destructive testing of inaccessible pipes," *Engineering Applications of Artificial Intelligence*, Vol. 19, No. 7, 2006, pp. 753–760.

[167] Acciani, G., et al., "Angular and axial evaluation of superficial defects on non-accessible pipes by wavelet transform and neural network-based classification," *Ultrasonics*, Vol. 50, No. 1, 2010, pp. 13–25.

[168] Lee, H., J. Yang, and H. Sohn, "Baseline-free pipeline monitoring using optical fiber guided laser ultrasonics," *Structural Health Monitoring*, Vol. 11, No. 6, 2012, pp. 684–695.

[169] Ahmad, R., and T. Kundu, "Cylindrical guided wave signals for underground pipe inspection using different continuous wavelet mother functions," *Journal of Civil Engineering and Architecture*, Vol. 5, No. 12, 2011, pp. 1103–1110.

[170] Lee, C., and S. Park, "Damage visualization of pipeline structures using laser-induced ultrasonic waves," *Structural Health Monitoring*, Vol. 14, No. 5, 2015, pp. 475–488.

[171] Mu, J., L. Zhang, and J.L. Rose, "Defect circumferential sizing by using long range ultrasonic guided wave focusing techniques in pipe," *Non-destructive Testing and Evaluation*, Vol. 22, No. 4, 2007, pp. 239–253.

[172] Ni, J., et al., "Effect of pipe bend configuration on guided waves-based defects detection: An experimental study," *Journal of Pressure Vessel Technology*, Vol. 138, No. 2, 2016.

[173] Wang, X., W. T. Peter, and A. Dordjevich, "Evaluation of pipeline defect's characteristic axial length via model-based parameter estimation in ultrasonic guided wave-based inspection," *Measurement Science and Technology*, Vol. 22, No. 2, 2011.

[174] Cobb, A. C., and J. L. Fisher, 2016, "Flaw Depth Sizing Using Guided Waves," *42nd Annual Review of Progress in Quantitative Nondestructive Evaluation: Incorporating the 6th European-American Workshop on Reliability of NDE, Minneapolis, Minnesota, U.S.A.,* AIP Publishing.

[175] Otero, R., E. Moreno, and B. Meza, 2011, "Generation of Focused Ultrasonic Guided Waves for Nondestructive Testing of Structures," *5th Pan American Conference for NDT*, *Cancun, Mexico,* NDT.net.

[176] Cheng, J.-W., S.-K. Yang, and S.-M. Chiu, "The use of guided waves for detecting discontinuities in fluid-filled pipes," *Materials Evaluation*, Vol. 65*,* No. 11, 2007, pp. 1129–1134.

[177] Gori, M., et al., "Guided waves by EMAT transducers for rapid defect location on heat exchanger and boiler tubes," *Ultrasonics*, Vol. 34, No. 2, 1996, pp. 311–314.

[178] Lu, B., B. R. Upadhyaya, and R.B. Perez, "Structural integrity monitoring of steam generator tubing using transient acoustic signal analysis," *IEEE Transactions on Nuclear Science*, Vol. 52, No. 1, 2005, pp. 484–493.

[179] Leinov, E., M.J.S. Lowe, and P. Cawley, "Investigation of guided wave propagation and attenuation in pipe buried in sand," *Journal of Sound and Vibration*, Vol. 347, 2015, pp. 96–114.

[180] Leinov, E., M.J.S. Lowe, and P. Cawley, "Ultrasonic isolation of buried pipes," *Journal of Sound and Vibration*, Vol. 363, 2016, pp. 225–239.

[181] Ahmad, R., 2005, *Guided Wave Technique to Detect Defects in Pipes Using Wavelet Analysis,* Doctoral Dissertation: University of Arizona, Tucson, Arizona, U.S.A.

[182] Lowe, M. J. S., and P. Cawley, *Long Range Guided Wave Inspection Usage–Current Commercial Capabilities and Research Directions,* 2006, Department of Mechanical Engineering, Imperial College London, London, United Kingdom.

[183] Cawley, P., 2002, "Practical Long Range Guided Wave Inspection – Applications to Pipes and Rails," *NDE2002: National Seminar of Indian Society for Non-Destructive Testing, Chennai, India,* NDT.net.

[184] Rose, J. L., 2009, "Successes and Challenges in Ultrasonic Guided Waves for NDT and SHM," *NDE2009: National Seminar & Exhibition on Non-Destructive Evaluation, Tiruchirappalli, India,* NDT.net.

[185] Mokhles, M., C. Ghavipanjeh, and A. Tamimi, 2013, "The Use of Ultrasonic Guided Waves for Extended Pipeline Qualification Prediction," *SINCE2013: Singapore International NDT Conference & Exhibition, Marina Bay Sands, Singapore,* NDT.net.

[186] Na, W. -B., and T. Kundu, "Underwater pipeline inspection using guided waves," *Journal of Pressure Vessel Technology*, Vol. 124, No. 2, 2002, pp. 196–200.

[187] Na, W. -B., and T. Kundu, "Underwater pipeline inspection using guided waves," *Journal of Pressure Vessel Technology*, Vol. 124, No. 2, 2002, pp. 196–200.

[188] Vasiljevic, M., et al., "Pipe wall damage detection by electromagnetic acoustic transducer generated guided waves in absence of defect signals," *The Journal of the Acoustical Society of America*, Vol. 123, No. 5, 2008, pp. 2591–2597.

[189] Ahmad, R., and T. Kundu, "Structural Health Monitoring of Steel Pipes Under Different Boundary Conditions and Choice of Signal Processing Techniques," *Advances in Civil Engineering*, 2012.

[190] Demma, A., et al., "The reflection of guided waves from notches in pipes: A guide for interpreting corrosion measurements," *NDT & E International*, Vol. 37, No. 3, 2004, pp. 167–180.

[191] Sun, P., et al., "An EMAT for inspecting heat exchanger tubes of stainless steel using longitudinal guided waves based on non-uniform static magnetic fields," *Insight-Non-Destructive Testing and Condition Monitoring*, Vol. 57, No. 4, 2015, pp. 221–229.

[192] Sinding, K., et al., 2013, "High Temperature Ultrasonic Transducers for the Generation of Guided Waves for Non-Destructive Evaluation of Pipes," *QNDE2013-ICBM2013: 40th Annual Review of Progress in Quantitative Nondestructive Evaluation: Incorporating the 10th International Conference on Barkhausen Noise and Micromagnetic Testing, Baltimore, Maryland, U.S.A.,* AIP Publishing.

[193] Bezdek, M., et al., 2008, "Structural Health Monitoring and Nondestructive Evaluation of Double Wall Structures," *SPIE6935: Health Monitoring of Structural and Biological Systems, San Diego, California, U.S.A.,* International Society for Optics and Photonics.

[194] Kwun, H., et al., "A torsional mode guided wave probe for long range, in bore testing of heat exchanger tubing," *Materials Evaluation*, Vol. 63, No. 4, 2005, pp. 430–433.

[195] Cheong, Y. -M., et al., "Analysis of the circumferential guided wave for axial crack detection in a feeder pipe," *Key Engineering Materials*, 2004, pp. *270–273*, pp. 422–427.

[196] Klein, K. A., et al., 1986, "Composite Piezoelectric Paints," *ISAF86: 6th IEEE International Symposium on Applications of Ferroelectrics, Bethlehem, Pennsylvania, U.S.A.,* Institute of Electrical and Electronics Engineers.

[197] Li, X., and Y. Zhang, 2007, "Piezoelectric Paint Sensor for Ultrasonic NDE," *SPIE6529: Sensors and Smart Structures Technologies for Civil, Mechanical, and Aerospace Systems, San Diego, California, U.S.A.,* International Society for Optics and Photonics.

[198] Li, X., and Y. Zhang, "Analytical study of piezoelectric paint sensor for acoustic emission-based fracture monitoring," *Fatigue and Fracture of Engineering Materials and Structures*, Vol. 31, No. 8, 2008, pp. 684–694.

[199] Zhang, Y., "In situ fatigue crack detection using piezoelectric paint sensor," *Journal of Intelligent Material Systems and Structures*, Vol. 17, No. 10, 2006, pp. 843–852.

[200] Yang, C., and C. -P. Fritzen, 2011, "Piezoelectric Paint as Spatially Distributed Modal Sensors," *8th International Workshop on Structural Health Monitoring, Stanford, California, U.S.A.,* DEStech Publications Inc.

[201] Yoo, B., et al., 2010, "Piezoelectric Paint Based 2-D Sensor Array for Detecting Damage in Aluminum Plate," *51st AIAA/ASME/ASCE/AHS/ASC Structures, Structural Dynamics, and Materials Conference, Orlando, Florida, U.S.A.,* American Institute of Aeronautics and Astronautics Inc.

[202] Yoo, B., et al., "Piezoelectric-paint-based two-dimensional phased sensor arrays for structural health monitoring of thin panels," *Smart Materials and Structures*, Vol. 19, No. 7, 2010, pp. 1–17.

[203] Kang, L. -H., and J. -R. Lee, 2014, "Piezoelectric Paint Sensor for Impact and Vibration Monitoring," *EWSHM2014: 7th European Workshop on Structural Health Monitoring and 2nd*

European Conference of the Prognostics and Health Management (PHM) Society, Nantes, France, National Institute for Research in Computer Science and Control.

[204] Payo, I., and J. M. Hale, 2010, "A Piezoelectric Paint Thick-Film Strain Sensor for Vibration Monitoring Purposes," *ISMA2010: 24th International Conference on Noise and Vibration Engineering and 3rd International Conference on Uncertainty in Structural Dynamics, Leuven, Belgium,* University of Leuven.

[205] White, J. R., et al., "Piezoelectric paint: Ceramic-polymer composites for vibration sensors," *Journal of Materials Science*, Vol. 39, No. 9, 2004, pp. 3105–3114.

[206] Hale, J. M., 2004, "Piezoelectric Paint: Thick-Film Sensors for Structural Monitoring of Shock and Vibration," *ESDA2004: 7th Biennial Conference on Engineering Systems Design and Analysis, Manchester, United Kingdom,* American Society of Mechanical Engineers.

[207] Zhang, Y., 2005, "Piezoelectric Paint Sensor for Real-Time Structural Health Monitoring," *SPIE5765: Smart Structures and Materials 2005: Sensors and Smart Structures Technologies for Civil, Mechanical, and Aerospace Systems*, *San Diego, California, U.S.A.,* International Society for Optics and Photonics.

[208] Raptis, P. N., et al., "Effect of exposure of piezoelectric paint to water and salt solution," *Journal of Materials Science*, Vol. 39, No. 19, 2004, pp. 6079–6081.

[209] Hale, J. M., and R. Lahtinen, "Piezoelectric paint: Effects of harsh weathering on aging," *Plastics, Rubber and Composites*, Vol. 36, No. 9, 2007, pp. 419–422.

[210] Yang, C., and C. -P. Fritzen, "Piezoelectric paint: Characterization for further applications," *Smart Materials and Structures*, Vol. 21, No. 4, 2012.

[211] Yang, C., and C. -P. Fritzen, 2012, "Characterization of Piezoelectric Paint and its Refinement for Structural Health Monitoring Applications," *SPIE8409: 3rd International Conference on Smart Materials and Nanotechnology in Engineering*, *Shenzhen, China,* International Society for Optics and Photonics.

[212] Egusa, S., and N. Iwasawa, "Piezoelectric paints as one approach to smart structural materials with health-monitoring capabilities," *Smart Materials and Structures*, Vol. 7, No. 4, 1998, pp. 438–445.

[213] Egusa, S., and N. Iwasawa, "Application of piezoelectric paints to damage detection in structural materials," *Journal of Reinforced Plastics and Composites*, Vol. 15, No. 8, 1996, pp. 806–817.

[214] Egusa, S., and N. Iwasawa, "Preparation of piezoelectric paints and application as vibration modal sensors," *Journal of Intelligent Material Systems and Structures*, Vol. 5, No. 1, 1994, pp. 140–144.

[215] Zhang, Y., C. Zhou, and L. W. Tong, 2014, "Fatigue Crack Growth Monitoring of Welded Tubular Structures Using Piezoelectric Film Acoustic Emission Sensor," *IABMAS2014: 7th International Conference of Bridge Maintenance, Safety and Management, Shanghai, China,* Taylor and Francis - Balkema.

[216] Yoo, B., D. J. Pines, and A. S. Purekar, 2009, "2-D Directional Phased Array Using Piezoelectric Paint to Detect Damages in Isotropic Plates," *SMASIS2009: ASME 2009 Conference on Smart Materials, Adaptive Structures and Intelligent Systems, Oxnard, California, U.S.A.,* American Society of Mechanical Engineers.

[217] Zhang, Y., 2003, "Dynamic Strain Measurement Using Piezoelectric Paint," *IWSHM2003: 4th International Workshop on Structural Health Monitoring: From Diagnostics and Prognostics to Structural Health Management, Stanford, California, U.S.A.,* DEStech Publications.

[218] Li, X., and Y. Zhang, 2008, "A Percolation Based Micromechanical Constitutive Model for Flexible Piezoelectric Paint," *SMASIS2008: ASME 2008 Conference on Smart Materials, Adaptive*

Structures and Intelligent Systems, Ellicott City, Maryland, U.S.A., American Society of Mechanical Engineers.

[219] Joint Research Plan on Structural Health Monitoring with the Electric Power Research Institute, INL/INT-16-38821, Revision 0, Idaho National Laboratory, May 2016